LIGHT-INDUCED ELECTRON TRANSFER REACTION OF AMPHIPHILIC COPOLYMERS IN AQUEOUS SOLUTION

by

YOSHIHIRO ITOH

Department of Macromolecular Science
Faculty of Scicence
Osaka University

1984

Approvals

1984

LIGHT-INDUCED ELECTRON TRANSFER REACTION OF AMPHIPHILIC COPOLYMERS IN AQUEOUS SOLUTION

A Doctoral thesis

by

Yoshihiro Itoh

This thesis is approved as to style and content by

野桜俊一

Member-in-Chief

藤田博

Member

中村晃

Member

林晃一郎

Member

森島洋太郎

Member

Acknowledgements

This research work was carried out in collaboration with Dr. Yotaro Morishima, Mr. Toshihiko Hashimoto, and Mr. Tohru Tanaka at Department of Macromolecular Science, Faculty of Science, Osaka University, under the direction of Professor Shun-ichi Nozakura. The author would like to express his gratitude to Professor Shun-ichi Nozakura for his continuing guidance and encouragement throughout the course of this work. The author also would like to express his utmost gratitude to Dr. Yotaro Morishima and other collaborators for their fruitful cooperations. Grateful acknowledgements are also made to Associate Professor Mikiharu Kamachi and Dr. Masaoki Furue for their helpful suggestions and also to all the members of the Nozakura Laboratory for their cooperation and friendship.

The author is greatly indebted to Mr. Atsuo Koreeda and Mr. Takeshi Ishibashi, Institute of Scientific and Industrial Research, Osaka University, for the measurements of the electron microscope. The author also expresses his thanks to Professor Shunji Kato and Dr. Takeshi Ohno, College of General Education, Osaka University, for the measurements of laser photolysis and their helpful discussion of the transient spectroscopy.

Nagano
August 1984

Yoshihiro Itoh

CONTENTS

Introduction

In the developement of energy resources other than fossil fuels, the chemistry of energy conversion has become a research subject of high priority. In particular, utilization of solar energy may play an important role in the ultimate solution to the world's energy problems because of it being infinite energy.

There are various types of energy conversion processes in natural and artificial systems (Table I)[1]. These processes are complicated and diverse, but have many points of similarity. For example, light-irradiation of a semiconductor electrode such as TiO_2 results in both the evolution of hydrogen and the generation of photovoltage[2]. Namely, conversions from light energy to chemical and electric energy take place at the same time. Analysis from the microscopic aspect reveals that the charge separation of electron and positive hole through the

Table I. Energy conversion processes

type of conversion	example
light ⟷ chemical	photosynthesis
	chemiluminescence
chemical ⟷ electric	fuel cell
	electrolysis
light ⟷ electric	photovoltaic cell
	electroluminescence
chemical ⟷ heat	exothermic reaction
	endothermic reaction

space charge region, which develops in the surface area of a semiconductor, occurs at the initial stage[3]. Also it is well known that the initial process in the plant photosynthesis is charge separation at the reaction center and the resulting cationic and anionic charges are ultimately linked with oxidation of water and reduction of carbon dioxide, respectively[4]. A detailed understanding of a common feature of the mechanisms could prove useful in the development of effective systems.

Recently, the photoinduced water cleavage by redox catalysis have received wide attention. Figure 1 illustrates a simplest model composed of an electron donor (D) and an acceptor (A) for the photochemical water splitting. Since the excited state of a molecule is a better electron donor, as well as a better electron acceptor, than its ground state, light energy can drive an electron transfer that is nonspontaneous. Energy of an amount ΔG can, thus, be stored in D^+ and A^-. Further, in the presence of appropriate catalysis, the photoinduced water decomposition may be realized. Photoinduced electron transfer reactions have been studied in great detail both from the experimental[5] and the theoretical[6] points of view. The rate of electron transfer between D^* and A (or D and A^*) in solution is expected to approach the diffusion-controlled limit when the driving force for the reaction exceeds a few hundred millivolts. On the other hand, the backward electron transfer between D^+ and A^- to D + A which is thermodynamically strongly favored is

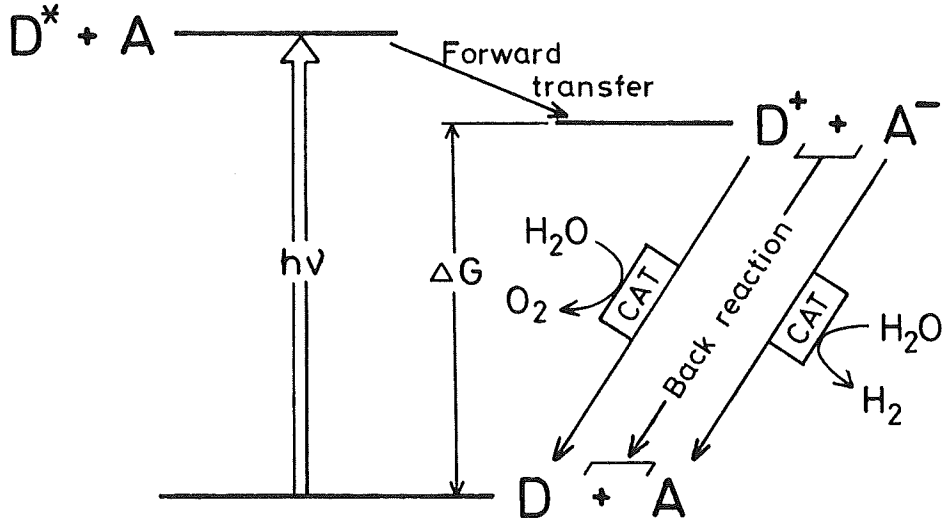

Figure 1. Schematic illustration of photochemical water splitting device.

always diffusion controlled in solution. This undesired back reaction precludes the practical use of such a homogeneous system in an energy conversion device, because it prevents the achievement of high overall quantum efficiency. Grätzel et al.[7] reported the photoinduced water cleavage by using tris(2,2'-bipyridine)ruthenium (II) chloride ($Ru(bpy)_3^{2+}$) as photosensitizer and methyl viologen (MV^{2+}) as electron acceptor. The electron transfer from $Ru(bpy)_3^{2+}$ to MV^{2+} yields $Ru(bpy)_3^{3+}$ and MV^{+}, which could oxidize water to oxygen and reduce water to hydrogen in the presence of catalysts. In fact, hydrogen and oxygen evolution was observed in the presence of RuO_2 and Pt colloids with a very low quantum yield ($\phi \sim 10^{-3}$)[7].

In the photosynthesis the efficiency of initial charge separation is essentially 100 %. Although the mechanism has not yet been fully unraveled, it is implied that some sort of heterogeneous phase might be playing a key role for the complete charge separation and hence the achievement of high overall quantum efficiency. Many workers have studied how suitable systems may be developed that allow the retardation of the undesired back reaction.

Fundamental phenomena in the photoinduced electron transfer in heterogeneous systems have extensively been investigated with semiconductor-electrolyte systems[3,8] and with micellar systems[9,10]. In the former systems electrons transfer across the space charge region which develops in the surface area of a semiconductor when it is in contact with a

suitable redox system. In the latter systems electrons often transfer, in analogy with the former, through the electric double layer between the organic interior and the aqueous exterior of a micelle, resulting in charged products separated in different phases. The back reaction in this system is far less likely than in homogeneous solutions. Utilization of micelles has actively been investigated by Grätzel et al.[10], Matsuo et al.[11], and Mataga et al.[12]. Matsuo et al.[13] studied the photoreduction of an amphipathic derivative of $Ru(bpy)_3^{2+}$ by dimethylaniline (DMA) in a micellar system and indicated that the decay of photoproducts strongly depends on the nature of microenvironments surrounding the primary redox pair. In the CTAC micelle, the decay of photoproduct is considerably retarded due to the Coulombic repulsion between DMA^+ and the micellar surface. Grätzel et al.[14] demonstrated the light-induced charge separation using a sensitizer (S) solubilized in functional micelles such as copper (II) lauryl sulfate ($Cu(LS)_2$). The forward electron transfer occurred very fast because S and Cu^{2+} are held in close proximity through the micellar organization and the charge separation was achieved by replacement of Cu^+ (photoproduct) with Cu^{2+} in the aqueous phase.

Bilayer membranes with two heterogeneous phase boundaries afford a better model system for biomembranes. Fendler et al.[15] and Calvin et al.[16] have extensively investigated the characterization and utilization of surfactant vesicles, which are phospholipids (liposomes) or synthetic surfactant

vesicles containing entrapped water. Fendler et al.[17] have studied the photoelectron transfer from N-methylphenothiazine (MPTH) to a surfactant derivative of $Ru(bpy)_3^{2+}$ in cationic surfactant vesicles. The MPTH cation radicals formed are efficiently expelled both into the vesicle-entrapped water pool and into bulk water. The photoinduced electron transport across the bilayer membrane has also been reported[18,19]. Microemulsions[19] have been demonstrated also as workable systems for charge separation.

A pronounced effect of polyelectrolyte on the reaction rate of small charged molecules has well been established[20,21]: Two charged species of the same sign would both be attracted to a polyelectrolyte with opposite sign to be locally concentrated, leading to the increase of the reaction rate. If the two has different signs, one would be attracted and the other repelled by the polyion, resulting in a pronounced reduction of the reaction rate. These effects have been demonstrated in photo-induced electron transfer reactions by Meisel et al.[22,23] and Rabani et al.[24]. Recently, Meisel et al.[22] have exhibited intriguing phenomena; i.e., in the photochemical systems with $Ru(bpy)_3^{2+}$ and neutral electron acceptors, they have observed a marked effect of poly(vinyl sulfate) on the yields of the photo-electron transfer as a result of enhanced charge separation. Sassoon and Rabani[24] have demonstrated that polybrene (a positively charged polyelectrolyte) has an effect on separating the photoelectron transfer products of cis-dicyanobis(2,2'-bipyridine)ruthenium (II) and potassium hexacyanoferrate (III) in aqueous solution.

From all these investigations on the semiconductor, micellar, vesicle, microemulsion, and polyelectrolyte systems, it is evident that very powerful electric field with unsymmetrical gradient developed in the vicinity of the surface area of the heterophase is a major force, if not a decisive one, for driving charge separation.

Introduction of photosensitive groups into the macromolecular chain has been widely investigated in relation to practical application: i.e., the development of polymer materials of photoresist, photoconductor, and photosensor etc[25]. Photoreaction with the polymer photosensitizer is expected to have some advantages compared to the monomeric system. First, heterogeneity of sensitizer makes easy to separate the reaction products and increases the photo-stability of the sensitizer itself. Second, the assembly effect of sensitizers enables the efficient collection of photoexcitation energy. It is reported that the photoredox reaction is facilitated as a result of singlet or triplet energy migration along the polymer chain[26]. Third, the microenvironmental effects of the polymer matrix will control the reaction kinetics. These include the ionic effect of polyelectrolyte as described above.

In this context, amphiphilic copolymers consisting of hydrophobic and electrolyte segments are interesting media for electron transfer reactions. These polyions carrying hydrophobic residues, when dissolved in water, tend to form "polysoap" in which hydrophobic aggregates are confined in a

powerful potential field generated by polyions with a high density of fixed charge along the macromolecular chain. One might expect a few advantages with these types of polymers as media for the photosensitized electron transfer:

(1) The forward electron transfer is facilitated due to uptake of hydrophobic or amphiphilic substrates such as electron donors or acceptors through hydrophobic interaction.

(2) The back reaction between the electron transfer products is retarded due to the electrostatic repulsion of the photoproduct with the electric charges on the electrolyte sequences.

(3) When the hydrophobic groups act as photosensitizers, photoexcitation energy may be efficiently collected and transfered to "reactive sites" as a result of energy migration along the polymer chain.

This idea is shown schematically in Figure 2.

An object of this research is to design a suitable polymer of this type as reaction media for the photoelectron transfer. In this thesis, we describe synthesis of a series of amphiphilic copolymers and investigation on the effect of these polymers on the forward and backward processes in the photoinduced electron transfer.

Chapter 1 describes the syntheses of various types of amphiphilic copolymers. These polymers were prepared by radical copolymerizations of aromatic vinyl compounds with strong electrolyte monomers. Block copolymers of this type

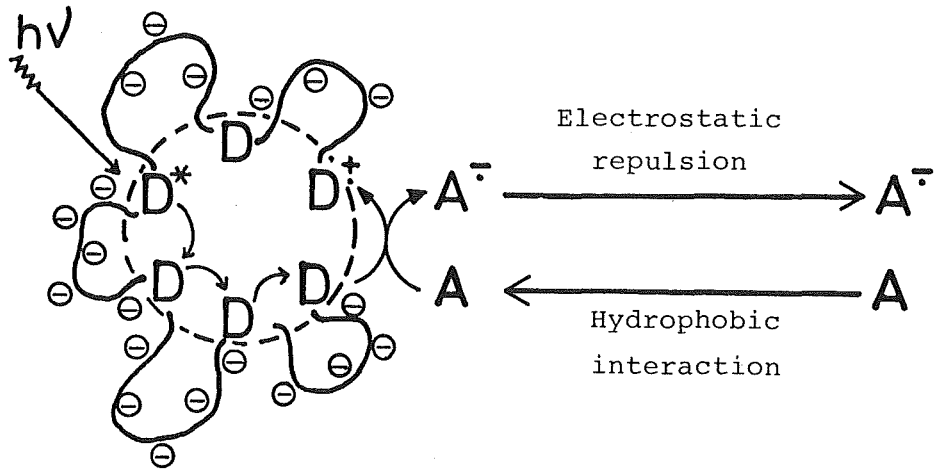

Figure 2. Schematic representation of the photoinduced electron transfer of amphiphilic copolymers in aqueous solution: D, chromophore (electron donor); A, electron acceptor.

type were prepared by anionic copolymerization of vinyl-phenanthrene and trimethylsilyl methacrylate.

In Chapter 2, the solution behaviors of these amphiphilic copolymers were studied. Hydrophobic microdomains are thus found with random and block copolymers in aqueous solutions. The hydrophobicity of these microdomains and the hydrophobic interaction of those with small molecules were studied.

In Chapter 3, in order to investigate the forward electron transfer, the fluorescence quenching of amphiphilic copolymers with amphiphilic quenchers in aqueous solution was studied. The fluorescence from the phenanthryl groups in such amphiphilic polymers is quenched by amphiphilic quenchers far more effectively than predicted by diffusional quenching. In these systems the quenching processes do not obey the fundamental rate laws of homogeneous kinetics. A specific model for such system was proposed.

Chapter 4 describes the fluorescence quenching of amphiphilic copolymers with ionic quenchers. Electrolyte segments of amphiphilic copolymers increase the rate of quenching by an order of magnitude in aqueous solutions.

In Chapter 5, electrostatic effect of amphiphilic copolymers on the back electron transfer was studied. It was demonstrated by the steady-state photoreduction and laser photolysis that the charged segments in these polymers can retard the back reaction of the photoproducts. Furthermore, the potential field effect of macroions on electron transfer reactions was simulated by the electrochemical redox reactions.

Abbreviations used in this thesis are as follows:

AM : sodium 9-phenanthrylmethanesulfonate

AMPS : 2-acrylamido-2-methylpropanesulfonic acid

ANS : sodium 8-anilino-naphthalenesulfonate

APh : poly(9-vinylphenanthrene-co-sodium 2-acrylamido-2-methylpropanesulfonate)

APy : poly(1-vinylpyrene-co-sodium 2-acrylamido-2-methylpropanesulfonate)

ASt : poly(styrene-co-2-acrylamido-2-methylpropanesulfonic acid)

BHET : bis(2-hydroxyethyl)terephthalate

b-VPh : poly(9-vinylphenanthrene-b-methacrylic acid)

CyD : 5,5'-diphenyl-3,3'-diethylbenzoxazolecarbocyanine nitrate

DHEA : N,N-di(2-hydroxyethyl)aniline

DHT : 1,6-diphenyl-1,3,5-hexatriene

DMAPMA : N-(N',N'-dimethylaminopropyl)methacrylamide

FA : fumaric acid

MA : methacrylic acid

MHEA : N-methyl-N-(2-hydroxyethyl)aniline

MPh : poly(9-vinylphenanthrene-co-methacrylic acid)

MV^{2+} : 1,1'-dimethyl-4,4'-bipyridinium dichloride (methyl viologen)

PyS : sodium 1-pyrenesulfonate

QM : 2-(3-phenanthrylacetylamino)ethyltrimethylammonium methylsulfate

QPh : poly(9-vinylphenanthrene-co-3-methacryloylaminopropyl-

trimethylammonium methylsulfate)

SPV : 4,4'-bipyridinium-1,1'-bis(trimethylenesulfonate)

TEA : triethylamine

TEOA : triethanolamine

TMSM : trimethylsilyl methacrylate

VPh : 9-vinylphenanthrene

VPy : 1-vinylpyrene

References

1) S. Nagakura Ed., "Enerugi henkan no kagaku", Iwanami, Tokyo, 1980.

2) A. Fujishima and K. Honda, Nature (London), 238, 27 (1972).

3) M. S. Wrighton, Acc. Chem. Res., 12, 303 (1979).

4) K. Shibata, Kagaku Sosetsu, 12, 45 (1976).

5) D. G. Whitten, Acc. Chem. Res., 13, 83 (1980).

6) R. A. Marcus, Ann. Rev. Phys. Chem., 15, 155 (1964).

7) K. Kalyanasundaram and M. Grätzel, Angew. Chem. Int. Ed. Engl., 18, 701 (1979).

8) T. Watanabe, T. Takizawa, and K. Honda, Shokubai, 20, 370 (1978).

9) K. Kalyanasundaram, Chem. Soc. Rev., 7, 453 (1978).

10) M. Grätzel, Acc. Chem. Res., 14, 376 (1981).

11) T. Matsuo, Pure Appl. Chem., 54, 1693 (1982).

12) N. Mataga, Hyomen, 16, 288 (1978).

13) Y. Tsutsui, K. Takuma, T. Nishijima, and T. Matsuo, Chem. Lett., 617 (1979).

14) Y. Moroi, A. M. Braun, and M. Grätzel, J. Am. Chem. Soc., 101, 567 (1979).

15) J. H. Fendler, Acc. Chem. Res., 13, 7 (1980).

16) M. Calvin, Photochem. Photobiol., 37, 349 (1983).

17) P. P. Infelta, M. Grätzel, and J. H. Fendler, J. Am. Chem. Soc., 102, 1479 (1980).

18) M. S. Tunuli and J. H. Fendler, J. Am. Chem. Soc., 103, 2507 (1981).

19) W. E. Ford, J. W. Otovos, and M. Calvin, Proc. Natl. Acad. Sci., USA, 76, 3590 (1979).

20) H. Morawetz, Acc. Chem. Res., 3, 354 (1970).

21) N. Ise, J. Polym. Sci., Polym. Symposium, 62, 205 (1978).

22) D. Meyerstein, J. Rabani, M. S. Matheson, D. Meisel, J. Phys. Chem., 82, 1879 (1978).

23) C. D. Jonah, M. S. Matheson, and D. Meisel, J. Phys. Chem., 83, 257 (1979).

24) R. E. Sassoon and J. Rabani, J. Phys. Chem., 84, 1319 (1980).

25) S. Tazuke, Yukigoseikagaku, 40, 806 (1982).

26) S. Tazuke, H. Tomono, N. Kitamura, K. Sato, and N. Hayashi, Chem. Lett., 95 (1979).

Chapter 1

Syntheses of Various Types of Amphiphilic Copolymers

1-1. Introduction

Photosensitized electron transfer reaction has been a subject of great interest because it may be a possible means of solar energy conversion and storage, and also be a simple model to simulate photosynthesis. A heterogeneous system, such as micelles and surfactant vesicles, offers several advantages over homogeneous solvent systems[1]. Through hydrophobic or electrostatic interaction different substrates (e.g., sensitizers, and electron donors and acceptors) can be held in the micro-heterogeneous phase. Also, charged interface provides a microscopic barrier for the prevention of undesirable back electron transfer to achieve the charge separation. In this context, amphiphilic polymers consisting of hydrophobic and electrolytic segments may also serve as promising media.

A number of amphiphilic polymers having a microphase-separated structure have been prepared for the purpose of various applications (e.g., biomedical materials[2]). However, syntheses of amphiphilic polymers consisting of strong electrolyte groups (e.g., $-SO_3^-$, $-NR_3^+$) and strong hydrophobic groups such as polycyclic aromatic compounds have been scarcely reported[3,4]. This chapter concerns with the syntheses of amphiphilic polymers used in this study. Amphiphilic copolymers of this type were prepared by radical and anionic copolymerizations.

1-2. Experimental

Monomers

2-Acrylamido-2-methylpropanesulfonic acid (AMPS) and N-(N',N'-dimethylaminopropyl)methacrylamide (DMAPMA) were provided by the courtesy of Nitto Chemical Industry Co. Ltd., and used without further purification.

9-Vinylphenanthrene (VPh) was prepared according to the method of Märkl[5] with some modifications: To a solution containing 4.13 g (20 mmol) of 9-phenanthrenecarboxyaldehyde[6] and 7.15 g (20 mmol) of triphenylmethylphosphonium bromide in 15 ml of methylene chloride, 50 % aqueous sodium hydroxide (10 ml) was added dropwise in 10 min with vigorous stirring at room temperature. The mixture was stirred for another 30 min. After the reaction, the organic layer was separated, washed with water, and dried over magnesium sulfate. Evaporation of methylene chloride left a yellow oil. The crude product was purified by passing through a silica-gel column (5 cmϕ x 30 cm) with n-hexane as eluent, and then recrystallized from n-hexane: mp 37-39 °C; yield 1.46 g (35 %).

1-Vinylpyrene (VPy) was prepared from 1-pyrenecarboxyaldehyde[7] and purified in the same way: mp 88-89 °C; yield 2.27 g (50 %).

Trimethylsilyl methacrylate (TMSM)[8] was synthesized as follows: To a stirred dispersion of 150 g (1.2 mol) of dried potassium methacrylate in 1 L of benzene was added 129 ml (1.0 mol) of trimethylchlorosilane in a 1 h at room

temperature and then the mixture was stirred for 48 h. After white crystals had been removed by filtration, the solvent was evaporated. The resulting monomer was purified by a fractional distillation through a 40-cm column containing Heli-Pak packing: bp 45 °C/20 mmHg; yield 27 %. The middle portion was divided into four or five storage ampoules which were directly sealed at the distillation setup under nitrogen. Absence of impurity was carefully checked and assured by GLPC using Apiezon as a liquid phase. The monomer was throughly dried immediately before use over CaH_2 and finally with a Na mirror by flash distillation on a vacuum line.

Styrene (St) and methacrylic acid (MA) were purified by distillation under reduced pressure.

Initiators

2,2'-Azobisisobutyronitrile (AIBN) was purified by recrystallization from methanol.

For the preparation of all initiators used for the anionic polymerization, the reagents and apparatus were manipulated on a high-vacuum line and the reactions were always carried out in an evacuated Pyrex flask to which the reagents were added by way of break-seals. After the reaction, the aliquots of the initiator solutions were passed through a sintered glass filter to remove the remaining solids and stored in a pencil-type Pyrex tube fitted with a break-seal at one end.

n-Butyllithium (n-BuLi) was commercially obtained as a

1.6 M solution in n-hexane. This solution was diluted to 8×10^{-2} M with dried n-hexane before use.

Tetrameric dianion of α-methylstyrene (α-MeSt) with Na^+ as a counterion was prepared according to the literature[9]; i.e., 0.52 ml (4×10^{-3} mol) of α-MeSt was allowed to react with a Na mirror in 19.5 ml of tetrahydrofuran (THF) at room temperature overnight and 2-ml aliquots of reddish-brown solution were stored.

1,1-Diphenyl-n-hexyllithium was prepared in the following way: To a 1.5 ml solution of n-BuLi (2.4×10^{-3} mol) in n-hexane was added 0.5 ml (2.5×10^{-3} mol) of highly dried 1,1-diphenylethylene in 15 ml of THF. The reaction flask was shaken occasionally at room temperature over a period of 2 h, and then the solution was divided into 0.72-ml aliquots.

Sodium biphenyl was prepared from 0.46 g (3×10^{-3} mol) of highly dried biphenyl treating with a Na mirror in 15 ml of THF at room temperature overnight and the 1-ml portions were stored.

A lithium biphenyl solution was prepared in the same way using about 1 g of lithium wire instead of the Na mirror.

Lithium naphthalene was prepared as follows: 0.38 g (3 mmol) of highly purified naphthalene was treated with 1 g (140 mmol) of lithium wire in 30 ml of THF with stirring at room temperature overnight. Aliquots of the initiator solution, varying in volume from 1 ml to 2 ml, were stored.

Syntheses of Polymers

Poly(styrene-co-2-acrylamido-2-methylpropanesulfonic acid) (ASt)

An ampoule containing 25 mmol of AMPS and St in a known ratio, 0.1 mol % of AIBN on the basis of monomers, and 10 ml of N,N-dimethylformamide (DMF) was evacuated at -78 °C and filled with nitrogen. This procedure was repeated five times and the ampoule was sealed under reduced pressure. Polymerizations were carried out in a thermostat at 60 °C. After the required time of polymerization the ampoule was opened and the contents, diluted with DMF, were poured into a large excess of ether with vigorous stirring to precipitate the polymer. All polymerizations were stopped at conversions below 15 %. The copolymers with a St fraction (f_s) lower than 0.72 were further purified by reprecipitation from methanol solution into an excess of ether. This was repeated three times. The polymers were dried, dissolved in pure water, dialyzed against pure water for 10 days, and finally recovered by freeze-drying. Copolymers with higher f_s were purified by reprecipitation five times from a DMF solution into a large excess of a mixture of ether and methanol (1:1,v/v) and dried. The copolymer compositions were determined by elemental analysis.

Poly(9-vinylphenanthrene-co-sodium 2-acrylamido-2-methylpropanesulfonate) (APh) and Poly(1-vinylpyrene-co-sodium 2-acrylamido-2-methylpropanesulfonate) (APy)

An ampoule containing AMPS and VPh (or VPy) in a known ratio (25 mmol in total), equimolar triethylamine (TEA) with

AMPS, 0.1 mol % (on the basis of total monomers) of AIBN, and 15 ml of THF was evacuated by five freeze-pump-thaw cycles and then sealed under vacuum. Polymerizations were carried out at 60 °C. After the specified period, the ampoule was opened and the content diluted with THF was poured into a large excess of hexane with vigorous stirring to precipitate the copolymer. The copolymer was further purified by precipitation from a THF solution into an excess of hexane. Copolymers with a VPh fraction (f_{Ph}) lower than 0.60 were water-soluble. These polymers were dissolved in dilute aqueous sodium hydroxide and the liberated TEA was removed by extraction with hexane several times. The polymer solution was dialyzed against pure water for 10 days, and finally the copolymers were recovered by freeze-drying. The copolymer compositions were determined by elemental analysis.

Poly(9-vinylphenanthrene-co-3-methacryloylaminopropyltrimethylammonium methylsulfate) (QPh)

Copolymerizations of VPh and DMAPMA were carried out as follows: An ampoule containing VPh and DMAPMA in a known ratio (20 mmol in total), 0.25 mol % (on the basis of total monomers) of AIBN, and 25 ml of THF was evacuated by five freeze-pump-thaw cycles and then sealed under vacuum. Polymerizations were carried out at 60 °C for 40 h. The ampoule was opened and the contents diluted with THF were poured into a large excess of hexane with vigorous stirring to precipitate the copolymers. The copolymer was further purified by precipitation from a THF solution into an excess of hexane. The total conversions for the copolymerizations with various VPh/DMAPMA ratios fell in

the range of 11-20 %. The copolymer compositions were determined by elemental analysis.

Quaternization of these polymers was carried out as follows: To a solution of 0.3 g of the copolymer in 5 ml of dimethylsulfoxide (DMSO) was added dimethyl sulfate in a 2.5 times excess of the molar quantity of the tertiary amino group in the copolymer. The reaction mixture was stirred at 30 °C for 3 days and then poured into an excess of acetone. The white product was isolated by filtration, washed with acetone, and dried in vacuo. In the 100-MHz ^{1}H NMR spectra of the quaternized copolymer (QPh), a characteristic sharp singlet peak at 3.16 ppm due to $-N^{+}(C\underline{H}_3)_3$ appeared in place of a 2.23-ppm peak due to $-N(C\underline{H}_3)_2$ in poly(VPh-co-DMAPMA), indicating quantitative quaternization. From the C/N and C/S ratios in microanalysis, quaternization was confirmed to be quantitative.

Poly(9-vinylphenanthrene-b-methacrylic acid) (b-VPh)

A solution of VPh in THF was prepared as follows: A known amount of VPh crystals varying from 2.0 to 8.8 mmol were placed in a glass ampoule fitted with a break seal and a sidearm tube containing 1 g of CaH_2 and dried on a high-vacuum line for a day. Further evacuation was carried out by melting the crystals by warming them up to about 50 °C for a few minutes until bubbling had ceased. This was followed by a flash distillation of THF (10 ml) into the ampoule, which was then sealed off.

Polymerizations were carried out in a four-necked 150-ml round-bottomed Pyrex flask to which the ampoules containing the

individual monomer solutions and an initiator solution had been connected (Figure 1). General procedures are as follows: The flask was evacuated on the high-vacuum line (ca. 10^{-5} mmHg) and throughly dried by flaming. After 10 ml of THF was flash distilled into the flask, it was sealed off at (a) and the whole body was cooled in a dry-ice/methanol bath. The initiator solution and the VPh solution were added into the flask in that order under vigorous agitation. The characteristic violet-brown color appeared and the solution viscosity increased. After 1 h, about 0.5 ml of the living polyVPh solution was forced into a sampling tube (B) by tilting the whole body and the tube was sealed off at (b) (this living polyVPh sample was terminated with aqueous THF and subjected to GPC analysis). TMSM solution was then added to the polymerization flask. The color rapidly disappeared and the solution became more viscous. Vigorous stirring was continued for 1 h at -78 °C. About 20 ml of aqueous methanol was added to terminate the polymerization and the polymer solution was allowed to stand overnight at room temperature to complete hydrolysis of the trimethylsilyl ester group and then poured into a large excess of ether to precipitate polymer. The resulting block copolymer was washed with methanol and with ether. The copolymer was further washed with benzene in a Soxhlet extractor overnight and washed with ether, and dried.

Poly(9-vinylphenanthrene-co-methacrylic acid) (MPh)

An ampoule containing 2.92 g (34 mmol) of MA, 1.24 g

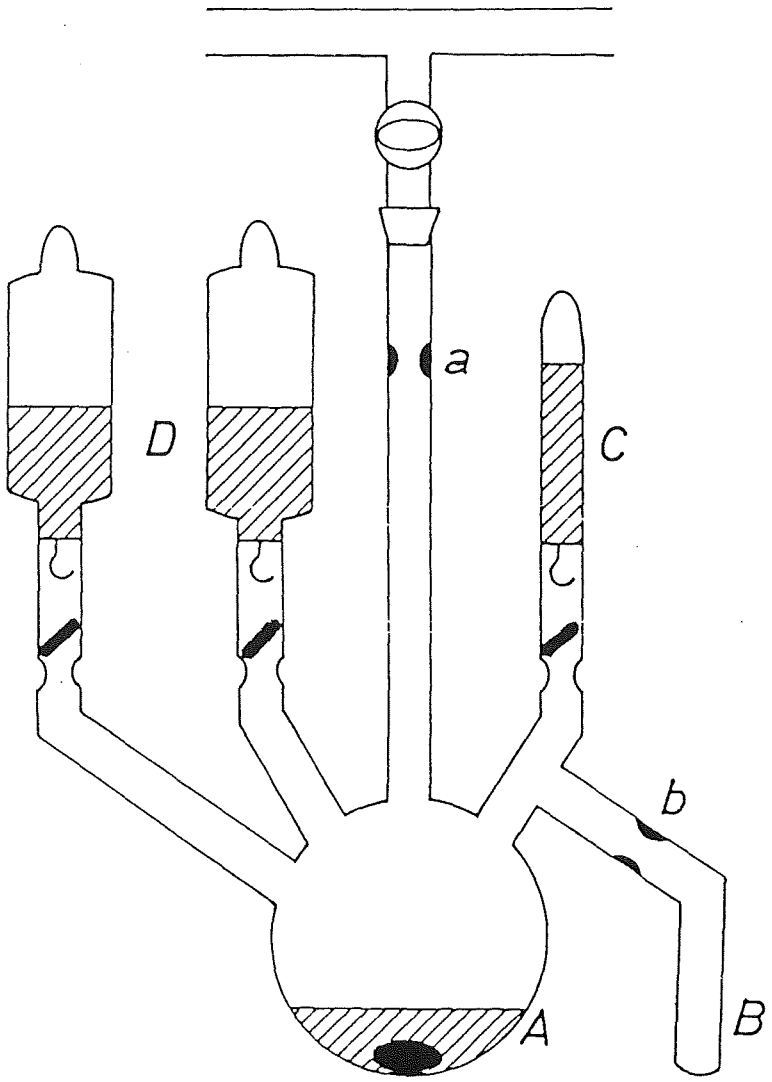

Figure 1. Block copolymerization apparatus.

(6 mmol) of VPh, 32.8 mg (0.2 mmol) of AIBN, and 20 ml of DMF was evacuated by several freeze-pump-thaw cycles and then sealed under vacuum. Polymerization was carried out at 60 °C for 38 h. The content was poured into a large excess of ether to precipitate the copolymer. The product was purified by reprecipitation from a DMF solution into an excess of ether three times and dried under vacuum at room temperature: yield 2.40 g (total conversion, 58 %). The content of VPh in the copolymer was calculated from UV absorption of the phenanthrene (Ph) residue to be 21 mol %.

Solvents and Reagents

THF used for anionic polymerization was dried with $LiAlH_4$, fractionally distilled onto Na wire, placed in a storage vessel connected with the vacuum line containing a Na block and benzophenone. Whenever necessary, a desired amount of solvent was flash distilled out of the storage vessel into a graduated ampoule and then into an ampoule with a Na mirror, successively.

Other reagents and solvents were purified, whenever necessary, in the usual way.

Measurements

GPC measurements for b-VPh were carried out with a Toyo Soda high-speed liquid chromatograph HLC-801A. THF was used as a solvent. Since the block copolymers are insoluble in THF, the MA sequences of these polymers were converted into

methyl methacrylate (MMA) sequences prior to the measurements according to the following procedure: To a suspension of about 50 mg of the block copolymer in 5 ml of benzene was added 20 ml of an ethereal solution of diazomethane (prepared according to the method of Arndt[10]). The mixture was allowed to stand overnight at room temperature and the solvents were replaced with THF to result in a clear solution of poly(VPh-b-MMA).

1-3. Results and Discussion

1-3-1. Syntheses of Copolymers of Aromatic Vinyl Compounds and 2-Acrylamido-2-methylpropanesulfonic Acid (ASt, APh, and APy)

In this section, the polymerizability of anionic electrolyte monomer, 2-acrylamido-2-methylpropanesulfonic acid (AMPS), was investigated. AMPS serves as a useful strong electrolyte monomer with balanced solubility in polar organic solvents and in water owing to its partial hydrophobicity, which allows one to perform copolymerization with hydrophobic comonomers in homogeneous organic solution.

First, styrene (St) was used as a hydrophobic comonomer simply because of its relatively straightforward nature in polymerizability, hydrophobic characteristics, and photochemistry.

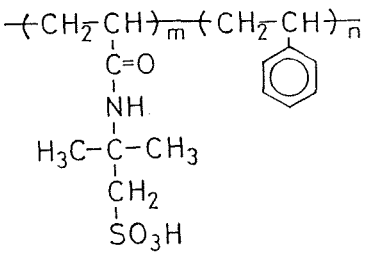

ASt

A copolymer composition curve for St (M_1) and AMPS (M_2) in DMF at 60 °C is exhibited in Figure 2. The monomer reactivity ratios were determined from the Fineman-Ross plot as follows:

$$r_1 = 1.13 \pm 0.10$$

$$r_2 = 0.31 \pm 0.06$$

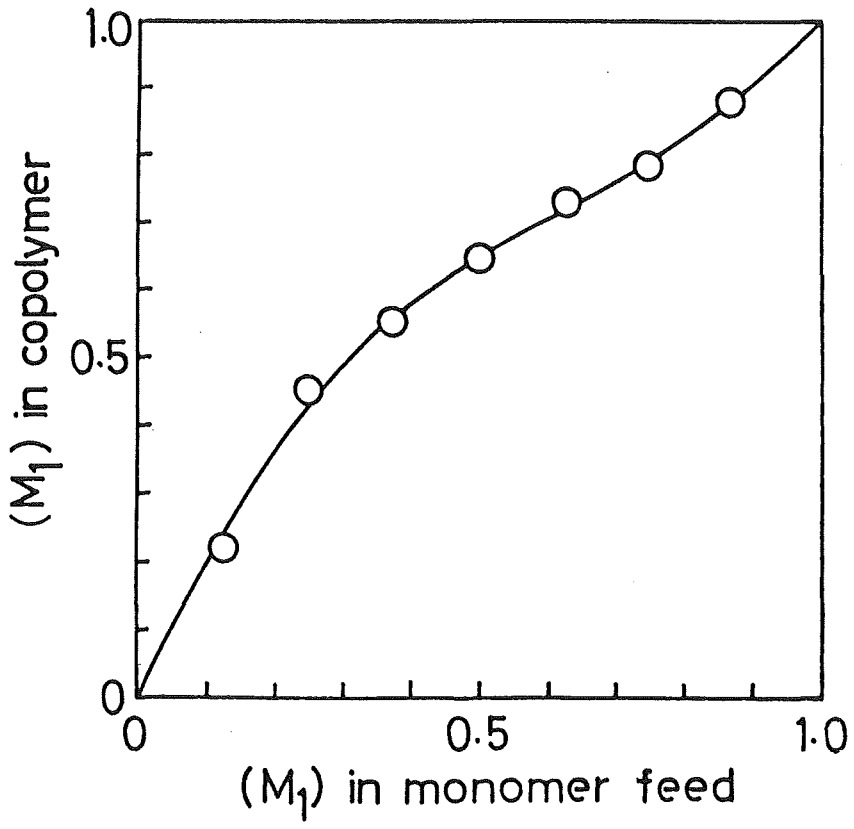

Figure 2. Copolymerization composition curve for St (M_1) and AMPS (M_2): $[M_1]+[M_2]$=25 mmol; DMF, 10 ml; AIBN, 0.1 mol% with respect to monomers; temp. 60 °C.

The values of Q = 0.39 and e = 0.22 were obtained for AMPS. It was found that AMPS has similar reactivity compared to that of acrylamide[11,12] in spite of a bulky and highly acidic substituent attached on the amide group. It should be noted that copolymers with St mole fraction (f_s) up to about 0.72 are soluble in water, which indicates that AMPS unit have remarkable solubilizing power for hydrophobic sequences placed along a polymer chain.

In the second step of the study, 9-vinylphenanthrene (VPh) and 1-vinylpyrene (VPy) were chosen as comonomers of AMPS. These monomers are more hydrophobic than St and the phenanthryl and pyrenyl groups would act as photosensitizers.

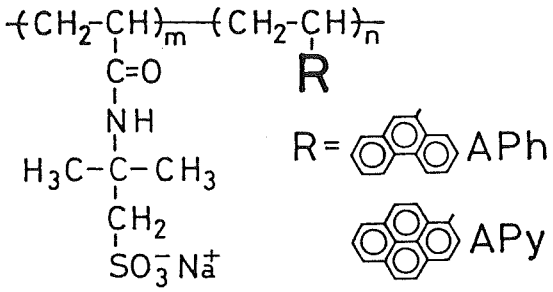

Copolymerization of AMPS and St was carried out in DMF. This solvent, however, could not be used for the copolymerizations in this case because of the lower solubilities of VPh, VPy, and the resulting copolymers. Instead, THF could conveniently be employed for the copolymerizations by using AMPS in a salt form with triethylamine (TEA), since its solubility in THF is highly improved as compared with the monomer in the acid form. The results of the copolymerization are summarized in Table I.

1-3-2. Synthesis of Copolymer of 9-Vinylphenanthrene and 3-Methacryloylaminopropyltrimethylammonium methylsulfate (QPh)

For comparison with an anionic amphiphilic copolymer (APh), the corresponding cationic copolymer was prepared by the radical copolymerization of VPh and N-(N',N'-dimethylaminopropyl)-methacrylamide (DMAPMA) followed by quaternization with dimethyl sulfate.

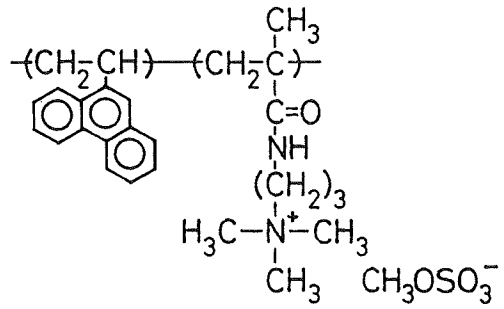

QPh

A copolymer composition curve for VPh (M_1) and DMAPMA (M_2) in THF at 60 °C is shown in Figure 3. The monomer reactivity ratios determined from the Fineman-Ross plot are as follows:

$$r_1 = 3.26 \pm 0.25$$

$$r_2 = 0.23 \pm 0.03$$

Quantitative quaternization of poly(VPh-co-DMAPMA) with dimethyl sulfate could be achieved in DMSO in which the reaction proceeded homogeneously throughout.

Table II lists the solubility characteristics of QPh with various VPh content in various polar solvents. It is noted that QPh with a VPh mole fraction (f_{Ph}) up to about 0.47 was found to be soluble in water and in methanol. In DMSO, copolymers with a wide range of f_{Ph} were soluble while in DMF those with f_{Ph} lower than 0.14 were insoluble.

The TEA salt of the sulfonic acid groups of copolymers was replaced by sodium salt because TEA was found to act as a quencher toward the photoexcited Ph and Py[13]. It was also confirmed that AMPS units have remarkable power to solubilize the hydrophobic units into water; i.e., the copolymers with mole fraction of VPh (f_{Ph}) up to about 0.60 and those with mole fraction of VPy (f_{Py}) up to about 0.35 were found to be soluble in water. These copolymers were also soluble in methanol, DMF, and DMSO, but not in the most of other organic solvents.

Table I. Radical copolymerization of AMPS and VPh or VPy[a)]

	Monomers			
Polymer	AMPS[b)] (mmol)	Comonomer (mmol)	Conversion (%)	Copolymer composition[c)]
APh-58	20.0	VPh 5.1	8.7	f_{Ph} 0.58
APh-32	22.5	2.5	10.6	0.32
APh-15	23.8	1.3	13.8	0.15
APh- 8	24.4	1.0	23.6	0.08
APh- 3	24.8	0.4	47.9	0.03
APy-32	23.8	VPy 1.3	7.7	f_{Py} 0.32
APy-16	24.4	0.6	6.2	0.16
APy-0.6	24.8	0.2	5.6	0.006[d)]

a) Initiator, AIBN 0.1 mol% based on total monomers; solvent, THF 15 ml; temperature, 60 °C.
b) Used as TEA salt.
c) Mole fraction of VPh or VPy in the copolymer.
d) Determined by UV spectra.

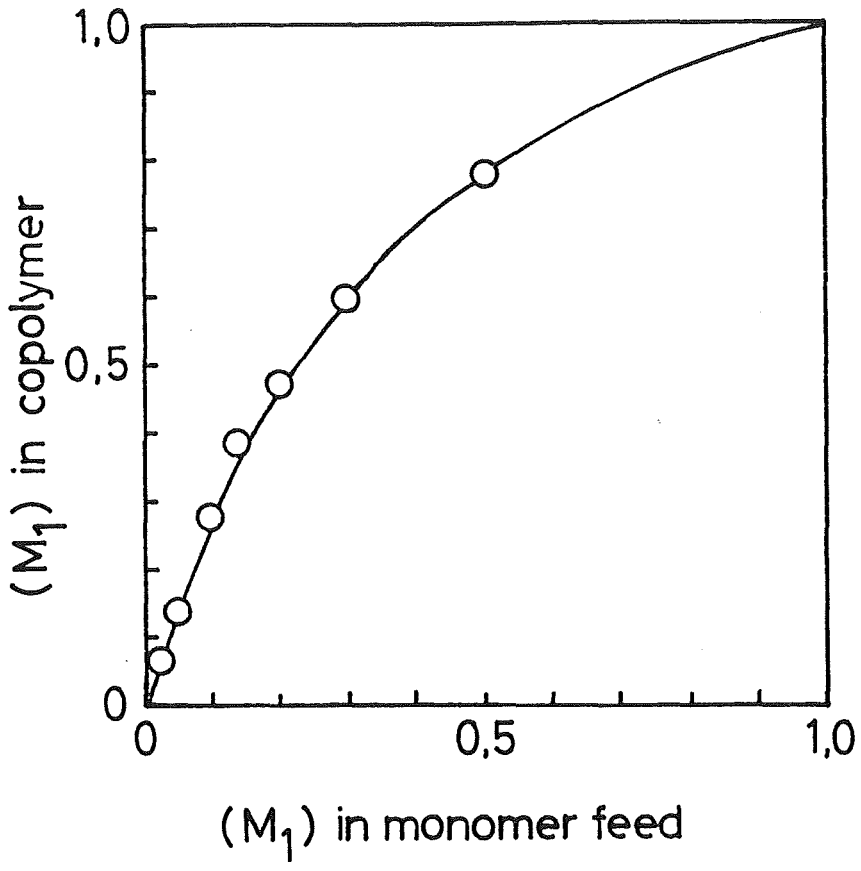

Figure 3. Copolymerization composition curve for VPh (M_1) and DMAPMA (M_2): $[M_1]+[M_2]$=20 mmol; THF, 25 ml; AIBN, 0.25 mol% with respect to monomers; temp. 60 °C.

Table II. Solubility of QPh

Polymer	f_{Ph}	solvent[a)]			
		water	MeOH	DMSO	DMF
QPh-78	0.78	I	I	S	S
QPh-60	0.60	I	I	S	S
QPh-47	0.47	S	S	S	S
QPh-39	0.39	S	S	S	S
QPh-28	0.28	S	S	S	S
QPh-14	0.14	S	S	S	I
QPh- 7	0.07	S	S	S	I

a) S, soluble; I, insoluble

1-3-3. Synthesis of Block Copolymer of 9-Vinylphenanthrene and Methacrylic Acid (b-VPh)

In the previous sections, various types of water-soluble amphiphilic polymers were prepared by radical copolymerization of aromatic vinyl monomers and electrolyte monomers. These studies are now extended to block copolymers, which frequently exhibit much clearer phase separation in the "selective" solvent than do random copolymers. Block copolymers in such a solvent consist of aggregates of poorly soluble blocks of one monomer and a dispersed phase of soluble blocks of another monomer unit.

The anionic polymerization is in fact the best technique by which well-defined block copolymers essentially free from contaminating homopolymers can be synthesized. A disadvantage of this technique, however, is that none of the electrolyte monomers can directly be employed as such. Trimethylsilyl-

methacrylate (TMSM) proved to be one of the best candidates to overcome this disadvantage because of its susceptibility to the living anionic polymerization and the ease of the hydrolysis of the trimethylsilyl ester group to yield methacrylic acid sequences[14].

Thus, block copolymers consisting of methacrylic acid (MA) and VPh were synthesized by a two-step process of the living anionic polymerization of VPh and TMSM followed by hydrolysis of the trimethylsilyl ester groups.

The preparation of the block copolymers are shown in Scheme I. The TMSM sequences are quantitatively converted into the MA sequences under mild conditions[14] (aqueous methanol at room temperature). In view of the fact that that the range of monomers susceptible to the anionic polymerization is limited, TMSM is indeed an useful monomer with which one can obtain polyelectrolyte sequence by the anionic polymerization. An important feature of the anionic polymerization, with respect to the synthesis of block copolymers, is the absence of the termination reaction under appropriate conditions. During the course of the present study, however, we have realized that the complete prevention of premature termination in the anionic polymerization of TMSM could only be achieved under limited conditions. Since the monomer is extremely susceptible to hydrolysis even on exposure to the ambient air, the final purification was found to have a vital effect on the conversion

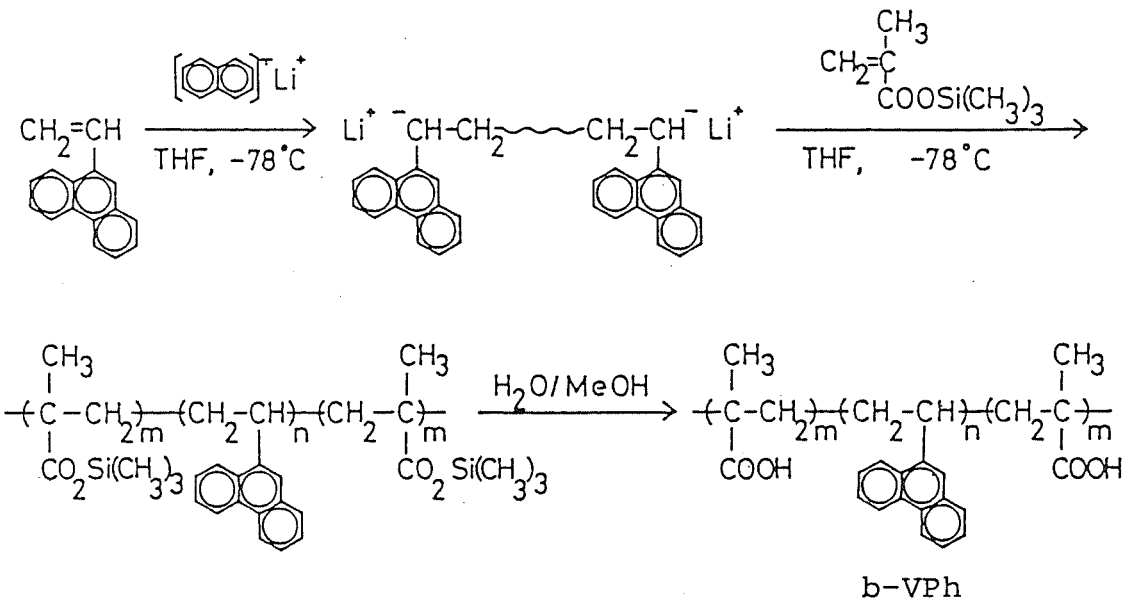

Scheme I

of this monomer. Besides, we have found that during the anionic polymerization the counterion has a remarkable effect on conversion. Therefore, prior to the syntheses of the block copolymers, we investigated the homopolymerization of TMSM in THF employing various anionic initiators; the results are presented in Table III. With Li^+ as a counterion, quantitative conversion was achieved, whereas with Na^+ the polymerization was prematurely terminated. To corroborate these observations, anionic polymerizations of TMSM were initiated by polystyryl living anions with different counterions. As obviously seen in Table IV, the conversion of TMSM was again quantitative

Table III. Anionic polymerization of TMSM by various initiators[a)]

Initiator	Polymerization time (hr)[b)]	Conversion (%)
n-BuLi[c)]	1	100
$(\alpha\text{-MeSt})_4^{2-}\,2Na^+$[d)]	3	13
$n\text{-}C_5H_{11}\text{-}\overset{\phi}{\underset{\phi}{C}}^-Li^+$[e)]	1	100
$Na^+\,^-\overset{\phi}{\underset{\phi}{C}}CH_2\text{-}(\alpha\text{-MeSt})_4\text{-}CH_2\overset{\phi}{\underset{\phi}{C}}^-Na^+$[f)]	2	16

a) TMSM 2×10^{-2} mol/THF 20 ml.
b) Under cooling in dry-ice/MeOH bath.
c) 1×10^{-4} mol/n-hexane 1.25 ml.
d) α-MeSt tetramer 1×10^{-4} mol/THF 2.0 ml.
e) 1,1-Diphenylhexyl lithium 1×10^{-4} mol/THF 0.7 ml.
f) 1×10^{-4} mol/THF 2.0 ml.

for Li^+ as a counterion, whereas with Na^+ the propagation reaction seems to compete unfavorably with side reactions.

In general, anionic polymerizations of methacrylates and acrylates are not as straightforward as those of hydrocarbon monomers because the polar ester groups cause numerous side reactions such as the solvation of the counterion[15,19] and the nucleophilic attack of carbanions onto the ester carbonyl group[16-19]. Recently Schulz and co-workers[19] reported that intramolecular termination by back-biting, in which growing carbanions attack the antepenultimate ester carbonyl groups in the nucleophilic way, is a predominant side reaction in the anionic polymerization of methacrylate (MMA) in THF with Na^+ as a counterion. They suggested that if the

Table IV. Anionic polymerization of TMSM initiated by polystyryl living anion[a)]

Preparation of living PSt[b)]		Polymerization time (hr)[c)]	Conversion of TMSM(%)[d)]
Initiator	mol /solvent (ml)		
n-BuLi	$1x10^{-4}$/n-hexane (1.25)	1.5	100
$(\alpha\text{-MeSt})_4^{2-}$ $2Na^+$	$1x10^{-4}$/ THF (2.0)	1	17
Biphenyl$^-Na^+$	$2x10^{-4}$/ THF (1.0)	1.5	8
Biphenyl$^-Li^+$	$2x10^{-4}$/ THF (1.0)	1.5	100

a) TMSM $2x10^{-2}$ mol/THF 20 ml.
b) St $1x10^{-2}$ mol/THF 20 ml.
c) Under cooling in dry-ice/MeOH bath.
d) Calculated on the assumption that the conversion of St is 100 %.

counterion in an ion pair is solvated by the antepenultimate ester group, then the conformation strongly favors the carbanion attack of the respective ester group. Their suggestion seems to be particularly useful at the present stage of our study to help us interpret the observations about the effect of the counterion presented in Tables III and IV, although further investigations are needed before we can draw any conclusion. In the case of TMSM, the intramolecular backbiting seems likewise to be possible because trimethylsilyl groups, in spite of their bulkiness, would not hinder the conformation favorable to the backbiting:

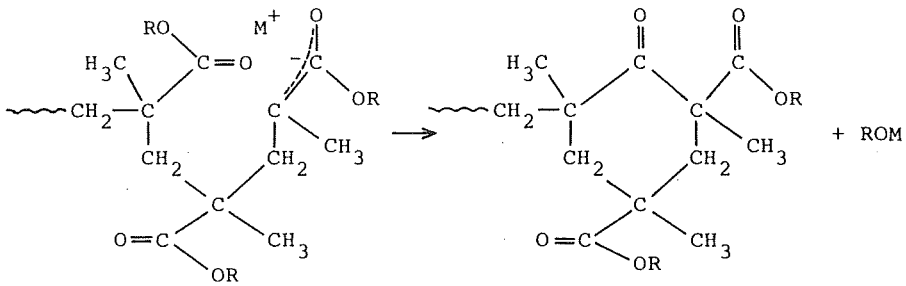

$R = Si(CH_3)_3$

In general, living anion pairs with Li^+ as a counterion in THF are more dissociable than those with Na^+, and thus an increased fraction of free ions leads to an increase of the propagation rate[20]. If these considerations are taken for granted, it follows that the highly solvated Li^+ would favor the propagation process over the backbiting termination for which the counterion may have to be partially solvated by the antepenultimate ester carbonyl group in the ion pair[19]. The other possibility could be competition between the propagation

and the "killing" process possibly caused by impurities that may have not been completely removed despite the efforts taken in purification. The enhanced rate of propagation achieved with Li^+ as a counterion may well predominate over the killing reaction to some extent.

Consequently, we have decided to use lithium naphthalene as an initiator for the block copolymerization. The results of the block copolymerization of VPh and TMSM are listed in Table V. It may be reasonable to assume, on the basis of the initiation mechanism of St in the presence of the naphthalene radical anion[21], that the anionic polymerization of VPh proceeds through a dicarbanionic chain, which would lead to an ABA triblock[22]. However, the block copolymer is most likely a mixture of di- and triblocks, because premature termination to a certain extent is not avoidable. Before TMSM, the second monomer, was added, a portion of the living PVPh was sampled out and subjected to GPC analysis (Figure 4 (a)). The degree of polymerization of the VPh sequences estimated from GPC was found to be much smaller than that expected from the monomer/ initiator ratio on assumption of a dicarbanionic propagation as presented in Table V. The titration of the initiator solution revealed the apparent concentration of the initiator to be 2,3 times higher than the calculated value, implying the presence of lithium metal contaminating the initiator solution. It can be speculated that the lithium metal reacts with the Ph groups of the monomer and/or polymer to generate phenanthryl radical anions which also participate in the initiation

Table V. Anionic block copolymerization of VPh and TMSM by lithium naphthalene in THF[a)]

Copolymer	Initiator[b)] (10^{-4} mol)	VPh (mmol)	TMSM (10^{-2} mol)	Total conversion (%)	$\overline{DP}_{VPh}$[c)] calc.[d)]	$\overline{DP}_{VPh}$[c)] obs.[e)]
b-VPh-43	1.0	8.8	1.0	100	176	43
b-VPh-23	1.0	5.0	1.0	100	100	23
b-VPh-16	2.0	5.0	2.0	97	50	16
b-VPh- 7	2.0	2.0	2.0	100	20	7

a) Polymerization was carried out under cooling in a dry-ice/methanol bath for 1 h each for VPh and TMSM.

b) Calculated amount of naphthalene radical anion, assuming naphthalene is quantitatively converted into the radical anion.

c) Degree of polymerization of the VPh sequence.

d) Calculated from ([VPh]/[Initiator])x2 on the assumption of a dicarbanionic propagation.

e) Determined by GPC of PVPh sampled out of the living solution before adding TMSM.

process. This could be responsible for the lower degree of polymerization than anticipated.

Figure 4 shows the GPC elution curves for the polymers before and after the second monomer was added. Since the block copolymers are not soluble in THF (solvent for GPC) the carboxylic acid groups were converted into methyl ester groups prior to GPC analysis. A large increase in molecular weight occurred on addition of TMSM to the living PVPh, which evidently indicates the formation of block copolymers. Extraction of the resulting block copolymers with benzene separated contaminating homo-PVPh in the amount of only 1-2 wt % of the total polymer. Therefore, a shoulder peak appearing in GPC of the block copolymer in the lower molecular weight region is not associated with remaining homo-PVPh but may be ascribable to the block copolymers with short MA sequences formed by premature termination. Extraction of the homo-poly(MA) with cold water, on the other hand, turned out to be unsuccessful, because a large amount of the block copolymer was also found in the extract.

The copolymer compositions were determined by NMR spectra (Table VI). The degree of polymerizations of VPh block sequences was estimated by GPC of the VPh living polymer sampled out during the synthetic process immediately before the second monomer was added. The copolymer compositions were also calculated on the basis of the degree of polymerization of the VPh sequence and that of the block copolymer estimated by GPC. The MA/VPh mole ratios thus estimated are not much different

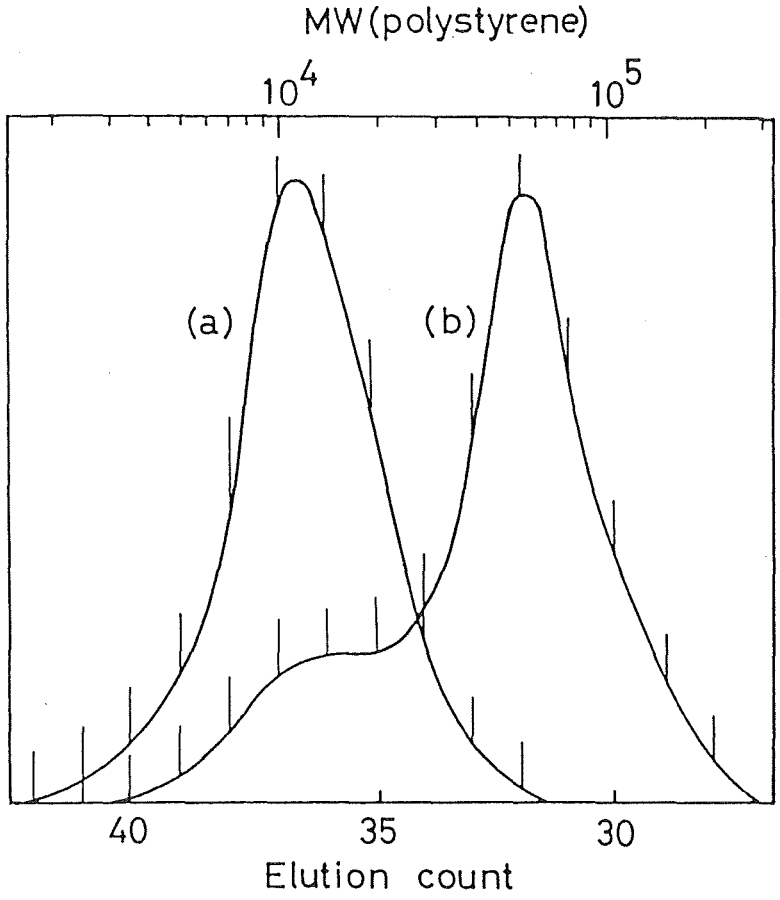

Figure 4. GPC elution curves of the VPh sequence (a) and the block copolymer (b-VPh-43, cf. Table V) after homo-PVPh was extracted with benzene (b): The methacrylic acid groups in the block copolymer were converted into methyl methacrylate groups; 1 elution count, 1.7 ml.

from those determined by NMR, indicating that the chain length of these block copolymers estimated by GPC is not far from reality. Table VI also contains the degree of polymerization of each block sequences calculated on the assumption that the block copolymers are ABA triblocks.

Table VI. Degree of polymerization and composition of the block copolymer

Block copolymer	$\overline{DP}_{MA}$-$\overline{DP}_{VPh}$-$\overline{DP}_{MA}$ [a]	Composition (MA/VPh) [b]	
		NMR	GPC
b-VPh-43	77-43-77 [c]	3.6	2.3
b-VPh-23	54-23-54 [c]	4.7	3.5
b-VPh-16	53-16-53 [c]	6.6	9.0
b-VPh- 7	23- 7-23 [d]	—	6.6

a) $\overline{DP}$ of each block sequence estimated on the assumption of ABA triblock.
b) Mole ratio.
c) Calculated from the GPC of VPh living polymer and the MA/VPh ratio determined by NMR.
d) Calculated from the GPC of VPh living polymer and the methyl ester of the block copolymer.

1-4. Conclusion

We prepared amphiphilic polymers consisting of aromatic and electrolyte segments. Anionic copolymers were prepared by the radical copolymerization of AMPS and aromatic vinyl compounds. Copolymers with a wide range of mole fraction of hydrophobic groups were found to be soluble in water. Cationic copolymers were prepared by the radical copolymerization of VPh and DMAPMA followed by quaternization with dimethyl sulfate. Amphiphilic block copolymers consisting of MA and VPh were prepared by a two-step process of living anionic polymerization of VPh and TMSM followed by hydrolysis of the trimethylsilyl groups.

References

1) P. P. Infelta, M. Grätzel, and J. H. Fendler, J. Am. Chem. Soc., 102, 1479 (1980) and references cited therein.

2) Y. Imanishi, K. Takakura, H. Tanzawa Ed., "Biomedical Polymer", Kagaku-zokan, 84, Kagaku-Dojin, Kyoto (1980).

3) S. Tazuke and Y. Suzuki, J. Polym. Sci., Polym. Lett. Ed., 16, 223 (1978).

4) Y. Suzuki and S. Tazuke, Macromolecules, 13, 25 (1980).

5) G. Märkl and A. Merz, Synthesis, 295 (1973).

6) C. A. Dornfeld and G. H. Coleman, "Organic Syntheses" Collective Vol. III, John Wiley and Sons Inc., New York, 1955, p701.

7) K. Tanikawa, T. Ishizuka, K. Suzuki, S. Kusabayashi, and H. Mikawa, Bull. Chem. Soc. Jpn., 41, 2719 (1968).

8) D. N. Andrew and E. V. Kukhurskaya, Zh. Obsch. Khim., 30, 2782 (1960); Chem. Abstr., 55, 15332 (1962).

9) C. L. Lee, J. Smid, and M. Szwarc, J. Phys. Chem., 66, 904 (1962).

10) F. Arndt, "Organic Syntheses" Collective Vol. II, John Wiley and Sons Inc., New York, 1943, p165.

11) A. Leoni and S. Franco, Macromolecules, 4, 355 (1971).

12) G. Saini, A. Leoni, and S. Franco, Makromol. Chem., 144, 235 (1971).

13) R. H. Young and R. L. Martin, J. Am. Chem. Soc., 94, 5183 (1972).

14) M. Kamachi, M. Kurihara, and J. K. Stille, Macromolecules,

5, 161 (1972).

15) W. Fowells, C. Schverch, F. A. Bovey, and F. P. Hood, J. Am. Chem. Soc., 89, 1396 (1967).

16) G. Lohr, A. H. E. Muller, V. Warzelhan, and G. V. Schulz, Makromol. Chem., 175, 497 (1974).

17) L. Lochmann, M. Rodova, J. Petranek, and P. Lim, J. Polym. Sci., A-1, 12, 2295 (1974).

18) J. Trekoval and P. Kratochvil, J. Polym. Sci., A-1, 10, 1391 (1972).

19) V. Warzelhan, H. Hocker, and G. V. Schulz, Makromol. Chem., 179, 2221 (1978).

20) D. N. Bhattacharyya, C. L. Lee, J. Smid, and M. Szwarc, J. Phys. Chem., 69, 612 (1965).

21) M. Szwarc, "Carbanions, Living Polymers, and Electron-Transfer Processes", Interscience, New York, 1968, chap. VI.

22) J. J. O'Malley, J. F. Yanus, and J. M. Pearson, Macromolecules, 5, 158 (1972).

Chapter 2

Behaviors of Amphiphilic Copolymers in Aqueous Solutions

2-1. Introduction

Polyelectrolytes carrying hydrophobic residues are known to form "polysoaps" in aqueous solution, which can provide the structural characteristics of both polyelectrolyte and micelles[1]. We have been interested in amphiphilic polymers of this type as media for light-induced electron transfer reactions in aqueous systems.

In Chapter 1, we described the syntheses of amphiphilic copolymers consisting of aromatic and electrolyte segments. This chapter concerns with the solution properties of these copolymers. In aqueous solution these polymers exhibit characteristic behavior in common; i.e., the formation of hydrophobic microdomains. Properties of these microdomains were also investigated.

2-2. Experimental

Materials

Syntheses of amphiphilic copolymers are described in Chapter 1.

Sodium 8-anilino-1-naphthalenesulfonate (ANS), 1,6-diphenyl-1,3,5-hexatriene (DHT), and 5,5'-diphenyl-3,3'-diethylbenzoxazolecarbocyanine nitrate (CyD) were obtained from Tokyo Kasei Ind. Co., Wako Pure Chemical Ind. Co., and Nippon Kanko-Shikiso Kenkyusho, respectively, and used without further purification.

Measurements

The reduced viscosities of the aqueous solutions of ASt were measured at 30 °C in a modified Ubbelohde viscometer. Ionic strength was adjusted by adding a known amount of KCl to the solutions.

The NMR spectra of ASt were measured on 7-wt % solutions in DMSO-d_6 and D_2O at room temperature by using a Varian T-60 Spectrometer. Special care was paid to maintain constant measuring conditions for all samples.

Fluorescence spectra were recorded on a Union FS-401 Spectrofluorometer or a Shimadzu RF-502A Spectrofluorometer at room temperature.

Electron micrographs were taken with a Hitachi Model HU-11DS at 100 kV as follows: (I) In the case of ASt, a few drops of a 2 % aqueous uranyl acetate solution were added to

0.5 ml of a 0.2 % aqueous polymer solution and the stained solution was applied to a 400-mesh copper grid covered with a carbon-coated collodion film, and air-dried. Thus prepared specimen was observed at the direct magnification of 6×10^4; (II) In the case of b-VPh, after casting the polymer solution on a copper grid, it was stained by applying a drop of 2-wt % aqueous uranyl acetate. The specimen was observed at the direct magnification of 5×10^4.

2-3. Results and Discussion

2-3-1. Solution Properties of ASt

We prepared water-soluble copolymers of St and AMPS (ASt) with a wide range of f_s as described in Chapter 1. In this section, the behaviors of these copolymers in aqueous solutions were investigated in detail.

Viscosity

Figure 1 shows the plots of the reduced viscosities of ASt with various compositions against the concentration of the copolymer in salt-free aqueous solution. An AMPS homopolymer and the copolymers with small St contents exhibited negative slopes of the reduced viscosity plots, reflecting a typical tendency of polyions to expand on dilution due to an increase in the mutual electrostatic repulsion. With increasing St content, however, the negative slope tends to turn into a slightly positive one combined with marked decrease in the reduced viscosities. This fact suggests that the mutual Coulombic repulsion is competing with attracting hydrophobic interaction between the St units along a polymer chain, and as a result the expansion of the chain is limited at balance. The hydrophobic association is well envisaged by the effect of ionic strength on the reduced viscosity. An increase in ionic strength would lead to a decrease of mutual Coulombic repulsion as well as an enhancement of hydrophobic interaction.

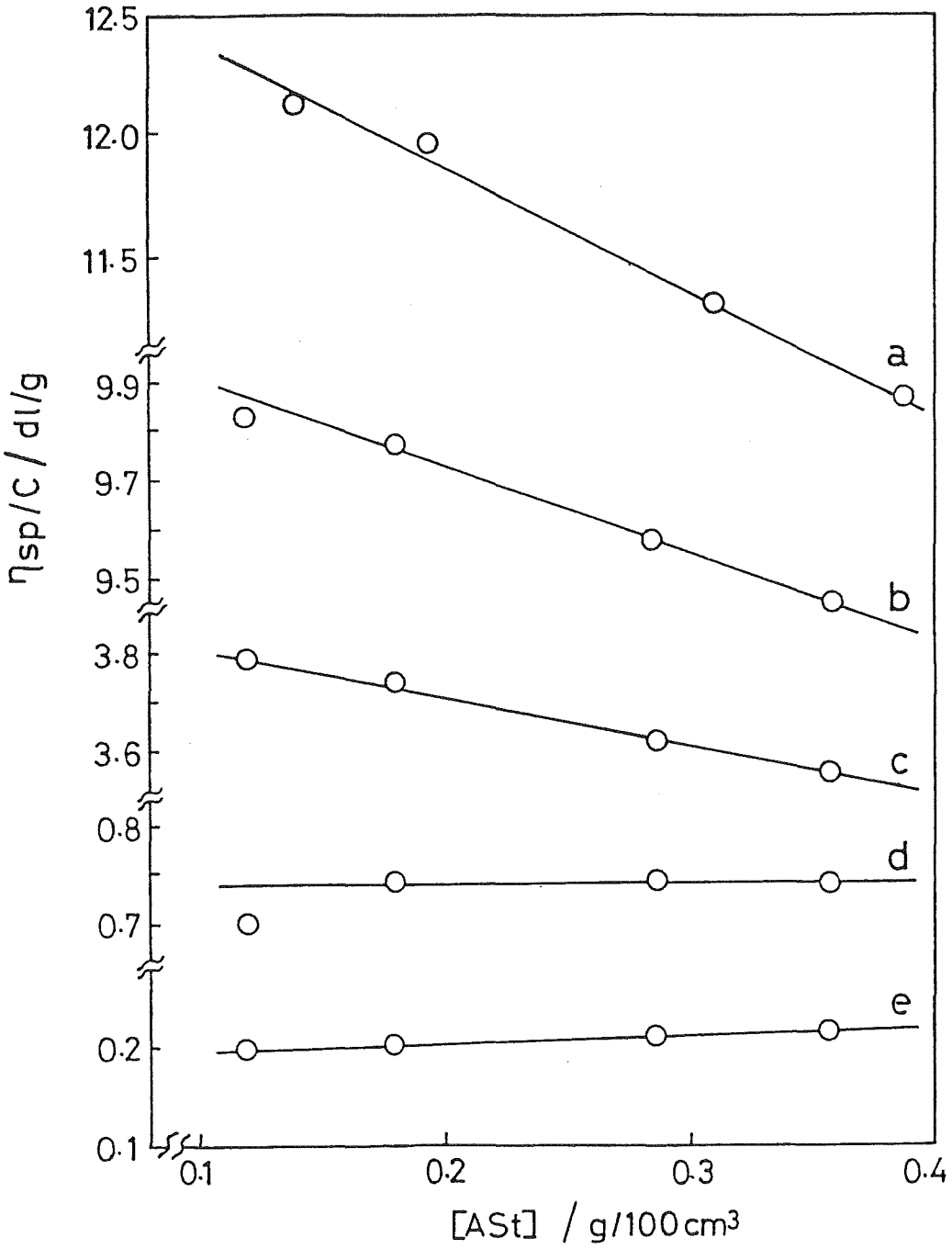

Figure 1. Reduced viscosity (η_{sp}/C) of ASt with various f_s in pure water at 30 °C: (a) f_s=0, (b) 0.46, (c) 0.54, (d) 0.64, (e) 0.72.

In Figure 2, the ratios of the reduced viscosities at the ionic strength of zero and 0.69 are plotted against St content of the copolymers. When a simple salt KCl was added to the aqueous solution of AMPS homopolymer, a marked salt-effect ($\eta/\eta \sim 8$) was observed, where reduced viscosity of the solution considerably decreased because of the shrinkage of the polymer molecules. It is interesting to note that a noticeable increase in salt-effect was observed with increasing St content, passing through a maximum at $f_s \simeq 0.55$ (Figure 2).
This tendency can be interpreted by taking into account the extra shrinkage of the copolymer resulting from enhanced hydrophobic association of styryl groups in addition to decreased mutual Coulombic repulsion caused by adding a salt to the aqueous solution. The copolymers with very high f_s, on the contrary, exhibited little salt-effect on the viscosities, which strongly suggests pronounced shrinkage of the polymer molecules due to preexisting hydrophobic association of styryl groups even under salt-free conditions. In this situation the extensive hydrophobic bonding among the styryl groups along the macromolecular chain could prevail over the electrostatic mutual repulsion of electrolyte groups of the polyions, which results in a compact random coil polymer conformation even in a salt-free solution.

^{1}H NMR Spectra

In the NMR spectra of polystyrene in CCl_4 the absorption due to the phenyl protons is split into two bands with

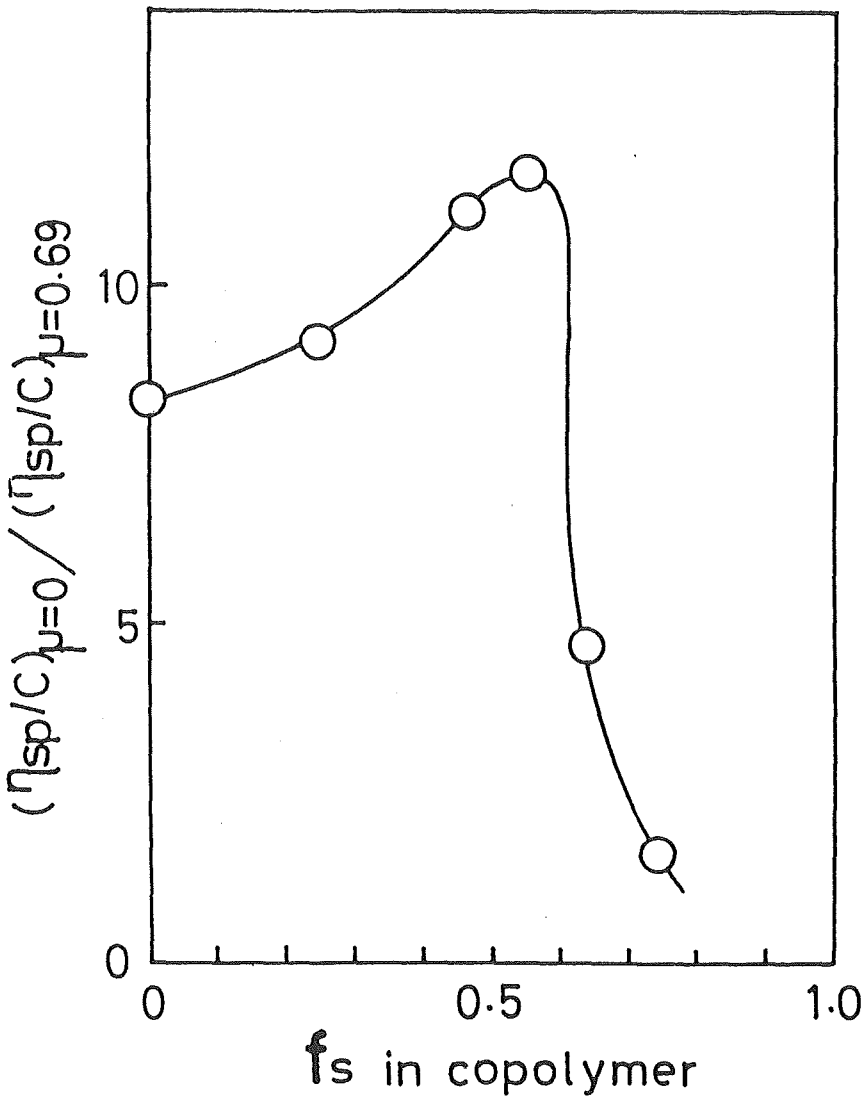

Figure 2. Effect of ionic strength on reduced viscosity vs. f_s.

intensities lying in the ratio of 3:2[2]. The upfield band is assigned to the shifted ortho-protons of the phenyl residues as a result of diamagnetic shielding by the π-electron systems of other aromatic residues of the chain[2]. It has been known that such shielding is sensitive to the sequence length of the St units in a copolymer and that at least four St units in a sequence are necessary for the split to occur[3,4]. These facts may allow a rough estimation of styryl sequence length in a copolymer. In Figure 3 the NMR spectra of the phenyl protons for ASt with various St contents are illustrated. All spectra were obtained from solutions with constant polymer concentration under constant measuring conditions. In DMSO-d_6 the intensity of the 7.2 ppm (from TMS) peak increases with increasing f_s in the copolymer. The 6.8 ppm peak due to the ortho-protons begins to show up at f_s = 0.55 and eventually a well separated peak clearly appears at f_s = 0.72. These facts suggest that the St residues distribute at random in the region of low f_s, whereas they do in blocks to some extent in the copolymers with high f_s. From a rough estimation of the peak ratio of the NMR spectra of ASt-72 (ASt with f_s = 0.72), it may be said that more than half of the St residues in this polymer are in block sequences with more than four monomeric units.

Conspicuous phenomena were observed on the NMR spectra obtained in D_2O solutions. As seen in Figure 3, the peak intensity due to the phenyl protons increases normally with the increase in the St fraction up to f_s = 0.46. However, it conversely decreases as the f_s increases beyond 0.55, and

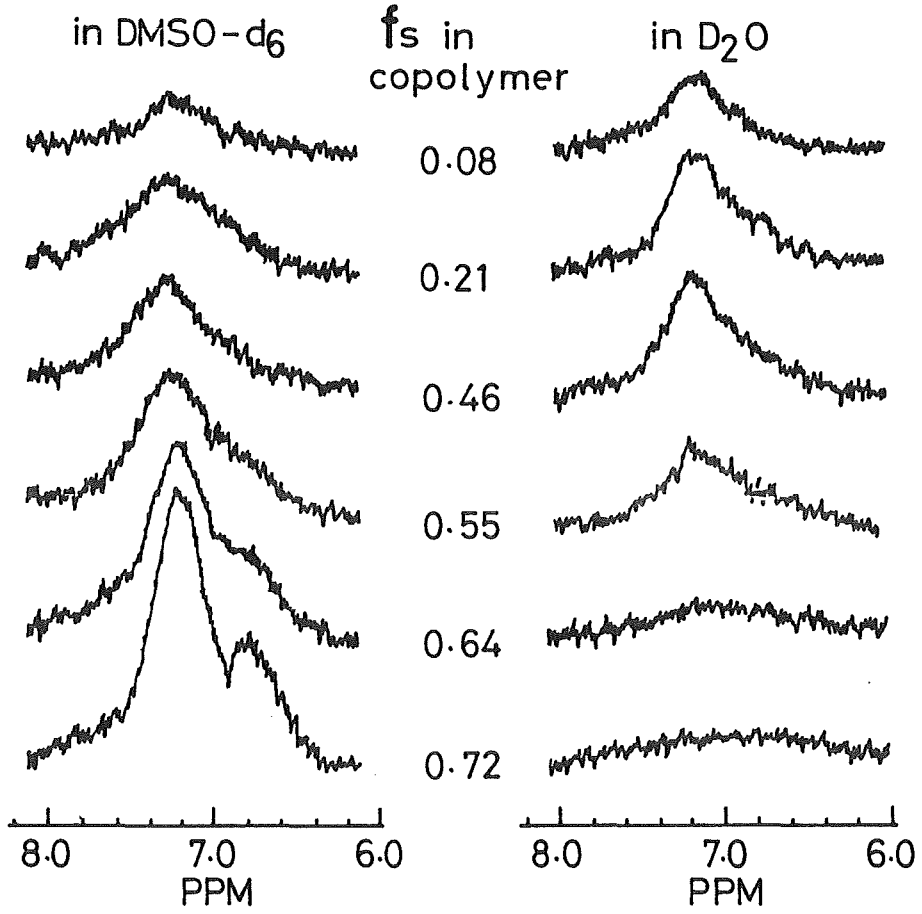

Figure 3. ^{1}H NMR spectra of ASt with various f_s in DMSO-d_6 and in D_2O: 7-wt% solution, at room temperature.

eventually it completely disappears at $f_s = 0.72$. This remarkable broadening effect stems obviously from the rigid structures where segmental motion of styryl groups is highly restricted as a result of pronounced extent of packing of styryl residues owing to hydrophobic association.

Fluorescence Spectra

The highly progressive hydrophobic association can also be evidenced by fluorescence emission spectra from styryl residues. The fluorescence of ASt shows an excimer emission at 325 nm besides a characteristic monomer emission at 285 nm. Figure 4 exhibits the facts that the intensity of excimer emission increases with the increase of St content in the copolymer, whereas that of monomer emission decreases with an isoemission point at 305 nm, and eventually the excimer emission predominates over the monomer emission at $f_s = 0.72$. An addition of alcohol that disrupts the iceberg structure of water is known to reduce hydrophobic interaction. In fact, Figure 5 shows that methanol has an effect to minimize the excimer emission. These facts are also in strong support of the contribution of hydrophobic association.

Uptake of Hydrophobic Fluorescent Probes

For a better clarification of the hydrophobic uptake of small molecules by the copolymers, where an additional complication is introduced by the concomitant electrostatic interactions, the following set of hydrophobic fluorescent probes with a negative or positive charge or without charge

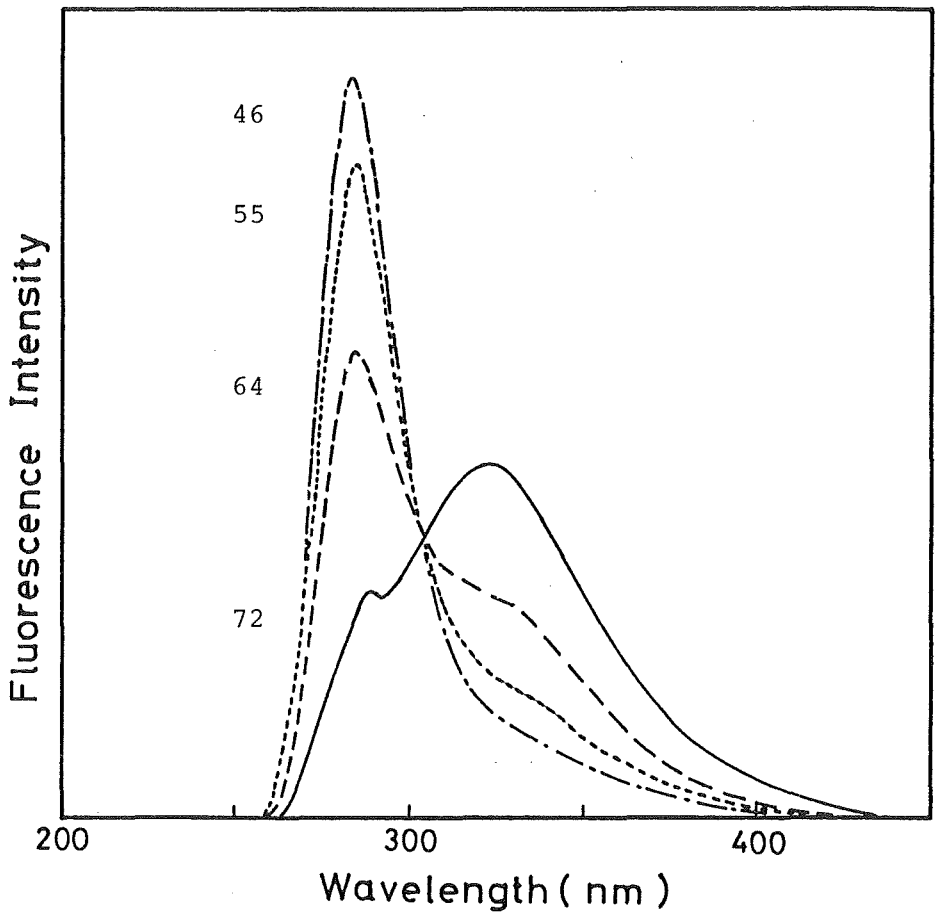

Figure 4. Fluorescence spectra of ASt with various f_s in pure water: $[St]_{residue}=5x10^{-3}$ M; excitation wavelength, 260 nm; ———, ASt-72; – – – –, ASt-64; -·-·-·-·-, ASt-55; —·—·—, ASt-46.

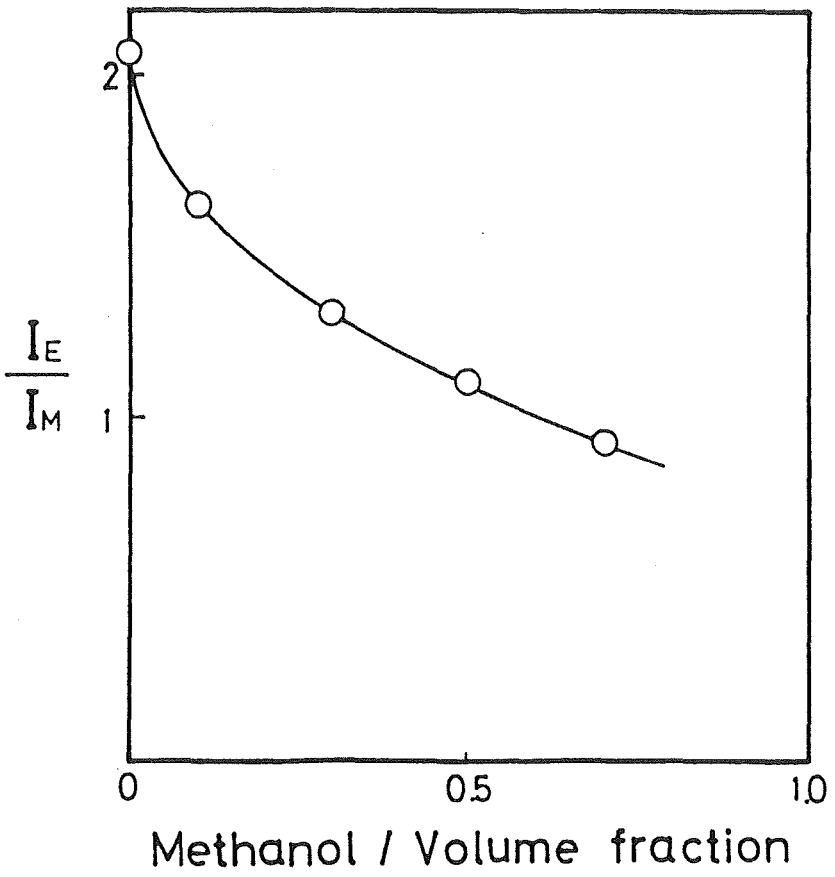

Figure 5. Excimer-to-monomer fluorescence intensity ratio (I_E/I_M) vs. volume fraction of methanol in the mixture of water and methanol for ASt-72.

was used in the present study:

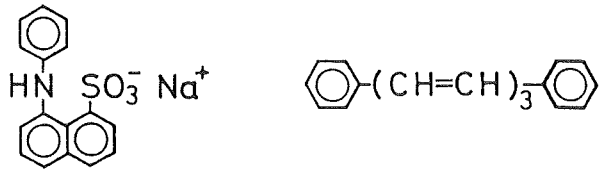

ANS DHT

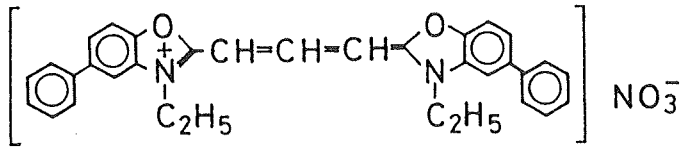

CyD

In all experiments the copolymers were employed in the sodium salt forms.

ANS, a commonly-used anionic probe, showed no noticeable enhancement of fluorescence intensity and no blue-shift of the emission maximum, when it was added to ASt of any f_s in salt-free aqueous solution. An addition of KCl, however, somehow facilitates the hydrophobic uptake on account of minimizing electrostatic repulsion as depicted in Figure 6. The fluorescence intensities I/I_0 (I_0 and I are emission intensity of ANS in the absence and presence of polymer, respectively) are relatively small compared with that of cetyltrimethyl-ammonium bromide (CTAB) micelle (I/I_0 $\sim$50) and exhibit a marked dependence on the concentration of styryl residues, whereas the maximum emission wavelength tends to level off after initial sharp dependence on the concentration of the

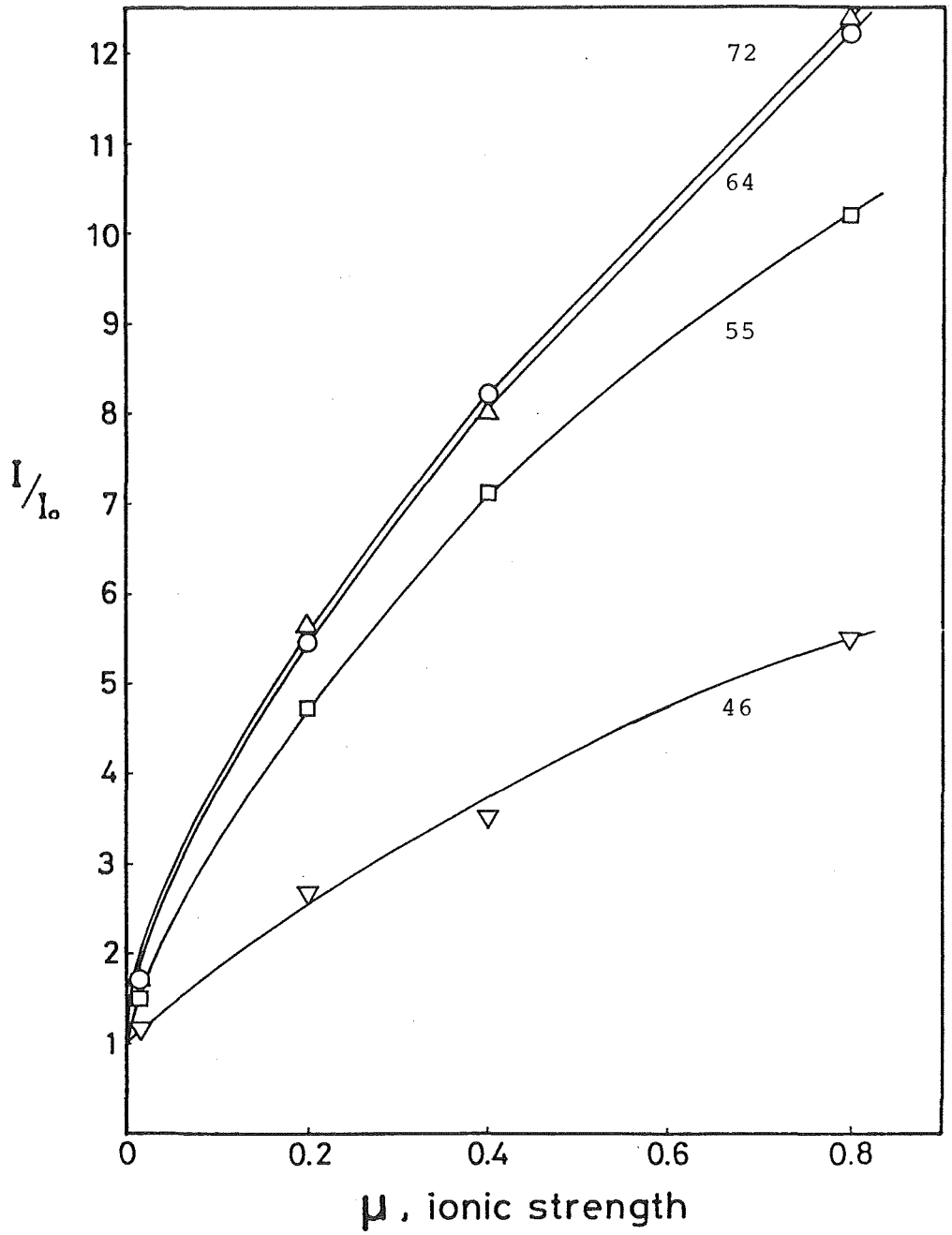

Figure 6. Effect of ionic strength (μ) on relative fluorescence intensity (I/I_0) of ANS: I_0 and I are fluorescence intensity of ANS at 500 nm in the absence and presence of ASt, respectively; $[St]_{residue}=5\times10^{-3}$ M; $[ANS]=5\times10^{-5}$ M; excitation wavelength, 365 nm; ○, ASt-72; △, ASt-64; □, ASt-55; ▽, ASt-46.

styryl residues and reach considerably lower wavelength than that of CTAB micelle (486 nm), especially for ASt-72 (Figure 7 and Figure 8). These phenomena imply that the size of the hydrophobic microdomain should be large so as to serve a hydrophobic binding site that is strong enough for ANS to be taken in by prevailing over electrostatic repulsion between ANS and the polyions. As judged from the blue-shift of the emission maximum, the aggregates of styryl residues have very strong hydrophobicity.

DHT, a neutral probe, is found to be taken up by ASt with high f_s in salt-free solution resulting in a drastic enhancement of its fluorescence intensity. Figure 9 shows that for ASt with high f_s fluorescence intensity tends to level off at a concentration of St residues $[St]_{residue} = 2 \times 10^{-3}$ M after an initial sharp dependence on the $[St]_{residue}$. This suggests the completion of the uptake of all DHT by the copolymers at this concentration, whereas for ASt with low f_s only a little portion of DHT is taken in by the copolymer in this concentration range presumably because of the lack of hydrophobic microdomain with a size large enough to take up the probe. An addition of salt has the effect to promote hydrophobic associations both among the styryl residues and between the hydrophobic domains in the copolymer field and the hydrophobic probe. Remarkable features of the salt-effect are presented in Table I. There is little or no salt-effect for ASt with higher f_s unequivocally because of there being

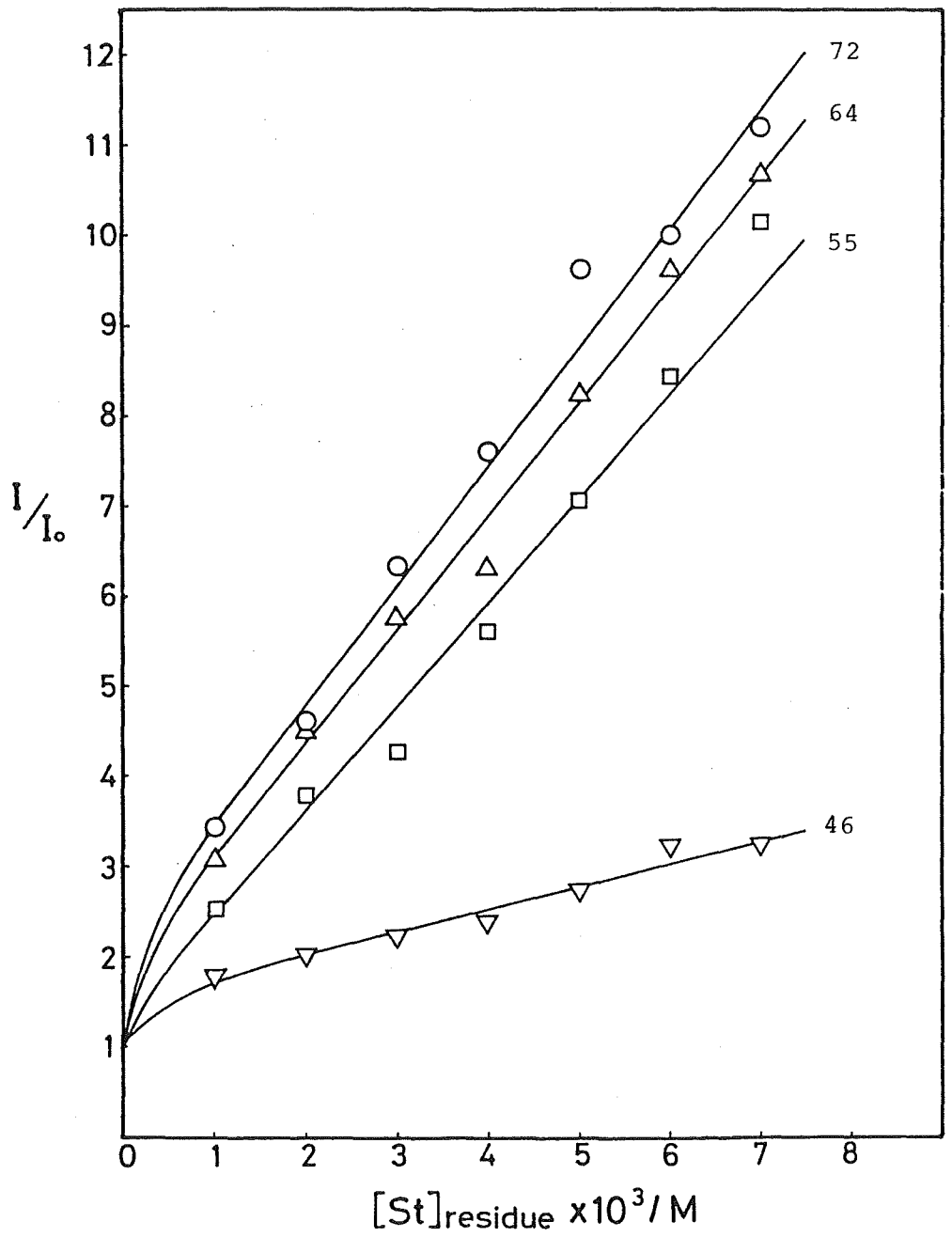

Figure 7. Effect of the concentration of St residues on relative fluorescence intensity of ANS at 500 nm in aqueous KCl solution (μ=0.2): [ANS]=5x10^{-5} M; excitation wavelength, 365 nm; ○, ASt-72; △, ASt-64; □, ASt-55; ▽, ASt-46.

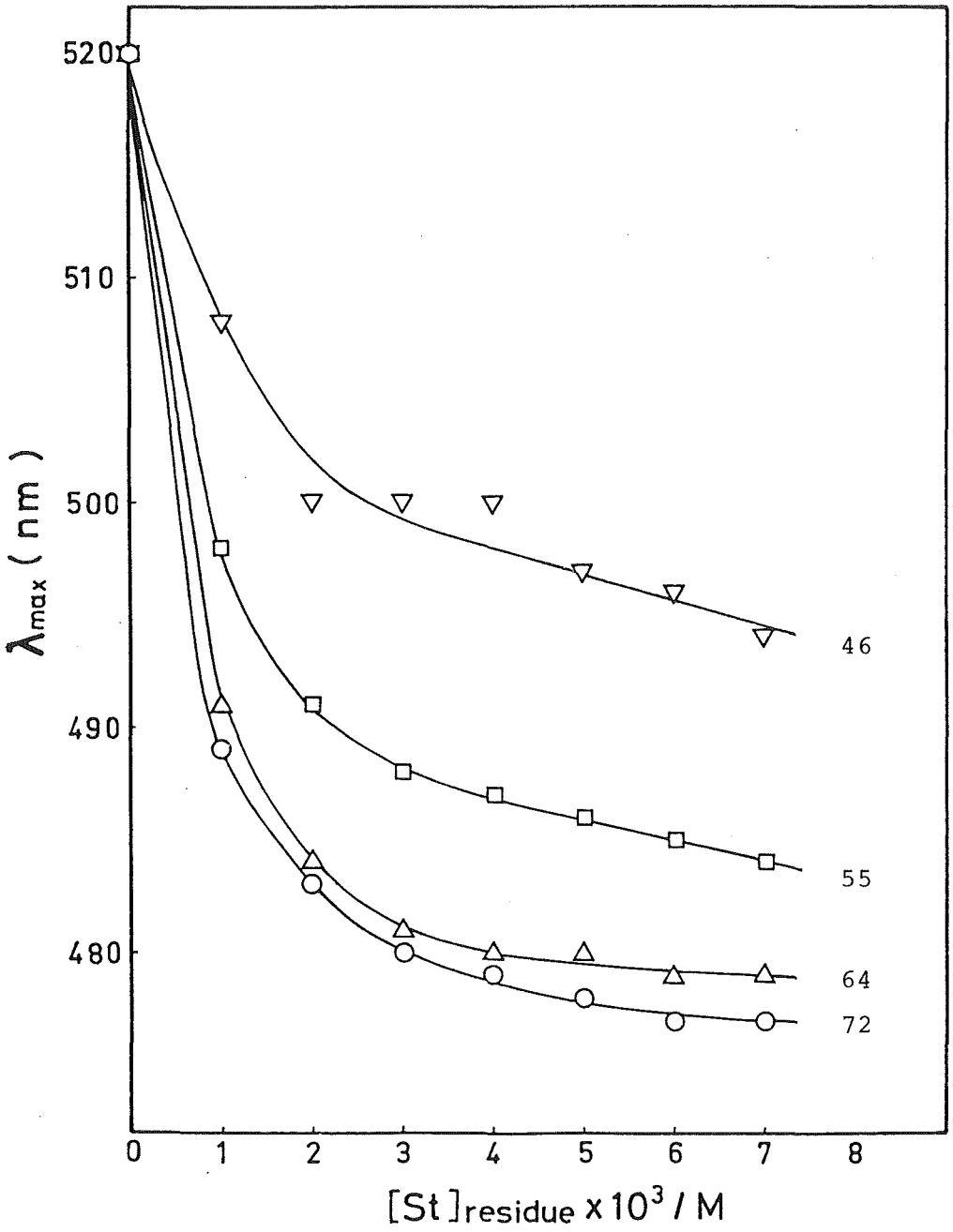

Figure 8. Effect of the concentration of St residues on maximum emission wavelength (λ_{max}) of ANS in aqueous KCl solution (μ=0.2): [ANS]=5x10^{-5} M; excitation wavelength, 365 nm; ○, ASt-72; △, ASt-64; □, ASt-55; ▽, ASt-46.

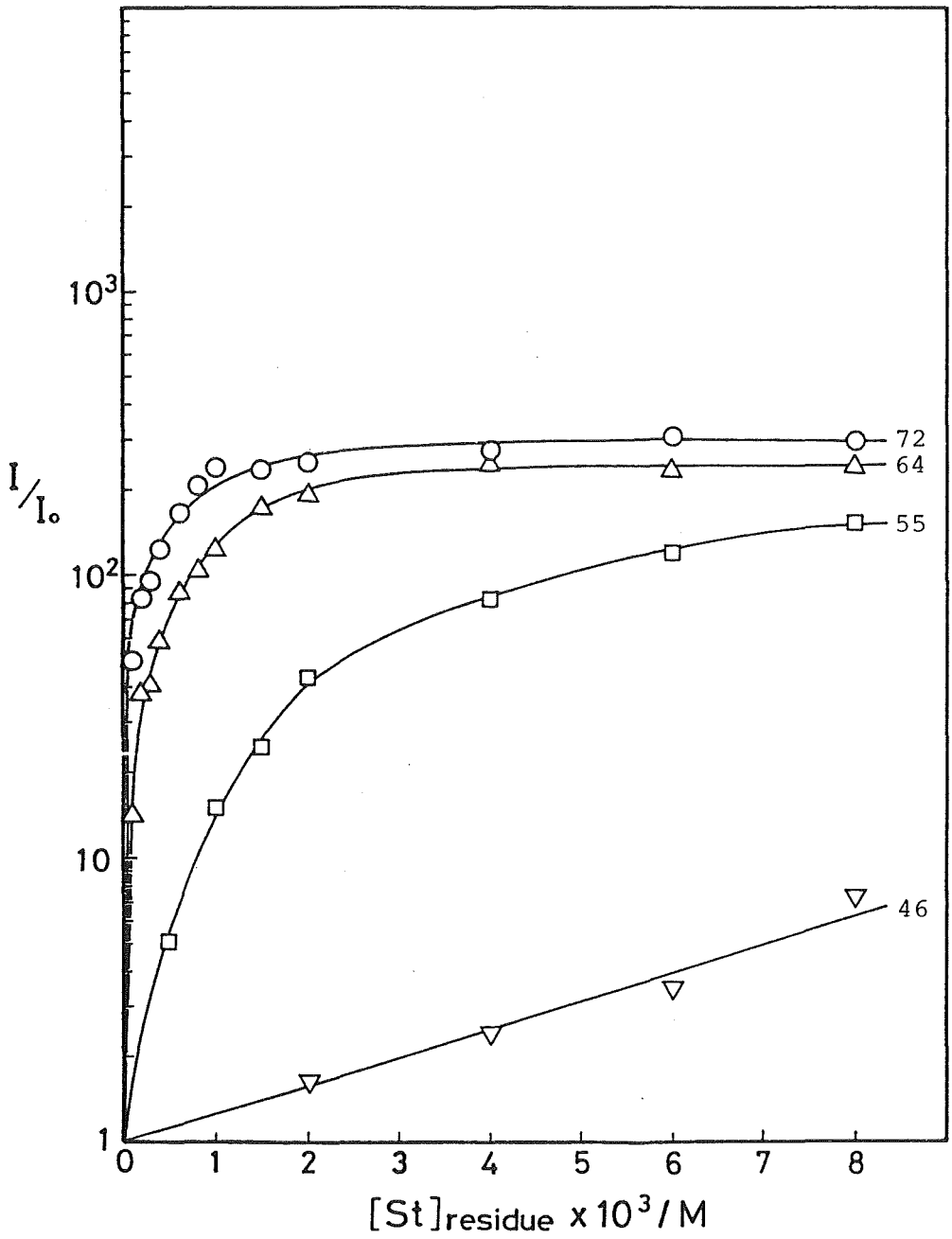

Figure 9. Effect of the concentration of St residues on relative fluorescence intensity of DHT in pure water: [DHT]=8x10^{-7} M; excitation wavelength, 370 nm; ○, ASt-72; △, ASt-64; □, ASt-55; ▽, ASt-46.

no necessity to increase hydrophobic interaction by adding salt for all DHT to be completely taken up. There is a marked salt-effect, on the other hand, for the copolymers with lower f_s, suggesting the increase of the hydrophobic microdomain in its size and number, that is caused by salt, enhances the uptake of the probe.

CyD has hydrophobic and cationic groups and hence an attractive electrostatic interaction between this dye and the polyanions is well expected to assist the hydrophobic uptake of the dye by the hydrophobic microdomains of ASt. According to Grätzel et al.[5], CyD shows drastic enhancement of the fluorescence intensity when it is associated with anionic surfactant micelles as a result of the immobilization of internal molecular motion of the dye. In this system the dye

Table I. Effect of ionic strength on the fluorescence intensity enhanced by the association with ASt

Copolymer	f_s	$I_{\mu=0.8}/I_{\mu=0}$ [a]		
		ANS[b]	DHT[c]	CyD[d]
ASt-72	0.72	12.2	1.06	1.10
ASt-64	0.64	12.4	1.07	1.13
ASt-55	0.55	10.2	2.23	1.23
ASt-46	0.46	5.48	9.89	3.76

a) Ratio of fluorescence intensities at μ=0.8 and μ=0.
b) [ANS]=5×10^{-5} M; $[St]_{residue}=5\times10^{-3}$ M.
c) [DHT]=8×10^{-7} M; $[St]_{residue}=6\times10^{-3}$ M.
d) [CyD]=5×10^{-7} M; $[St]_{residue}=4\times10^{-3}$ M.

is considered to be situated in the surface area of the micelle with the hydrophobic groups protruding into the lipoidic interior. These facts motivated us to use CyD in the present study as a positively charged hydrophobic probe. Figure 10 displays the large enhancement of fluorescence intensity of CyD when it is added to aqueous solutions of ASt. On the other hand, no noticeable enhancement of fluorescence intensity was confirmed when CyD was added to an aqueous solution of polyAMPS, where CyD is possibly bound electrostatically in the polymer field. It is notable that ASt-55 shows a similar ability in enhancing the dye fluorescence to that of ASt with higher f_s (Figure 10), although the former shows relatively less ability in the uptake of DHT than the latters do (Figure 9). It may be inferred, therefore, that the uptake of CyD is so assisted by the concurrent electrostatic attraction that the hydrophobic microdomains with smaller size (where DHT, a neutral probe, is unable to reside) may be able to associate with CyD through hydrophobic interaction. The emission maximum of CyD associated with ASt with high f_s was observed at 520 nm, which is identical to that of the monomeric dye[5], when $[St]_{residue}$ was higher than 1×10^{-4} M. This is indicative of CyD being taken up in isolation. In the lower concentration range of the polymer solution, however, a shoulder at about 550 nm, presumably due to the dimer or higher aggregates of the dyes, slightly appears at $[St]_{residue} = 5 \times 10^{-5}$ M for ASt-72. This shoulder had a tendency to gradually increase with the dilution of the polymer concentration. On the other hand, in the case of the copolymer

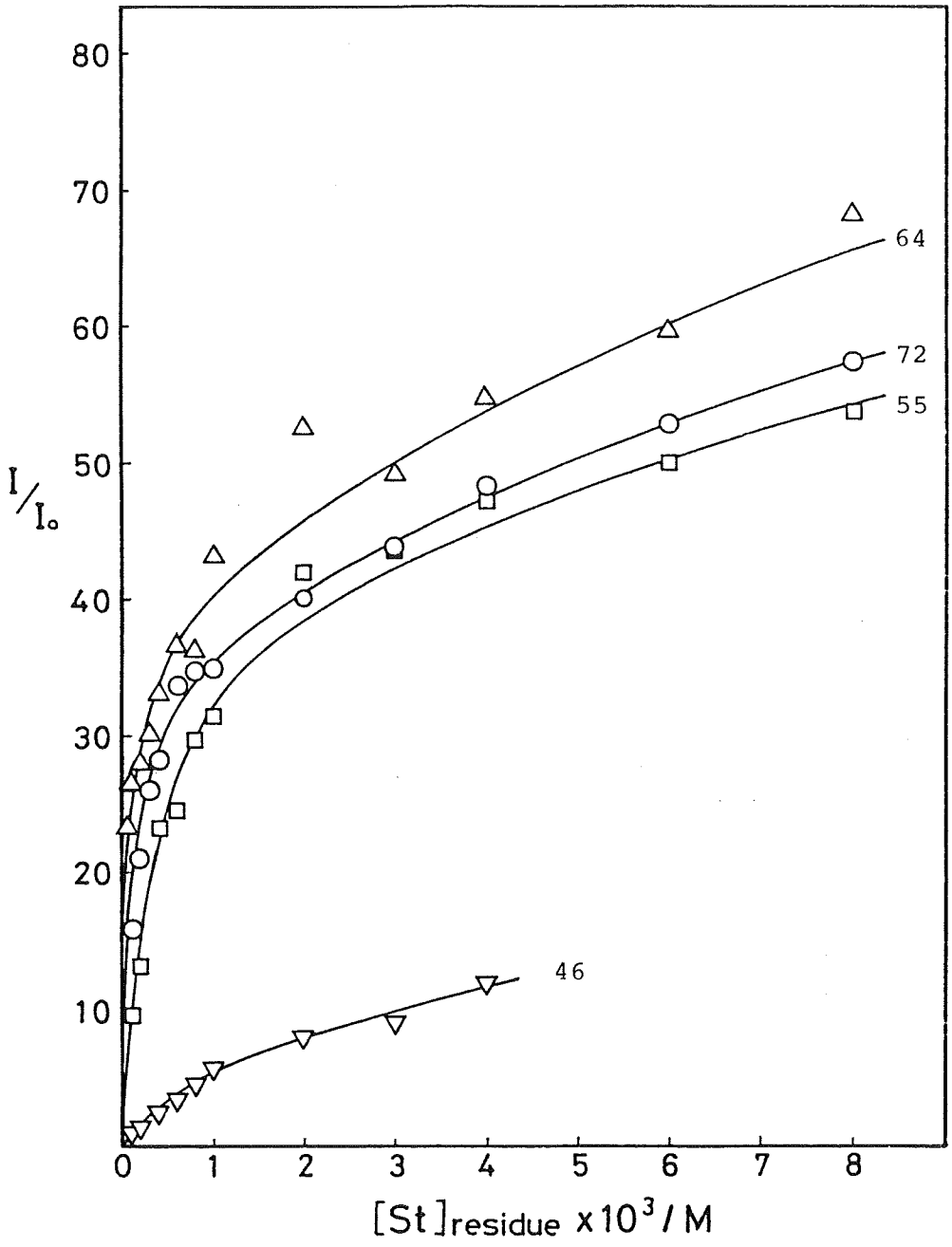

Figure 10. Effect of the concentration of St residues on relative fluorescence intensity of CyD in pure water: [CyD]=5x10^{-7} M; excitation wavelength, 485 nm; ○, ASt-72; △, ASt-64; □, ASt-55; ▽, ASt-46.

with the lowest f_s (ASt-46) contained in Figure 10, the emission spectra of CyD showed a significant amount of the shoulder peak at about 550 nm besides a main peak at 520 nm even at $[St]_{residue} = 4 \times 10^{-3}$ M. Consequently, it is conceivable that, under the conditions contained in Figure 10, all CyD are associated even with ASt-46 through hydrophobic interaction assisted by electrostatic attraction, although hydrophobic microdomains are not large enough to have CyD reside in isolation against its self-aggregation and to result in a drastic enhancement of monomeric fluorescence. Unlike DHT, the enhancement of CyD fluorescence shows no level-off with respect to the St concentration (Figure 10). We do not have an explanation for this. Since the enhancement of cyanine emission seems to be more sensitive to where the dye resides, it might be reflecting the change in the microenvironment of the hydrophobic domains in the polymer field caused by the increase of polymer concentration. The little effect of ionic strength on the enhancement of CyD fluorescence brought about by the copolymers with high f_s (Table I), however, does not seem to be in support of this assumption, because ionic strength may well be also a factor to cause the change in the microenvironment.

Recently, Tazuke and Suzuki[6,7] reported that a cationic polyelectrolyte of ionene type with pendant anthryl groups forms hydrophobic domains organized by a number of anthryl pendant groups. They clarified some of the general features of polyions bearing hydrophobic aromatic groups. Namely, they reported a

strong salt-effect on solution viscosity, and the destructive effect of methanol on the hydrophobic domains which results in a marked decrease in excimer emission. The results of the present study are qualitatively in agreement with their results. Furthermore, they investigated the dimerization of the anthryl groups and interpreted that the mobility of the anthryl group in the hydrophobic domain is apparently more restricted than that of the lipoidic core of micelles consisting of small molecular surfactants[7]. In the present study we also find ourselves in agreement with their explanations with respect to the qualitative nature of the hydrophobic microdomain. Namely, it may be said that the nature of the hydrophobic aggregates of aromatic groups differs in terms of structural rigidity from that of aliphatic long-chains presumanly because of the tendency of the aromatic rings to pack in stacks.

For a more straightforward evidence of the presence of hydrophobic microdomains, an electron micrograph was taken for ASt-72. As seen in Figure 11, unexpectedly large unstained portions due apparently to hydrophobic domains are observed. An electron microscopic image of AMPS homopolymer as a reference obtained under identical conditions showed no such pattern but was homogeneously stained. It should be kept in mind, however, that an electron micrograph of a polymer, having a strong propensity for molecular aggregation, is likely to be the one of an artifact no matter how special care may be paid for the preparation of the specimen. Accordingly, the size and shape of the hydrophobic domains in Figure 11 do not

necessarily represent those which are in the actual solution. Nevertheless, it should be still meaningful in the sense that an agreement on the presence of hydrophobic microdomains is secured, if not quantitatively, between the interpretations of above-mentioned various data on the copolymer solution and the more intuitive data of electron microscopic images.

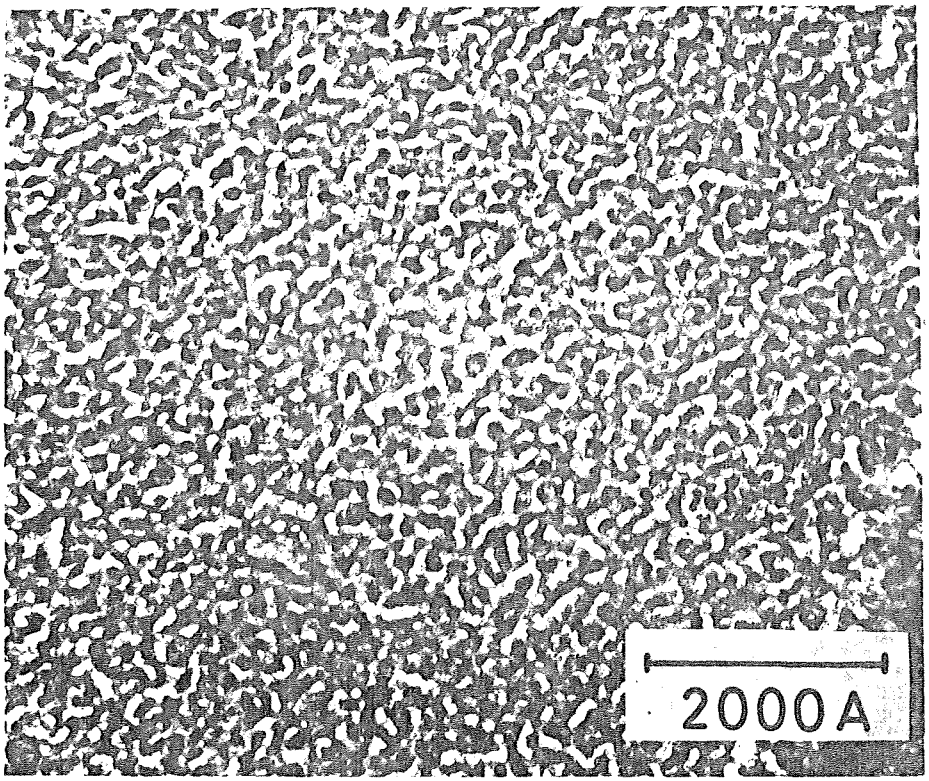

Figure 11. Electron micrograph of ASt-72.

2-3-2. Solution Properties of Other Amphiphilic Copolymers

Solution behaviors of other polymers were examined by spectroscopic measurements.

Solution Behaviors of APh and APy

In the NMR spectra of poly(AMPS-co-VPh) with f_{Ph} = 0.58 (APh-58), the peaks due to the phenanthryl protons were clearly observed in DMSO-d_6 but not at all in D_2O, presumably because of the compact packing of phenanthryl residues owing to an extensive hydrophobic association in an aqueous solution (Figure 12). The same phenomena had been observed for ASt.

Figure 13 shows the fluorescence spectra of APh with various f_{Ph} in aqueous soution. The fluorescence spectra of the copolymers with high f_{Ph} in aqueous solution are broad with significant tailing in the longer-wavelength region along with a significant decrease in the intensity at emission maximum; e.g., the fluorescence intensity of APh-58 at 376 nm was one-sixth that in DMF. On the other hand, in DMF the shape of the fluorescence spectra of all copolymers was identical to that of poly(vinylphenanthrene) (PVPh)[8].

In Figure 14, the relative intensities of the fluorescence of APh in various solvents are plotted against f_{Ph}. The fluorescence intensity decreased remarkably in aqueous solution with increasing f_{Ph}. It is known that the monomer fluorescence intensity decreases through excimer formation, whether radiative or nonradiative, when the chromophores are brought into close vicinity by being incorporated into the polymeric

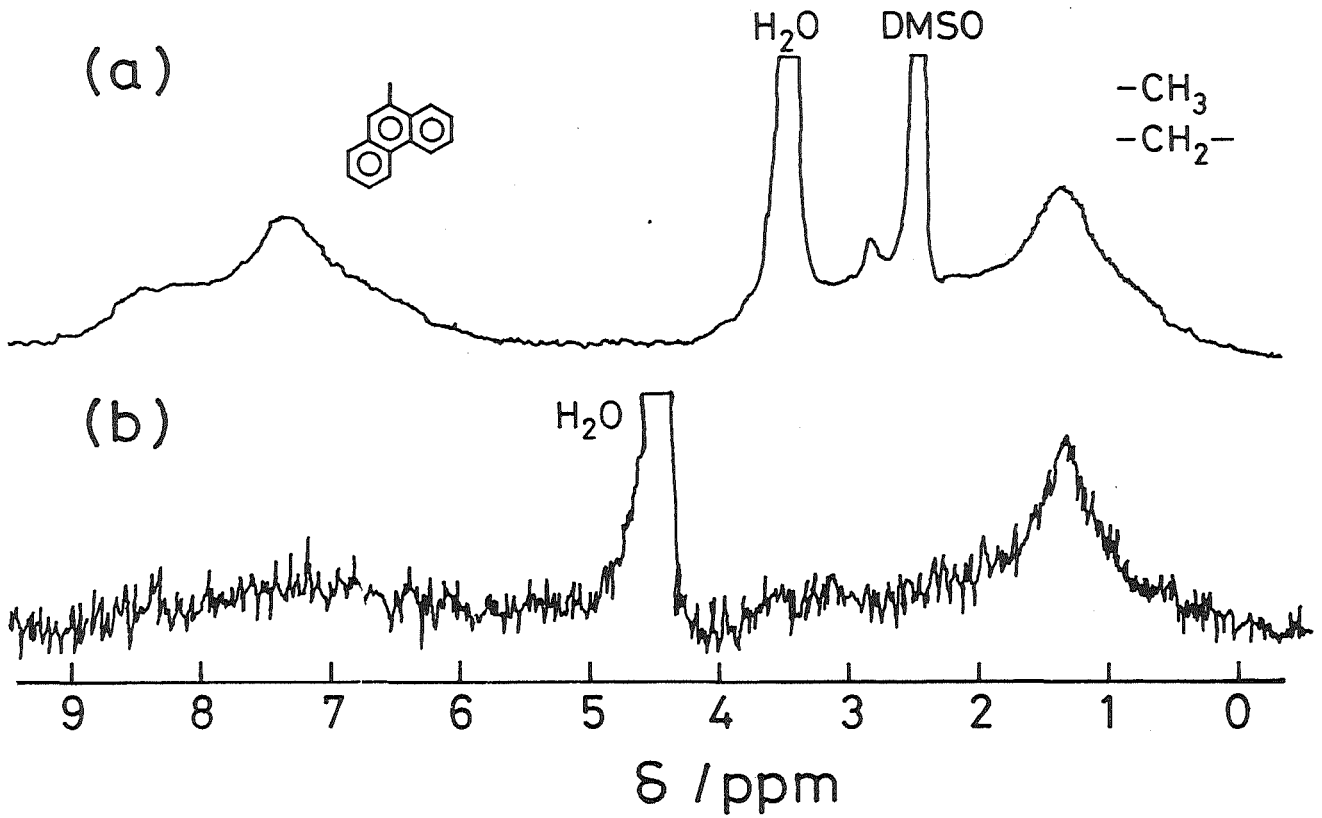

Figure 12. ^1H NMR spectra of APh-58 in DMSO-d_6 (a) and in D_2O (b) at room temperature: Intensity is not normalized.

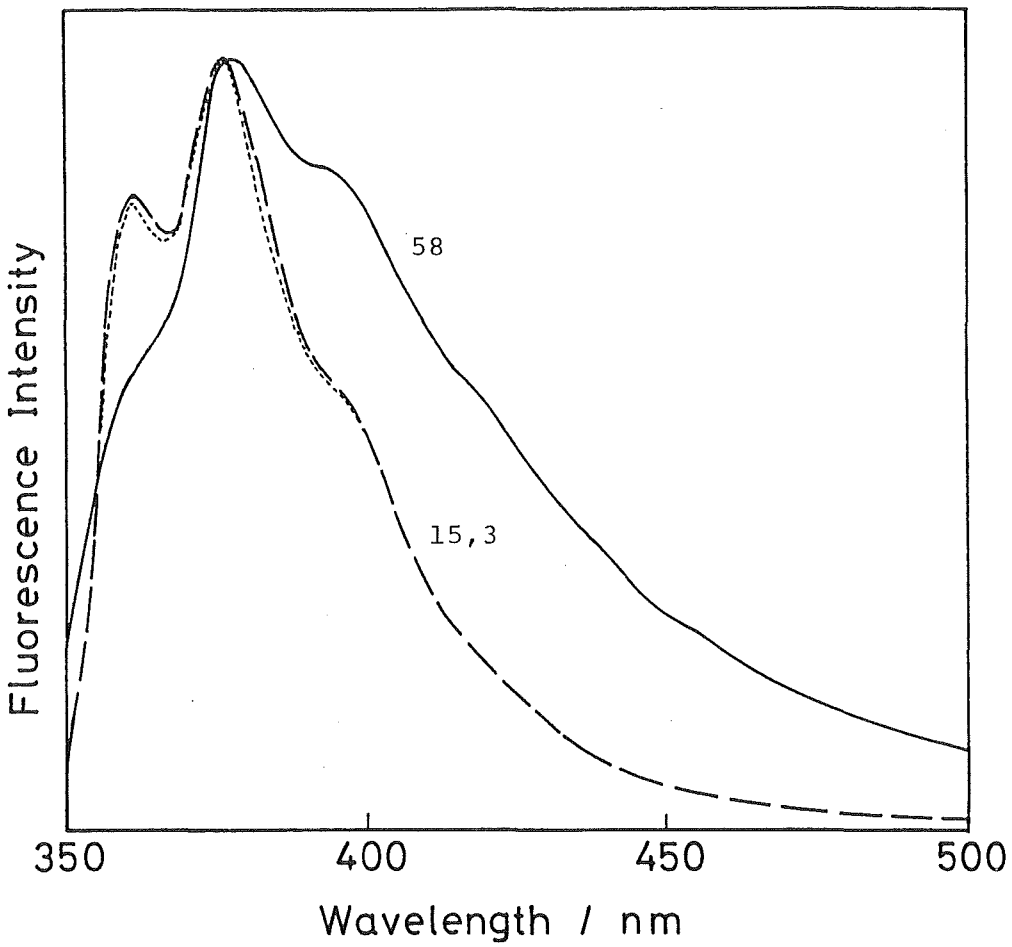

Figure 13. Fluorescence spectra of APh with various f_{Ph} in aqueous solution: $[VPh]_{residue}=3x10^{-4}$ M; excitation wavelength, 337 nm; ———, APh-58; – – – –, APh-15; --------, APh-3; fluorescence intensity normalized to peaking emission at 376 nm.

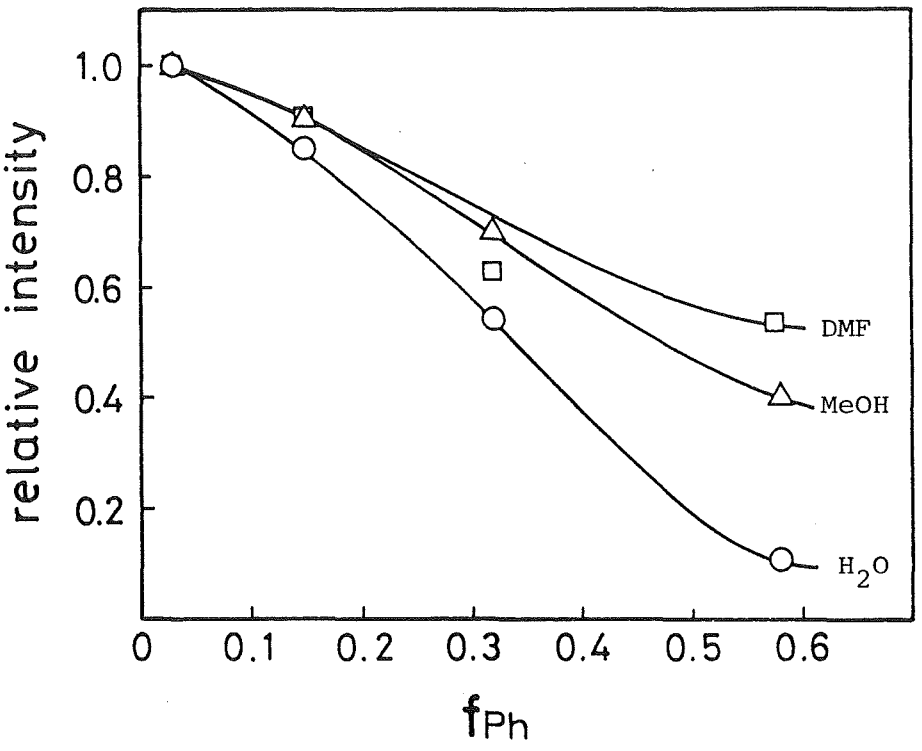

Figure 14. Relative fluorescence intensity of APh at 376 nm in various solvents as function of f_{Ph}: $[VPh]_{residue}=3x10^{-4}$ M; excitation wavelength, 352 nm; ○, in H_2O; △, in methanol; □, in DMF; fluorescence intensity normalized to that of APh-3 in each solution.

array[9]. In addition to this, the self-quenching of the excited Ph was probably facilitated further by the compact packing of the phenanthryl rings through the hydrophobic interaction. The decrease of the fluorescence intensity with increasing VPh content was more significant in methanol than in DMF, which suggests that the shrinkage of the copolymer with high f_{Ph} in methanol, a poor solvent, may facilitate self-quenching. In view of the shape of the fluorescence spectra, a possibility of the excimerlike interaction in APh may not be precluded in aqueous solution where the phenanthryl rings are probably stacked, although the fluorescence of Ph[10] and PVPh[8] shows no excimer emission and is almost independent of solvents.

Figure 15 shows the fluorescence spectra of APy with various compositions in aqueous solutions. The fluorescence of the copolymer with high f_{Py} shows an excimer emission at 490 nm besides a monomer emission at 390 nm. Addition of an equal volume of DMF to the aqueous solution reduced the relative intensity of the excimer emission to the monomer emission by ca. 30 % for APy-32 (Data not shown in figure). This indicates that more excimers are formed by packing of pyrenyl residues in aqueous solution than in DMF.

In order to clarify the hydrophobic interaction of small molecules with the copolymers in an aqueous solution, the uptake of a hydrophobic fluorescence probe, ANS, by APh with various compositions was investigated. This experiment was performed under the same conditions as those for ASt so that

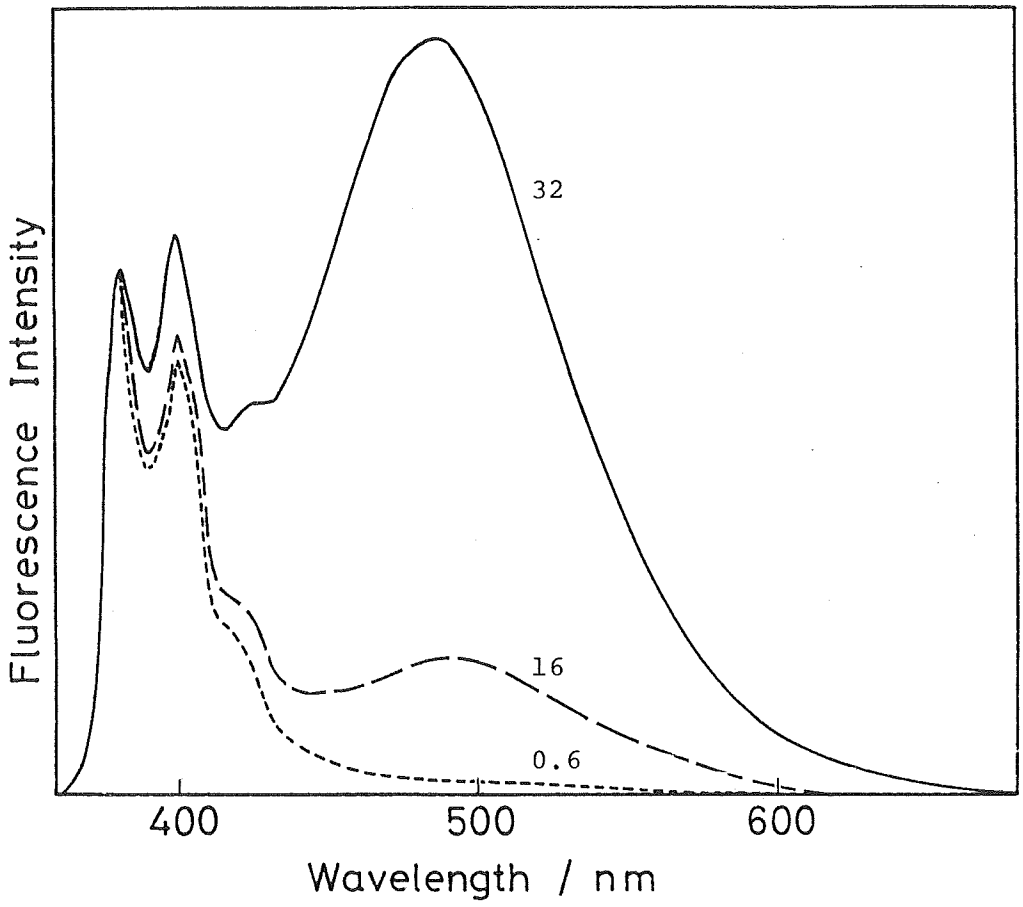

Figure 15. Fluorescence spectra of APy with various f_{Py} in aqueous solution: $[VPy]_{residue}=1x10^{-5}$ M; excitation wavelength, 346 nm; ———, APy-32; – – – –, APy-16; --------, APy-0.6; fluorescence intensity normalized to peaking emission at 380 nm.

the results could be compared (Figure 16). The relative fluorescence intensity I/I_0 was at most 10 even in the case of ASt-72. In the case of APh, ANS was taken up even by APh-8 and I/I_0 increased to more than 20. I/I_0 also increased with an increase in the VPh content of the copolymers. Because of the much higher hydrophobicity than ASt, APh was able to take up ANS to enhance its fluorescence intensity even in pure water (without any salt added) inspite of the electrostatic repulsion between ANS and the polyions, whereas ASt showed no enhancement of the fluorescence intensity in pure water. It should be noted that there was a striking difference in capacity for hydrophobic uptake of the fluorescence probe between St and VPh as hydrophobic components in the amphiphilic copolymers.

Solution Behavior of QPh

In the ^1H NMR spectra of the copolymer with $f_{Ph} = 0.47$ (QPh-47), peaks due to phenanthryl protons were observed in DMSO-d_6 but not at all in D_2O (Data not shown). This seems to be a common observation often encountered for amphiphilic copolymers of this type, whether the electrolyte sequences are cationic or anionic, because of the compact packing of the hydrophobic residues arising from an extensive hydrophobic association in an aqueous soution. The presence of the hydrophobic microdomain was also suggested by the uptake of a hydrophobic fluorescence probe, ANS, by the copolymer. As shown in Table II, an addition of QPh-28 to an aqueous solution of ANS induced drastic enhancement of the fluorescence intensity

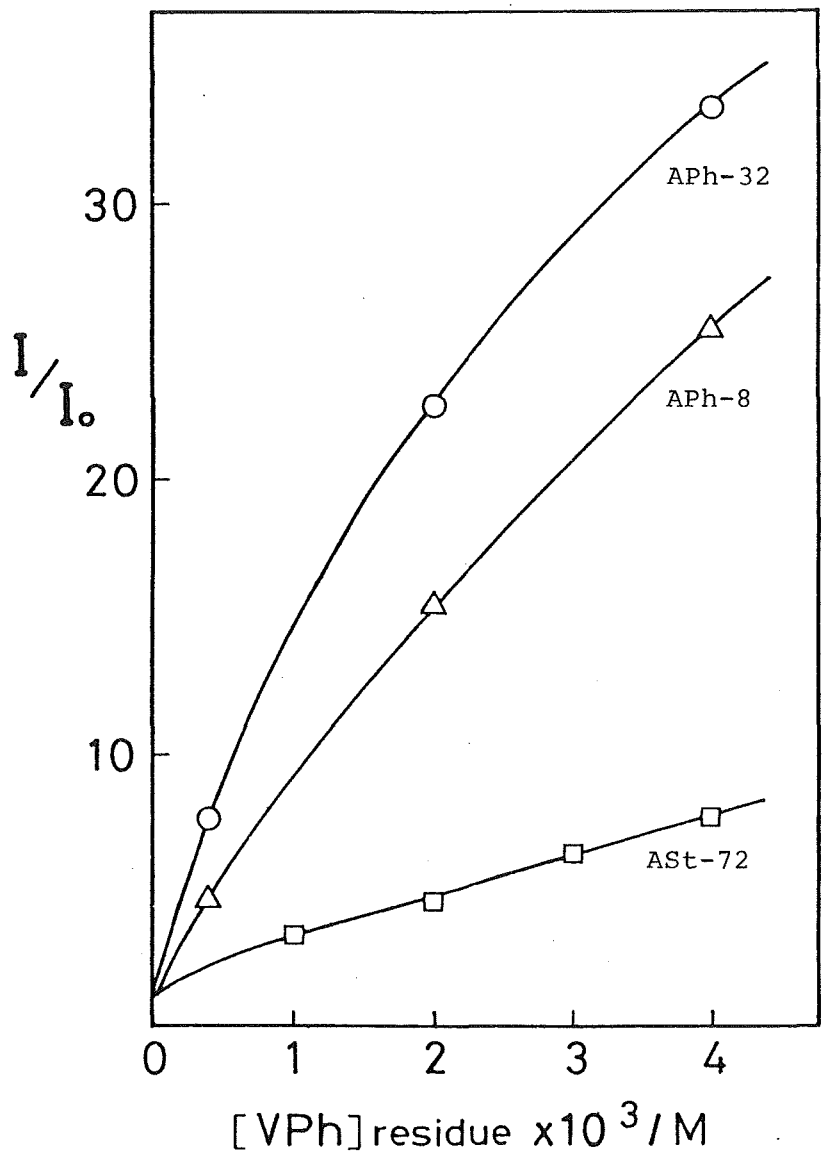

Figure 16. Relative fluorescence intensity of ANS at 500 nm in the presence of APh and ASt in aqueous KCl (μ=0.2) solution: [ANS]=5x10^{-5} M; excitation wavelength, 365 nm; ○, APh-32; △, APh-8; □, ASt-72.

of the probe with a marked blue shift of the emission maximum. In this case, since the attractive electrostatic interaction between ANS and the polycation assisted the hydrophobic uptake by the microdomains, the enhancement of intensity was far more favorable than the anionic polymers (ASt or APh).

Figure 17 shows the fluorescence spectra of QPh with various f_{Ph} in aqueous solution. The fluorescence spectra of the copolymers with high f_{Ph} in aqueous solution are broad with significant tailing in the longer-wavelength region accompanied with a significant decrease in intensity at the emission maximum. As seen in Figure 17, the fluorescence intensity of QPh-47 was about 40 % that of QPh-7 in aqueous solution. The

Table II. Relative fluorescence intensity at 500 nm and maximum emission wavelength of ANS in the presence of QPh-28 in aqueous solution[a)]

$[Ph]_{residue}$ (10^{-3} M)	λ_{max} (nm)	I/I_0[b)]
Nil	528	1
0.2	486	154
0.4	484	188
0.8	480	220
2.0	476	266

a) [ANS]=5×10^{-5} M; excitation wavelength, 365 nm.

b) I_0 and I are emission intensity of ANS in the absence and presence of QPh-28.

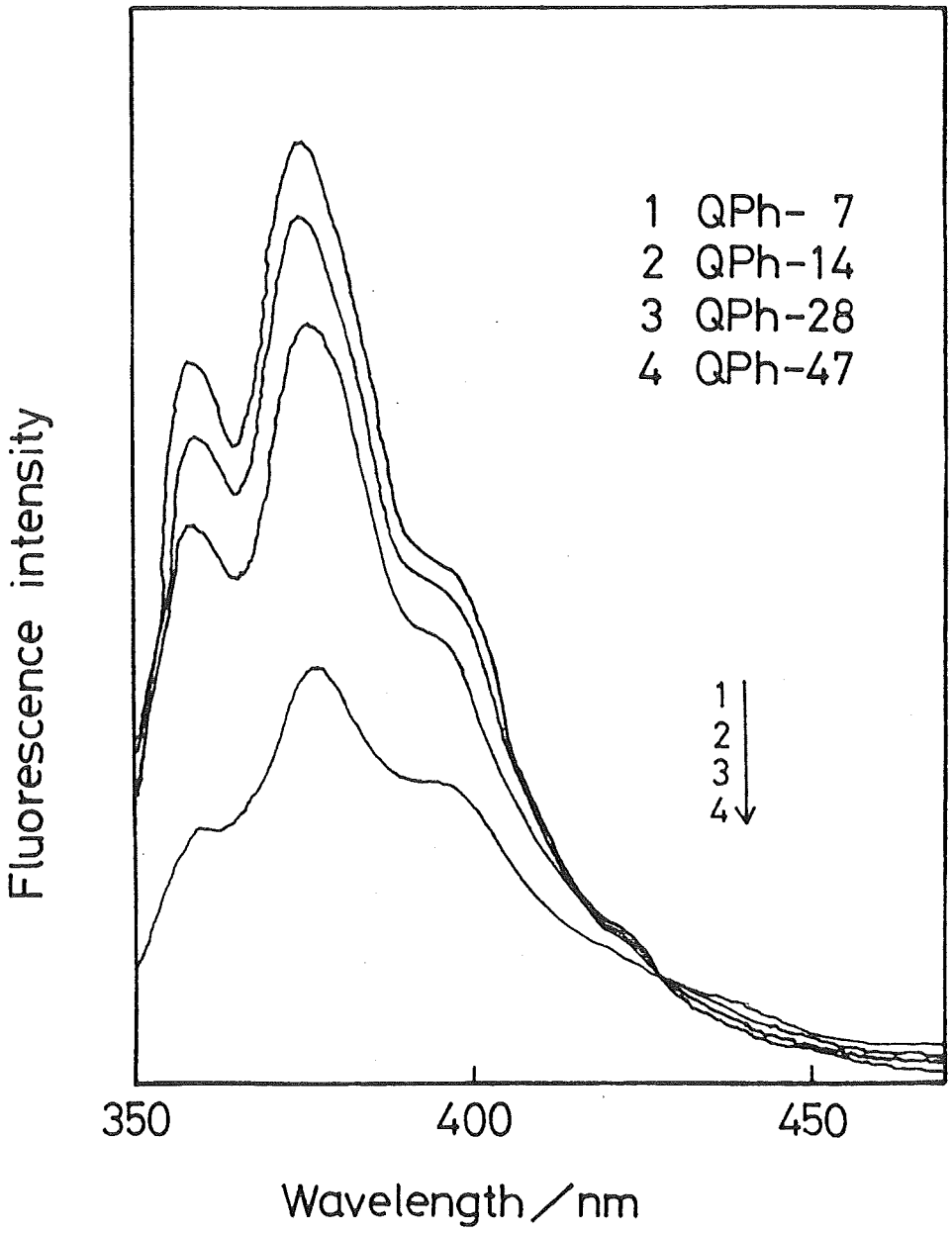

Figure 17. Fluorescence spectra of QPh in aqueous solution: $[VPh]_{residue}=1.5x10^{-4}$ M; excitation wavelength, 337 nm.

fluorescence lifetime was also found to decrease with increasing f_{Ph} in aqueous solution (Table III). In DMSO the shape of the fluorescence spectra of the copolymers were identical to each other over a wide range of f_{Ph} and also identical to that of PVPh. The fluorescence intensity in this solvent also decreased gradually as f_{Ph} increased; e.g., the intensity of QPh-47 was about 70 % that of QPh-7. These observations seem to be common to this type of amphiphilic copolymers regardless of the sign of the charge on the electrolyte segments (Table III).

Table III. Relative fluorescence intensities and fluorescence lifetimes of APh and QPh

Polymer	f_{Ph}	in H_2O		in DMF or DMSO[a]	
		I_{rel}[b]	τ/ns	I_{rel}[b]	τ/ns
APh-58	0.58	0.11	20	0.53	34
APh-32	0.32	0.54	—	0.63	—
APh-15	0.15	0.85	37	0.91	42
APh- 3	0.03	1.00	38	1.00	44
QPh-47	0.47	0.44	34	0.73	40
QPh-28	0.28	0.81	39	0.81	—
QPh-14	0.14	0.92	42	0.95	41
QPh- 7	0.07	1.00	44	1.00	—

a) Measured in DMF for APh and in DMSO for QPh.
b) Fluorescence intensity normalized to that of APh-3 or that of QPh-7 in each solution.

Solution Behavior of Block Copolymers (b-VPh)

For the block copolymers DMF was a good "nonselective" solvent, while water is a typical selective one. When the block copolymer was placed directly in water, it did not dissolve completely. However, when it was dissolved into a small amount of DMF first and then the solution was injected into an excess of water with vigorous agitation, neither precipitation nor turbidity appeared but an apparently clear solution was obtained. All aqueous solutions in the present study were prepared in this manner and, as a result, they eventually contain 1 vol % of DMF.

Figure 18 compares the fluorescence spectrum of the block copolymer in an aqueous solution and that in a DMF solution. In DMF the shapes of the fluorescence spectra of the block copolymer were identical to those of PVPh homopolymer. On the other hand, in water, the spectrum of the block copolymer was extremely broad with considerable tailing in the longer-wavelength region, the phenomena being parallel with a significant decrease in the intensity at the emission maximum of monomer fluorescence. It should be noted that the absorption spectrum of the block copolymer in aqueous solution was identical to that observed in DMF. Such observations were also encountered with APh and QPh. As described above, in particular circumstances where Ph rings are highly packed in a rigid stack, which is probably the case for the block copolymer in aqueous solution, one may not preclude a possibility of the excimerlike interaction to which the

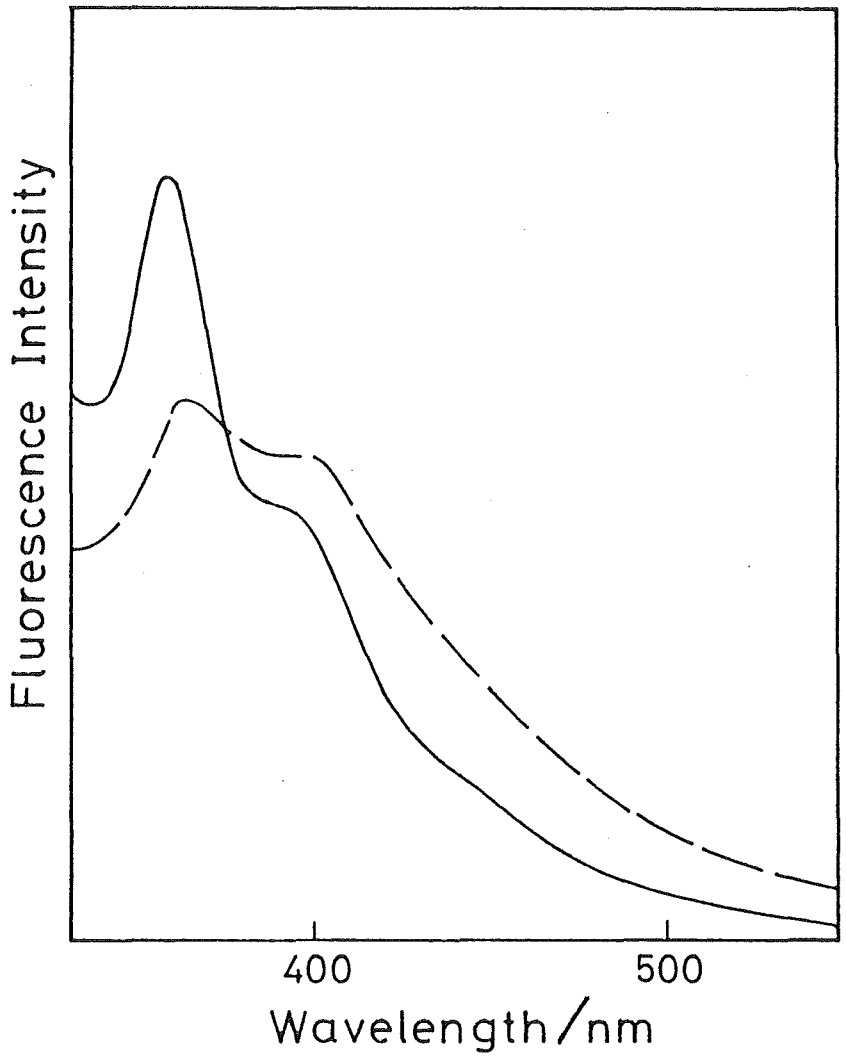

Figure 18. Fluorescence spectra of block copolymer (b-VPh-16): $[VPh]_{residue}=1x10^{-4}$ M; ———, in DMF; – – – –, in pure water.

emission in the longer-wavelength region may be attributable. In contrast, the emission spectrum of a related random copolymer (MPh) in aqueous solution was almost identical to that in DMF.

Addition of the aqueous solution of the block copolymer to an aqueous solution of ANS induced a drastic enhancement of the fluorescence intensity of the probe with marked blue shift of emission maxima (Figure 19). The longer VPh block sequence in the block copolymer led to a greater enhancement of the ANS fluorescence intensity. Since most of the MA groups in the polymer are believed to be dissociated at pH 9[11,12], the VPh block sequences must be surrounded by a negatively charged region with high electrostatic potential. Therefore, ANS, an anionic probe, must overcome the repulsive electrostatic interaction between the probe and polyions before it can be associated with the hydrophobic region of the block copolymer. In fact this could more favorably happen to the block copolymer with longer VPh block sequences. On the other hand, the random copolymer (MPh-21) showed no noticeable enhancement of the ANS fluorescence intensity, indicating that no association of ANS with the copolymer is possible. From these observations it may be inferred that as for the block copolymer the hydrophobic microdomain made up of VPh block sequences is large enough to serve as a hydrophobic binding site and is strong enough for ANS to be taken in even by prevailing over the electrostatic repulsion between ANS and the polyions.

Figure 20 illustrates a typical transmission electron

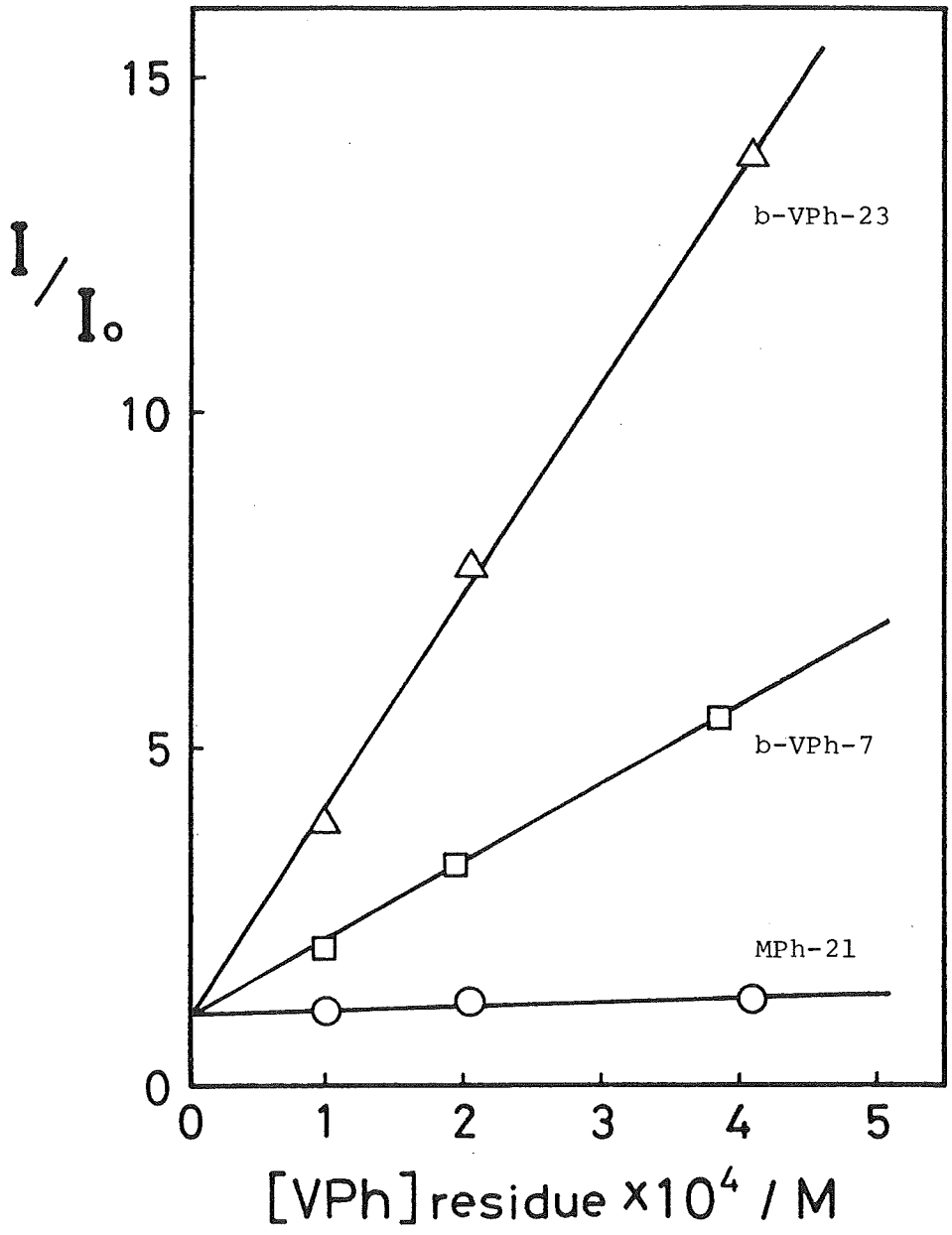

Figure 19. Enhancement of fluorescence intensity of ANS at 500 nm in the presence of block copolymer in borate buffer (pH 9): △, b-VPh-23; □, b-VPh-7; ○, MPh-21; [ANS]=5x10^{-5} M; excitation wavelength, 365 nm.

micrograph of a cast film of the block copolymer. Hydrophobic domains are clearly observed as unstained islands and the disperse phase as stained continuous portions. Although the size and shape of the hydrophobic microdomains in Figure 20 do not necessarily represent those in the diluted aqueous solution, it is conceivable that qualitatively the similar phase separation is already present even in the solution.

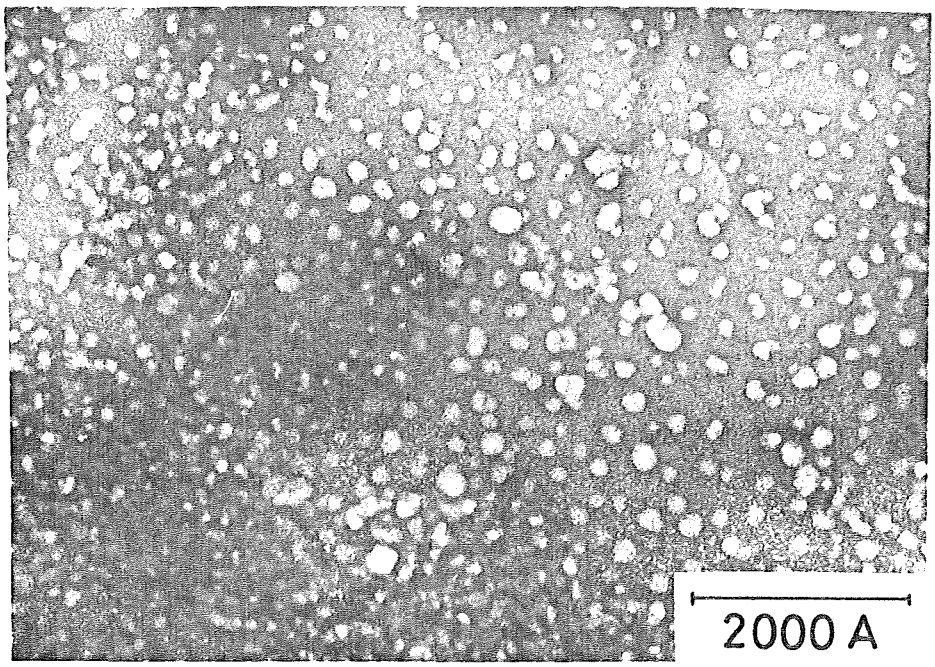

Figure 20. Electron micrograph of b-VPh-16.

2-4. Conclusion

Amphiphilic copolymers consisting of aromatic and electrolyte segments were found to form hydrophobic microdomains in aqueous solutions. These microdomains are highly hydrophobic in nature but less capable to solubilize the substrates than the surfactant micelles. These observations were more pronounced with the block copolymers than the random copolymers. These microdomains will be interesting media for the electron transfer in aqueous solutions.

References

1) S. Shinkai and T. Kunitake, Biopolymers, 15, 1129 (1976).

2) F. A. Bovey, G. V. D. Tiers, and G. Filipovich, J. Polym. Sci., 38, 73 (1959).

3) V. D. Mochel, Macromolecules, 2 , 537 (1967).

4) V. D. Mochel and W. E. Claxton, J. Polym. Sci., A-1, 9, 345 (1971).

5) R. Humphry-Baker, M. Grätzel, and R. Steiger, J. Am. Chem. Soc., 102, 847 (1980).

6) S. Tazuke and Y. Suzuki, J. Polym. Sci., Polym. Lett. Ed., 16, 223 (1978).

7) Y. Suzuki and S. Tazuke, Macromolecules, 13, 25 (1980).

8) A. Itaya, K. Okamoto, and S. Kusabayashi, Bull. Chem. Soc. Jpn., 50, 52 (1977).

9) T. Ishii, T. Handa, and S. Matsunaga, Macromolecules, 11, 40 (1978).

10) J. B. Birks, "Photophysics of Aromatic Molecules", Interscience, New York, 1970, chap. 7.

11) A. M. Kotliar and H. Morawetz, J. Am. Chem. Soc., 77, 3692 (1955).

12) J. C. Leyte and M. Mandel, J. Polym. Sci., A, 2, 1879 (1964).

Chapter 3

Hydrophobic Effect of Amphiphilic Copolymers on the Forward Electron Transfer

3-1. Introduction

We have been interested in amphiphilic polymers consisting of electrolyte and hydrophobic segments as media for electron transfer reactions in aqueous systems. In Chapter 2, it was demonstrated that these types of polymers, either random or block copolymers, formed the micellar structure in aqueous solutions. Such a microheterogeneous phase can be utilized for the modification and control of reactivity in various thermal[1] and photochemical[2] reactions. We may expect a few advantages with these amphiphilic polymers as media for the photosensitized electron transfer: (i) uptake of hydrophobic or amphiphilic substrates such as electron donors or acceptors through hydrophobic interaction, (ii) prevention of the back reaction between the electron transfer products due to electric charges on the electrolyte sequences, (iii) efficient collection and transport of excitation energy as a result of energy migration along the polymer chains[3].

In this chapter, we deal with the hydrophobic effect of these polymers on the facilitation of the forward electron transfer. The fluorescence quenching in aqueous solutions was studied by using amphiphilic and hydrophilic quenchers. The results are compared with those of the monomer model compound and the micellar systems. The quenching behavior characteristic of the polymer was also discussed kinetically.

3-2. Experimental

Monomer Model

Sodium 9-phenanthrylmethanesulfonate (AM) was prepared from 9-phenanthrenecarboxyaldehyde (I)[4] as follows: 9-Hydroxymethylphenanthrene (II) was obtained by reduction of I with $LiAlH_4$ in dry ether and purified by recrystallization from benzene: mp 146 °C; yield 73 %. 9-Bromomethylphenanthrene (III) was prepared by treating II with phosphorous tribromide in benzene and purified by recrystallization from ethanol: mp 118.5 °C; yield 55 %. A mixture of 2.7 g (0.01 mol) of III and 2.0 g (0.016 mol) of anhydrous sodium sulfite suspended in 40 ml of ethanol/water (3/1,v/v) mixture was heated at 130 °C for 16 h in an autoclave. The reaction mixture was evaporated to dryness and then extracted with hot ethanol. After removal of the unreacted starting material (III) by extraction with hot benzene, the crude product (AM) was recrystallized from water three times: yield 1.1 g (38 %);

NMR(D_2O) δ 4.5(s,2H) and 7.24-8.30 ppm(m,9H).

Anal. $C_{15}H_{11}O_3SNa \cdot 1.4H_2O$ Calcd: C, 56.39%; H, 4.35%; S, 10.03%

Found: C, 56.56%; H, 4.47%; S, 9.91%.

2-(3-Phenanthrylacetylamino)ethyltrimethylammonium methylsulfate (QM) was prepared from 3-phenanthreneacetic acid (IV)[5] via N-(N',N'-Dimethylaminoethyl)-3-phenanthrylacetamide (V)

as follows: To a refluxing solution of 4.75 g (0.02 mol) of IV in 50 ml of toluene was added 3.38 g (0.038 mol) of unsym-dimethylethylenediamine in 10 ml of toluene. Water was separated as the toluene azeotrope by distillation over a period of 5 h and toluene was finally evaporated under reduced pressure to dryness. The crude product was dissolved in methanol and passed through a silica gel column. Evaporation of methanol left 5.47 g of a crystalline product (V): mp 93.5-95.0 °C; yield 89.0 %;
NMR($CDCl_3$) δ 2.13(s,6H), 2.36(t,2H), 3.31(m,2H), 3.75(s,2H), 6.5(s,1H), 7.36-7.89(m,7H), and 8.48-8.60 ppm(m,2H).
Quaternization of V was performed by the following procedures: To a stirred solution of 5.0 g (0.016 mol) of V in 50 ml of the mixture of acetone-methanol (4/1,v/v) was added an equimolar (2.06 g) amount of dimethyl sulfate at one time. The reaction was performed at 30 °C for 24 h and the solvents were then evaporated under reduced pressure. A 30-ml chloroform solution of the residue was poured into 200 ml of ether to precipitate a solid product which was recrystallized from acetone-ethanol (4/1,v/v) to give 6.52 g of QM as pale yellow flakes: mp 163.5-165 °C; yield 91.6 %;
NMR(D_2O) δ 3.41(s,7H), 3.62-4.01(m,4H), 4.07(s,2H), 4.30(s,3H), 7.40-7.95(m,7H), and 8.60-8.84 ppm(m,2H).
Anal. Calcd: C, 61.09%; H, 6.53%; N, 6.48%; S, 7.41%
Found: C, 60.51%, H, 6.49%; N, 6.42%; S, 7.52%.

Sodium 1-pyrenesulfonate (PyS) was obtained by neutralization of 1-pyrenesulfonic acid[6] with equimolar

amounts of sodium hydroxide and then recrystallized from water:

Anal. $C_{16}H_9O_3Na \cdot H_2O$ Calcd: C, 59.62%; H, 3.44%; S, 9.95%

Found: C, 58.93%; H, 3.68%; S, 10.03%.

Quenchers

Bis(2-hydroxyethyl)terephthalate (BHET) was provided by Toyobo Co. and used without further purification.

Fumaric acid (FA) purchased from Wako Pure Chemical Ind. Co. was purified by recrystallization from water.

N-Methyl-N-(2-hydroxyethyl)aniline (MHEA) was prepared according to the literature[7] and purified by fractional distillation under reduced pressure: bp 106.5 °C/0.2 mmHg.

N,N-Di(2-hydroxyethyl)aniline (DHEA) was synthesized in accordance with the method of Benn et al.[8] and purified by recrystallization twice from ethyl acetate: mp 58.0 °C.

Materials

Syntheses of amphiphilic copolymers are described in Chapter 1.

Phenanthrene (Ph) and pyrene (Py) used for the fluorescence measurements were zone-refined reagents (Tokyo Chemical Ind. Co.). Sodium dodecylsulfate (SDS) and cetyltrimethylammonium bromide (CTAB) were obtained from Wako Pure Chemical Ind. Co. and used without further purifications.

Measurements

Fluorescence spectra were recorded on a Union FS-401

Spectrofluorometer or a Shimadzu RF-502A Spectrofluorometer at room temperature. In the case of APh and QPh systems, prior to the measurement sample solutions were deaerated by bubbling with nitrogen for 30 min. In the case of the b-VPh system, the measurements were carried out without deaeration. An aqueous stock solution of b-VPh was prepared by injecting 1.67 ml of a DMF solution of the polymer (3.99×10^{-2} M with respect to the VPh residue) into 48.3 ml of water under agitation. An appropriate volume of an aqueous solution of the quenching agent was mixed with the stock solution. To adjust the concentration of the solutes, the mixture was then diluted with water containing a small amount of DMF so that the final aqueous solution contained 1 vol % of DMF. All emission spectra were recorded 4 h after the sample solutions had been prepared. The concentrations of the VPh residue of the solutions were reconfirmed by measuring optical density.

The fluorescence lifetime was measured using a small Blumlein-type N_2 laser: N_2 pressure, 1 atm; peak output power, $\sim$30 kW; laser pulse width, 0.8-1 ns[9]. Prior to the measurement, the sample solutions (containing 3.3×10^{-3} M of the Ph residue) were evacuated and sealed in 2-mmϕ quartz tubes on a vacuum line. The lifetimes were calculated from the decay curves; first-order plots were obtained between about 5 and 80 ns after the pulse.

3-3. Results and Discussion

3-3-1. Fluorescence Quenching of APh and APy

In order to obtain some preliminary information regarding the photoinduced electron transfer reaction of the copolymers in aqueous solution, the fluorescence quenching of APh was studied. The quenchers used are the following two compounds, which satisfy the prerequisite of being water soluble and electron accepting but not energy accepting: an amphiphilic electron acceptor, BHET, and a hydrophilic acceptor, FA.

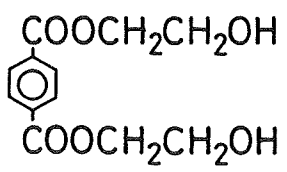

BHET

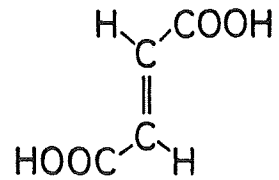

FA

The half-wave reduction potential $E_{red,1/2}$ for FA is reported to be -1.71 V vs. SCE[10], and since there has been no report on the $E_{red,1/2}$ for BHET, we determined it to be -1.42 V vs. SCE by cyclic voltammetry. These compounds are considered to act thermodynamically as electron acceptors toward Ph in its excited state because the $E_{ox,1/2}$ for the excited Ph can roughly be estimated as -2.07 V vs. SCE simply subtracting the excitation energy of Ph from the oxidation potential for Ph (+1.50 V vs. SCE[11]). Since the lowest-energy absorption band of these compounds appears at a shorter wavelength than that of Ph, the possibility of energy transfer from excited Ph to them is

precluded.

Figure 1 shows the fluorescence spectra of the 1 x 10^{-4} M Ph residue of APh-58 in pure water in the presence of various amount of BHET. Considerable quenching of the fluorescence intensity was observed.

The fluorescence quenching of the copolymer was characterized by the dependence of I_0/I on the concentration of the quencher [Q], where I_0 and I are emission intensity of the excited Ph in the absence and in the presence of the quencher, respectively. Figure 2 shows the dependence of I_0/I on [BHET] for APh with various VPh contents in aqueous solution. The fluorescence of APh was quenched more effectively with increasing VPh-unit content. The data for APh-15 and APh-3 as well as that for the monomer model (AM) gave linear plots, following the Stern-Volmer equation:

$$I_0/I = 1 + K_{SV}[Q]$$

$$K_{SV} = k_q\tau$$

where K_{SV} is the Stern-Volmer quenching constant, k_q the second-order rate constant for fluorescence quenching, and τ the fluorescence lifetime in the absence of quencher. This implies that the quenching of these copolymers is governed by dynamic processes. Further, it should be noted that the quenching for these polymers is less effective than that for AM. Figure 2

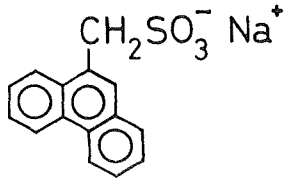

AM

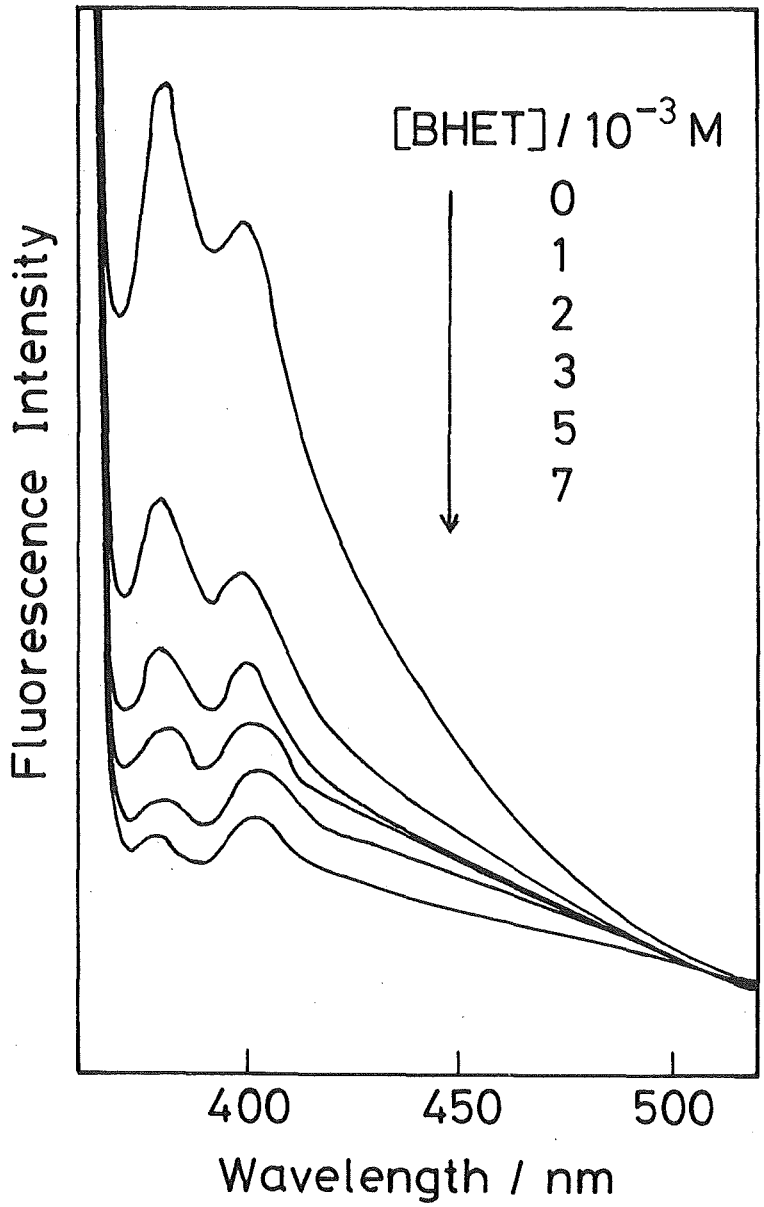

Figure 1. Fluorescence spectra of APh-58 in aqueous solution in the presence of various concentrations of BHET: excitation wavelength, 352 nm.

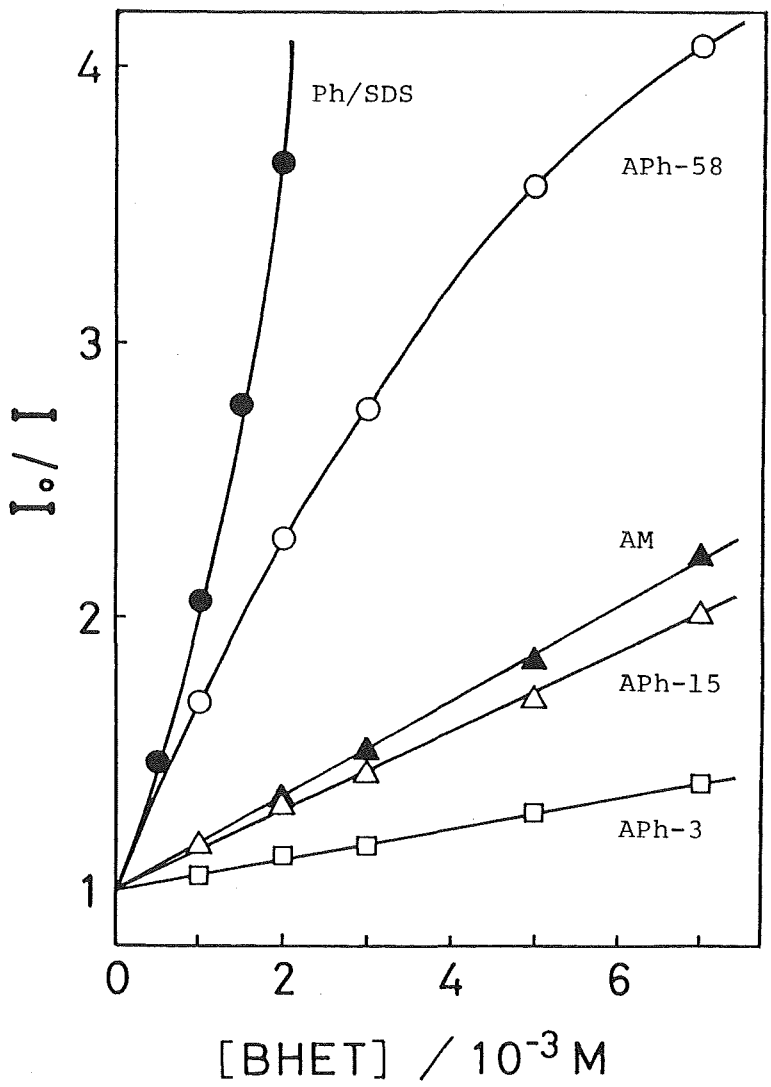

Figure 2. Stern-Volmer plots for the fluorescence quenching of APh with various f_{Ph}, AM, and Ph in SDS by BHET in aqueous solution: ○, APh-58; △, APh-15; □, APh-3; ●, Ph/SDS; ▲, AM.

also includes the plots for Ph solubilized in SDS micelles where the fluorescence is strongly quenched. The data for the micellar system and for APh-58, however, did not follow the Stern-Volmer equation; i.e., in the former case the plots deviated upward from the straight line, while in the latter downward. A model for interpreting fluorescence quenching results in micellar solutions has been proposed whereby the quenchers that are distributed in the micellar phase obey Poisson statistics and the quenching process in the micellar phase is described by a first-order rate constant[12]. This model also explains the upward deviation from the Stern-Volmer plots for the micellar system in the present study. On the other hand, the fluorescence quenching of APh-58 seems to be ruled by some other mechanism.

FA quenched the fluorescence of Ph in SDS micelles and of APh far less effectively than BHET. With FA as a quencher, the plots for all copolymers followed the Stern-Volmer dependence.

The K_{SV}'s for the linear plots were calculated by the least-squares method, while those for the nonlinear plots were estimated from their initial slope. The k_q's, calculated from the K_{SV}'s and the τ's, are summarized in Table I. The lifetime τ of the copolymer was reduced as the VPh content increased presumably because of the self-quenching of the excited VPh units. On the other hand, the rate constant k_q increased with increasing VPh content for both BHET and FA. The k_q value for BHET was always larger than that for FA for all the copolymers. The k_q for BHET was about 3×10^{10} $M^{-1}s^{-1}$ for APh-58, which

was considerably higher than the rate constant for a diffusion-controlled reaction in an aqueous solution [$k_{diff} \sim 7 \times 10^9$ $M^{-1}s^{-1}$ (ref. 13)]. However, the k_q for the monomer model (AM) was close to this value. These observations are explicable in terms of the increased local concentration of the quenching agent around the VPh sequences, which results from hydrophobic interaction. The mechanism for quenching could be a dynamic or a static process. The former process requires the collision between the fluorophore and quencher in a solution where the both can move freely. In this case the k_q approximates that of a diffusion-controlled process. The latter mechanism involves interaction of a "quenching sphere" with the fluorophore. Such a process can be favored by the proximity of quenchers to the fluorophore through hydrophobic association. As described above, from the

Table I. Rate constants for the fluorescence quenching of APh in aqueous solution

Sample	f_{Ph}	τ/ns	K_{SV}/M^{-1}		$k_q \times 10^{-9}/M^{-1}s^{-1}$	
			BHET	FA	BHET	FA
APh-58	0.58	20	610[a]	97.2	30	4.9
APh-15	0.15	37	145	72.1	3.9	1.9
APh- 3	0.03	38	57.3	52.3	1.5	1.3
Ph/SDS[b]	—	—	940[a]	49[a]	—	—
AM	—	34	171	116	5.0	3.4

a) Calculated from the initial slope of the Stern-Volmer plot.

b) Measured without deaeration; [SDS]=1×10^{-1} M.

value of k_q in Table I it is reasonable to consider that the quenching of APh-15 and APh-3 with BHET is a dynamic process[13]. However, the k_q for APh-58 appeared to be considerably higher than that predicted for the diffusion-controlled reaction[13]. This may be the consequence of the fact that for the Stern-Volmer analysis stoichiometric concentrations of BHET were used instead of local concentrations around fluorophores, although the quenching mechanism may be a totally dynamic process. Another possibility is that some of the quenchers are so closely bound to the rigid hydrophobic microdomains of VPh sequences that a static quenching process is also contributing to some extent. The latter idea seems to be in accord with the fact that a hydrophobic fluorescence probe (ANS) is quite effectively taken up by APh with higher f_{Ph}[14]. An increase of the cross section of the quenching reaction arising from energy migration along the aromatic sequences is a further factor to be taken into account. Enhancement of quenching assisted by energy migration was observed in polymer systems[15]. However, this effect seems not to be so large in homogeneous solutions[16]. Thus, we consider this effect to be rather a minor factor in the present system because the large k_q was obtained only for BHET (amphiphilic quencher) in aqueous solution (Table I) and the k_q depended mildly on f_{Ph} in DMF (vide infra). In DMF the effect of hydrophobic interaction is nil and that of charge is also minimized. Reference data obtained in this solvent are listed in Table II. Several interesting features emerge from the comparison of data obtained in aqueous and in DMF solutions. The k_q's in DMF are all smaller than those observed

in aqueous soution and fall in the range predicted from the diffusion-controlled reaction. It should be stressed that in DMF there was little difference in the k_q's for BHET and for FA. Furthermore, the Stern-Volmer plots of all copolymers in this solvent gave straight lines. An increase of k_q with increasing VPh content in DMF may be an implication of the contribution of energy migration as described above. These results strongly support the above-mentioned interpretation of the characteristic behavior of fluorescence quenching in aqueous media. Quenching mechanism in aqueous solution will be discussed in some details in the later section.

The presence of excimer emission makes the fluorescence quenching process of APy more complicated than that of APh. We found, however, that the Stern-Volmer plots showed little deviation from a straight line for both the monomer fluorescence and the excimer emission (plots are not illustrated). The life-times were not determined in this case because both the monomer-

Table II. Rate constants for the fluorescence quenching of APh in DMF solution

Sample	f_{Ph}	τ/ns	K_{SV}/M^{-1}		$k_q x10^{-9}/M^{-1}s^{-1}$	
			BHET	FA	BHET	FA
APh-58	0.58	34	50.8	61.3	1.5	1.8
APh-15	0.15	42	49.1	44.2	1.2	1.1
APh- 3	0.03	44	30.8	31.6	0.70	0.72
Ph	—	52[a)]	81.2	117	1.6	2.2
PVPh	1.0	22	34.1	40.6	1.6	1.8

a) Measured in dioxane.

and excimer-emission response curves were complex and did not exhibit simple exponential decay. Therefore the k_q could not be calculated. Table III lists K_{SV}'s for APy with various f_{Py}. K_{SV}'s for APy are larger than those for APh listed in Table I. These differences, however, are not considered to be associated with the differences in k_q but are probably ascribable to longer τ for APy than APh (we judge τ for the monomer emission to be roughly 100 ns from the decay patterns). It is also noted that K_{SV}'s for the excimer emission are always larger than those for the monomer emission for both BHET and FA. This apparent effectiveness of the excimer quenching is presumed to be a results of the fact that the quenching of the monomer emission

Table III. Stern-Volmer constants for the fluorescence quenching of APy in aqueous solution

Sample	f_{Py}	K_{SV}(monomer)/M^{-1} a)		K_{SV}(excimer)/M^{-1} b)	
		BHET	FA	BHET	FA
APy-32	0.32	340	220	1400	260
APy-16	0.16	320	230	890	330
APy-0.6	0.006	200	140	—	—
Py/SDS[c)]	—	2000[d)]	170[d)]	—	—
PyS[e)]	—	330	270	—	—

a,b) Stern-Volmer constants for the quenching of monomer and excimer emissions, respectively.

c) Measured without deaeration; [SDS]=$1x10^{-1}$ M.

d) Calculated from the initial slope of the Stern-Volmer plot.

e) Sodium 1-pyrenesulfonate.

indirectly contributes to the excimer quenching in addition to the direct quenching. While all these complexities and the uncertainty of the lifetime prevent further insight into the quenching mechanism, it can be safely concluded that the fluorescence of APy with high f_{Py} was quenched more effectively by BHET than by FA in aqueous solution, as was the case for APh.

3-3-2. Fluorescence Quenching of b-VPh

In the preceding section, it was reported that oxidative electron transfer quenching of the excited state of the Ph groups in amphiphilic random copolymers occurs efficiently with BHET, an amphiphilic quencher, in aqueous media. This section deals with the block copolymers. Figure 3 shows the fluorescence spectra of the 1×10^{-4} M Ph residue of the block copolymer in neat water in the presence of increasing amounts of BHET. Clearly, a considerable quenching of the fluorescence intensity is observed not only at the emission maximum but over the whole wavelength region even when the concentration of BHET added is considerably low.

Figure 4 illustrates the dependence of I_0/I on the concentration of BHET for the block copolymer and its related random copolymer (MPh-21) in the aqueous solution buffered at pH 9. The data for MPh-21 gave a linear plot obeying the Stern-Volmer equation. On the other hand, quenching of the block-copolymer fluorescence was far more effective than that of the random copolymer and the data showed deviation from the Stern-Volmer equation.

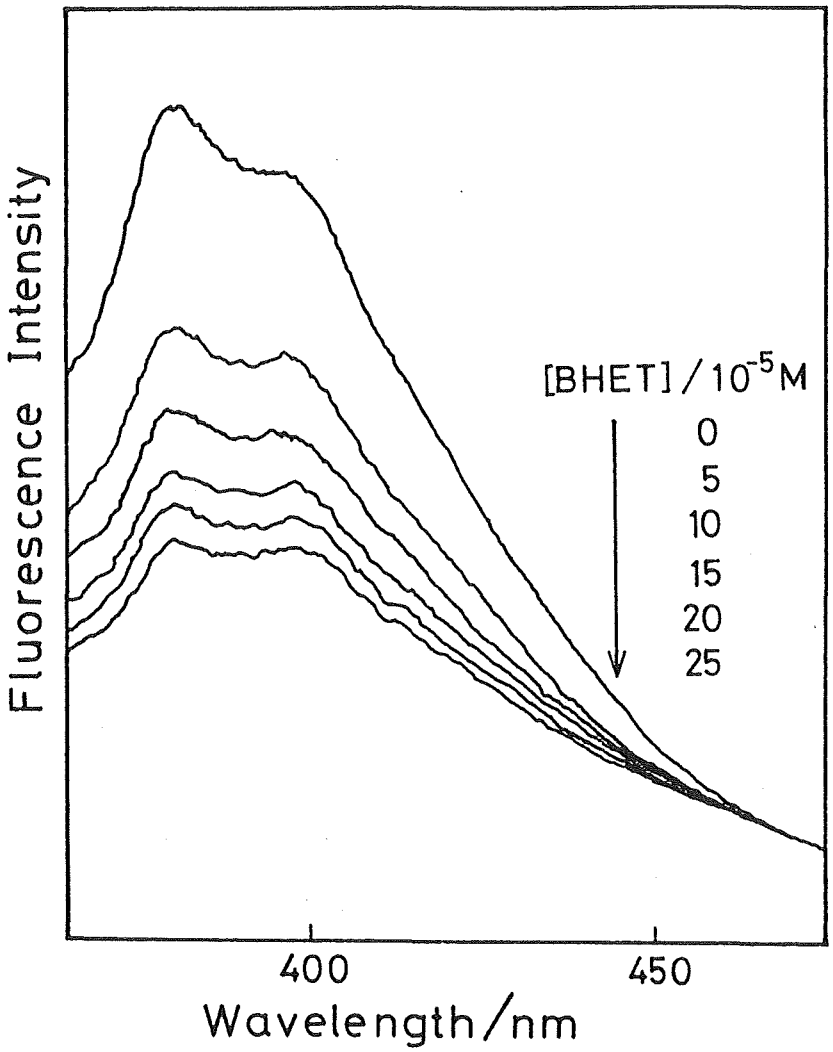

Figure 3. Effect of BHET on the fluorescence spectra of b-VPh-23 in pure water: $[VPh]_{residue}=1x10^{-4}$ M.

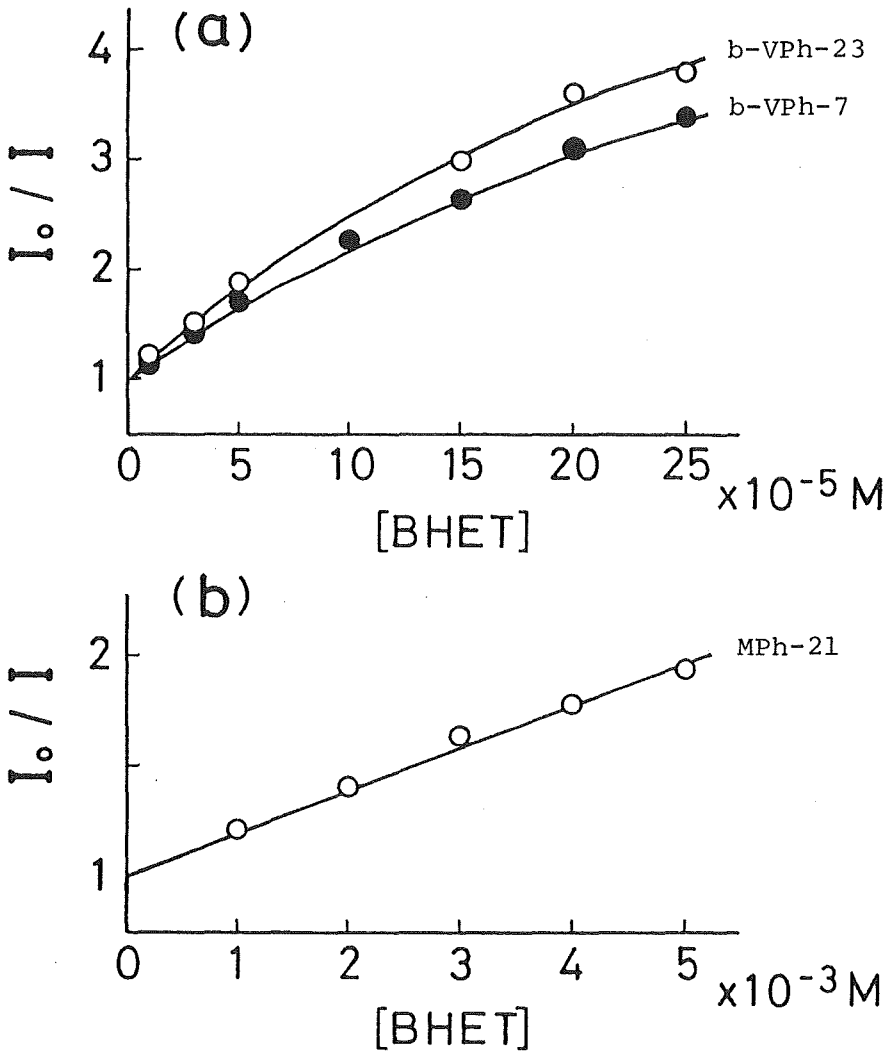

Figure 4. Stern-Volmer plots for the fluorescence of Ph by BHET in borate buffer (pH 9): (a) block copolymer; ○, b-VPh-23; ●, b-VPh-7; (b) random copolymer (MPh-21); $[VPh]_{residue}=4x10^{-4}$ M.

Quenching data for various block copolymers and a random copolymer were obtained in aqueous solutions of pH 9 and pH 7. The results are summarized in Table IV. K_{SV} and k_q were calculated in the same manner as described in the preceding section. The natural lifetime of fluorescence τ was measured in neat water because it was found to be almost independent of pH. These results in Table IV establish that the block and random copolymers exhibit vastly varying quenching efficiency toward the amphiphilic quenching agent; i.e., k_q's for block copolymers are approximately two orders of magnitude higher than that for the random copolymer. These observations are explicable in terms of the increased local concentration of the amphiphilic quencher around the microdomains of VPh block sequences resulting from the hydrophobic interaction as described in the preceding section. From the value of k_q in Table IV, it may be said that the quenching of the random copolymer is a dynamic process. However, k_q's for the block copolymer appeared to be considerably higher than that predicted for the diffusion-controlled reaction[13], implying the contribution of a static quenching process. In fact, we propose a kinetic model, which involves both dynamic and static mechanisms occurring concurrently, to explain the downward deviation of the Stern-Volmer plot for the block copolymer. This will be discussed in the later section. Reference data on the fluorescence quenching were obtained in DMF in which the effects of hydrophobic interaction are nil (Table V). The Stern-Volmer plots for the block copolymers in this solvent gave straight lines and k_q's

Table IV. Rate constants for fluorescence quenching of b-VPh by BHET at pH 9 and 7[a)]

Copolymer	$\overline{DP}_{VPh}$[b)]	τ/ns[c)]	at pH 9[d)]		at pH 7[e)]	
			K_{SV}/M^{-1}	$k_q/M^{-1}s^{-1}$	K_{SV}/M^{-1}	$k_q/M^{-1}s^{-1}$
b-VPh-43	43	12	—	—	38000[f)]	3.2×10^{12}
b-VPh-23	23	20	17000[f)]	8.5×10^{11}	29000[f)]	1.5×10^{12}
b-VPh-16	16	—	—	—	22000[f)]	—
b-VPh- 7	7	18	14000[f)]	7.8×10^{11}	21000[f)]	1.2×10^{12}
MPh-21	—	25	195	7.8×10^{9}	830	3.3×10^{10}

a) Measured without deaeration; $[VPh]_{residue}=4\times10^{-4}$ M.

b) $\overline{DP}$ of VPh sequence in the block copolymer.

c) Meadured in pure water.

d) Borate buffer (μ=0.02).

e) Phosphate buffer (μ=0.06).

f) Calculated from the initial slope of the Stern-Volmer plot.

thus obtained are more than two orders of magnitude lower than those obtained in aqueous solution. These values fall in the range predicted from the diffusion-controlled reaction[13]. It should be stressed that in DMF there was no difference in the magnitude of k_q between the block and random copolymers. These results strongly support the contribution of hydrophobic interaction to the quenching in aqueous media. It is interesting to note that k_q's for b-VPh were still an order of magnitude larger than that for the random copolymer with the highest hydrophobicity (APh-58) in aqueous solution (Table I and IV). This implies that the block copolymers exhibit much clearer phase separation than the random copolymer.

Being a weak acid, polyMA is not completely dissociated at pH 7[17,18]. Unlike poly(acrylic acid) undissociated polyMA sequences are known to somewhat hydrophobic in nature[19], which would favor the hydrophobic association of BHET around the polymer. In other words, undissociated portions of MA sequences

Table V. Rate constants for fluorescence quenching of b-VPh by BHET in DMF solution[a)]

Copolymer	$\overline{DP}_{VPh}$ [b)]	τ/ns	K_{SV}/M^{-1}	$k_q/M^{-1}s^{-1}$
b-VPh-43	43	14	25	1.8×10^{9}
b-VPh- 7	7	21	26	1.2×10^{9}
MPh-21	—	24	30	1.3×10^{9}

a) Measured without deaeration; $[VPh]_{residue}=3\times10^{-4}$ M.
b) $\overline{DP}$ of VPh sequence in the block copolymer.

may participate in the hydrophobic association of VPh sequences in a cooperative way and, as a result, the formation of hydrophobic microdomain is greatly facilitated. This seems to be a reason for k_q being higher at pH 7 than at pH 9, especially in the case of random copolymer (Table IV).

FA, a hydrophilic quenching agent with anionic nature, also acts as an oxidative quencher toward the excited state of Ph[20]. However, the fluorescence of the block and random copolymers was not virtually quenched at pH 7 and 9 even with 10^{-2} M of FA (approximately two orders of magnitude higher than the Ph residual concentration)*. These observations can be rationalized in terms of the electrostatic repulsion between the negative potential surrounding the fluorophores and the anionic quenchers, because FA is negatively charged due to dissociation of the dicarboxylates at these pH's.

In pure water only a part of MA sequences are expected to be dissociated[18]. Hence it is assumed that, as mentioned above, both block and random copolymers greatly increase their hydrophobicity and at the same time considerably decrease their ionic nature. Table VI shows the quenching data obtained in pure water. Interestingly, FA effectively quenched both block and random copolymers equally in pure water. This is

---

* Since K_{SV}'s are extremely small, it was impossible to obtain reliable values from the Stern-Volmer relation plotted in the range of 10^{-2} M of FA. However, it was obvious that all K_{SV}'s could not exceed 10 at the highest.

Table VI. Rate constants for fluorescence quenching of b-VPh by BHET and FA in pure water[a)]

Copolymer	$\overline{DP}_{VPh}$ [b)]	τ/ns	BHET		FA	
			K_{SV}/M^{-1}	$k_q/M^{-1}s^{-1}$	K_{SV}/M^{-1}	$k_q/M^{-1}s^{-1}$
b-VPh-43	43	12	21000[c)]	1.8×10^{12}	102	8.5×10^{9}
b-VPh-23	23	20	19000[c)]	9.5×10^{11}	84	4.2×10^{9}
b-VPh-16	16	—	11000[c)]	—	78	—
b-VPh- 7	7	18	10000[c)]	5.6×10^{11}	54	3.0×10^{9}
MPh-21	—	25	8400[c)]	3.4×10^{11}	71	2.8×10^{9}

a) Measured without deaeration; $[VPh]_{residue}=4\times10^{-4}$ M.

b) $\overline{DP}$ of VPh sequence.

c) Calculated from the initial slope of the Stern-Volmer plot.

probably the result of the increase of hydrophobic interaction parallel with the decrease of the electrostatic repulsion between the polymer and FA in pure water in which the dissociation of the carboxy groups is highly limited. Such a behavior of MA sequences would result in the random copolymer also being highly hydrophobic, as mentioned above. Thus the k_q for the random copolymer greatly increases in pure water and is of the same order of magnitude as those for the block copolymers.

3-3-3. Fluorescence Quenching of QPh

In the previous sections, we revealed that the oxidative electron transfer quenching of the excited Ph residues in various types of amphiphilic copolymers with anionic segments occurred effectively with BHET, an amphiphilic acceptor, in aqueous media. We demonstrated that these remarkable events originated from hydrophobic binding of the quencher molecules by hydrophobic microdomains consisting of Ph residues.

In this section, we used MHEA and DHEA, amphiphilic electron donor quenchers, to examine the photoinduced electron transfer processes in aqueous media. The half-wave oxidation

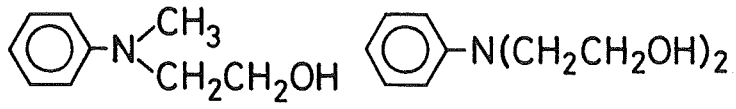

MHEA DHEA

potentials $E_{ox,1/2}$ for both MHEA and DHEA were determined by cyclic voltammetry to be +0.65 V vs. SCE. The lowest-energy absorption band of these compounds shows up at 297 nm, which is a shorter wavelength than that of the Ph group. These compounds are expected to act thermodynamically as electron donors toward excited Ph groups since the $E_{red,1/2}$ for excited Ph groups can roughly be estimated as +1.07 V vs. SCE by simply additing the excitation energy to the reduction potential for Ph (-2.51 V vs. SCE[21]).

Figure 5 shows the fluorescence spectra of the 1×10^{-4} M Ph residue of QPh-47 in pure water in the presence of various

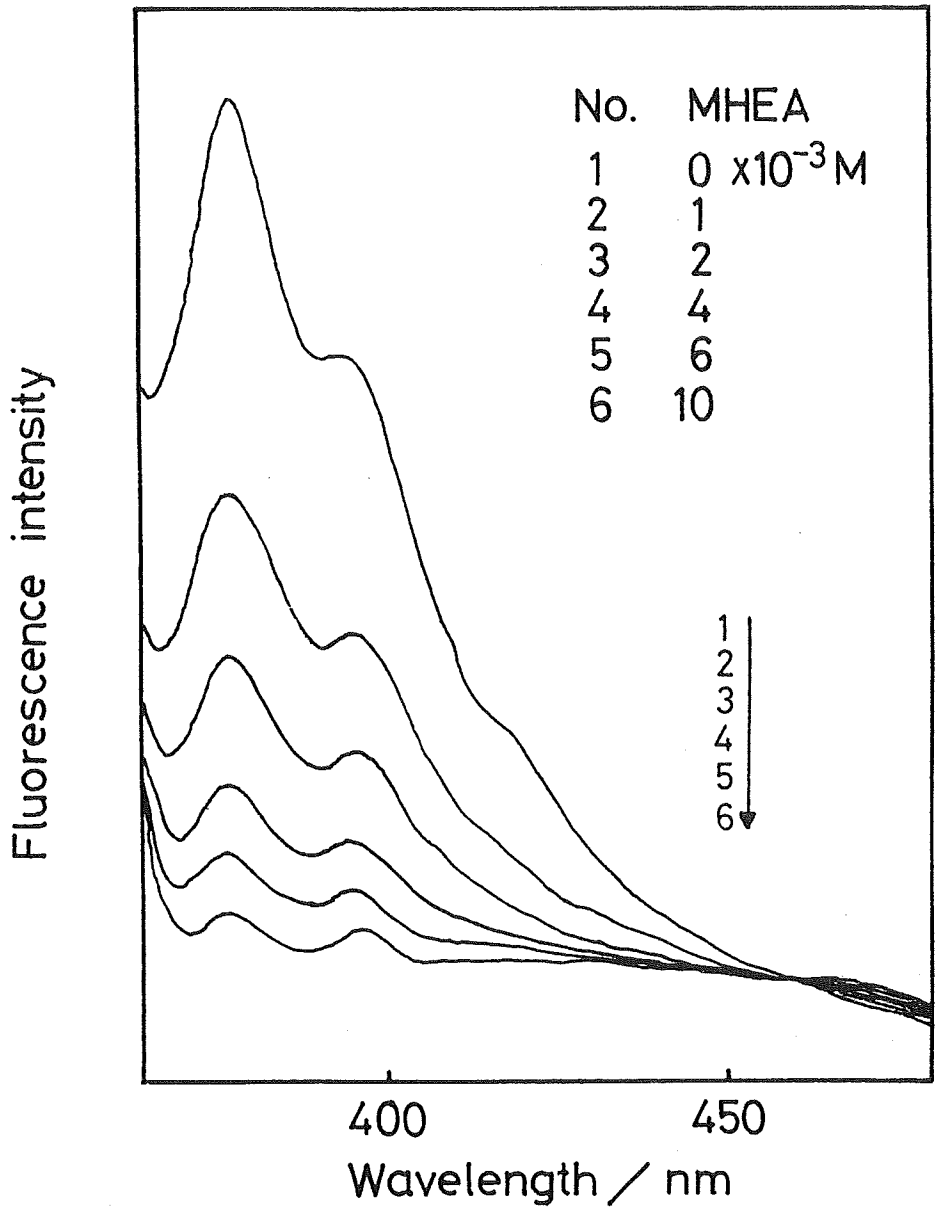

Figure 5. Fluorescence spectra of QPh-47 in aqueous solution in the presence of various concentrations of MHEA: excitation wavelength, 352 nm.

amounts of MHEA. Considerable quenching of the fluorescence intensity at the emission maximum was observed, whereas this intensity in the longer wavelength region slightly increased with an isoemissive point appearing at 460 nm as the amount of quencher increased. We have no explanation for this except that the possibility of exciplex formation cannot be precluded.

Figure 6 illustrates the typical example of the Stern-Volmer plots for the copolymers and the monomer model (QM) in

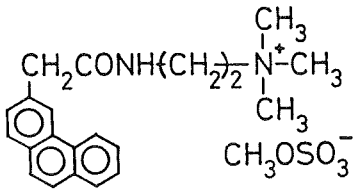

QM

aqueous solution. A distinctive feature in Figure 6 is that, qualitatively speaking, the fluorescence of the copolymer with a higher f_{Ph}, QPh-47, is quenched far more effectively by MHEA and that the plots fail to follow the Stern-Volmer equation. These phenomena were often encountered with various amphiphilic copolymers hitherto investigated in previous studies (section 3-3-1 and 3-3-2). On the other hand, the fluorescence quenching of the copolymer with lower f_{Ph}, QPh-14, and the related monomer model, QM, by MHEA exactly followed the Stern-Volmer equation. Table VII summarizes the results for the copolymers of various VPh content. The k_q for both MHEA and DHEA with QPh-47 were considerably higher than the rate constant predicted from the diffusion-controlled kinetics in an aqueous solution. These values for QM were about the same order of

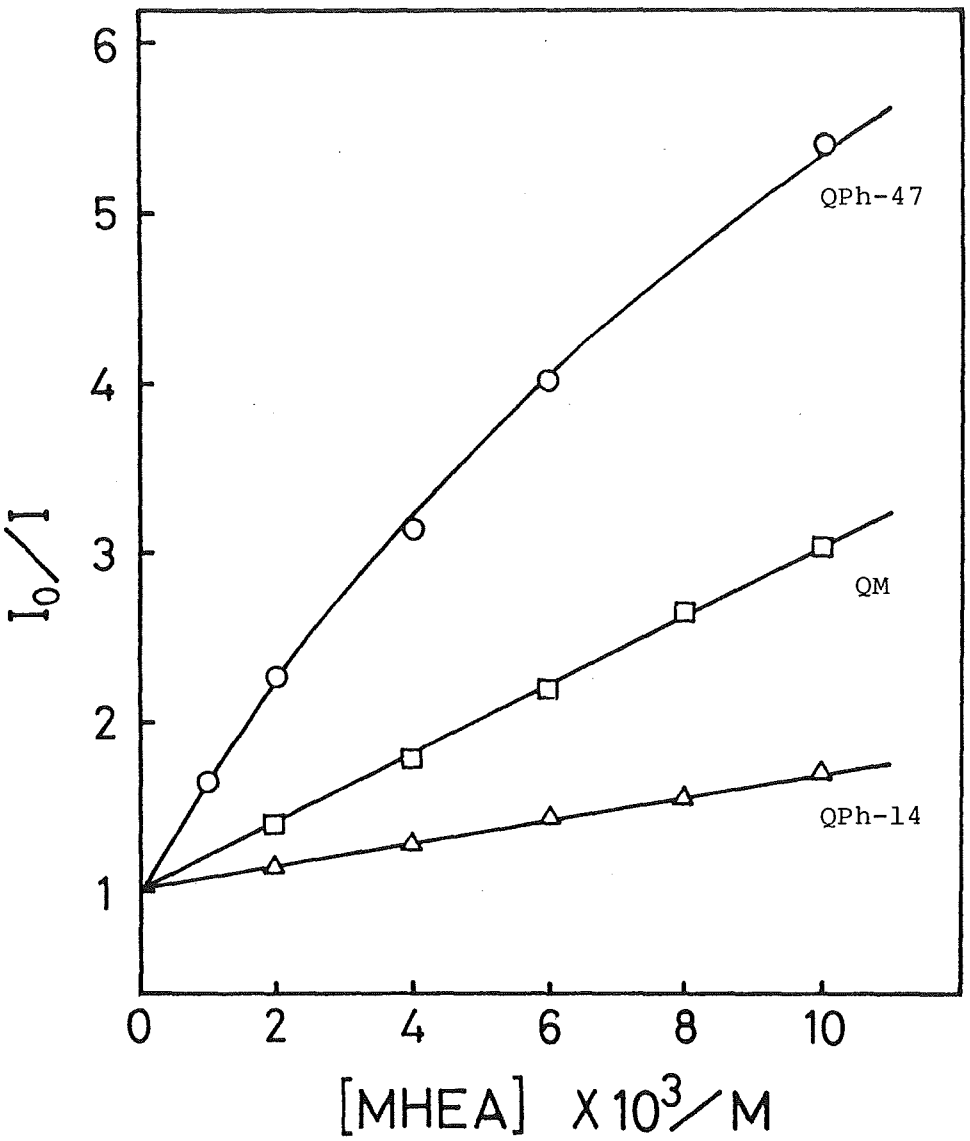

Figure 6. Stern-Volmer plots for QPh-MHEA system in aqueous solution: ○, QPh-47; △, QPh-14; □, QM.

Table VII. Rate constants for the fluorescence quenching of QPh by MHEA and DHEA in aqueous solution

Copolymer	f_{Ph}	τ/ns	K_{SV}/M^{-1}		$k_q x10^{-9}/M^{-1}s^{-1}$	
			MHEA	DHEA	MHEA	DHEA
QPh-47	0.47	34	630[a)]	400[a)]	18	12
QPh-28	0.28	39	153	120	3.9	3.1
QPh-14	0.14	42	73.0	71.3	1.7	1.7
QPh- 7	0.07	44	45.4	53.7	1.0	1.2
QM	—	44	203	184	4.6	4.2

a) Calculated from the initial slope of the Stern-Volmer plot.

Table VIII. Rate constants for the fluorescence quenching of QPh by MHEA and DHEA in DMF solution

Copolymer	f_{Ph}	τ/ns	K_{SV}/M^{-1}		$k_q x10^{-9}/M^{-1}s^{-1}$	
			MHEA	DHEA	MHEA	DHEA
QPh-47	0.47	40	28.4	21.8	0.71	0.55
QPh-14[a)]	0.14	41	16.3	10.0	0.39	0.24
QM	—	53	179	144	3.4	2.7
PVPh	—	22	23.8	11.2	1.1	0.51
Ph	—	52	210	130	4.0	2.5

a) Measured in DMSO solution.

magnitude as that of the diffusion-controlled reaction[13]. However, k_q for the copolymers with f_{Ph} less than 0.28 were all much lower than those for QPh-47 and even lower than those of the monomer model (QM). These observations are consistent with those for APh and also explicable in terms of the increased local concentration of amphiphilic quencher around the fluorophore resulting from the hydrophobic interaction. Reference data obtained in DMF support the presence of hydrophobic interaction between QPh-47 and the quencher in aqueous solution (Table VIII). Namely, the Stern-Volmer plots for QPh-47 in this solvent gave a linear relationship and k_q's thus obtained were much lower than those obtained in aqueous solutions. On the other hand, k_q's for QM observed in DMF were only slightly lower than those in aqueous solution. It should be also noted that k_q's for the polymers were lower than those for QM in both solvents (except for QPh-47 in water). Table VIII also includes the rate constants for PVPh homopolymer and Ph itself for reference. In this comparison, k_q's for Ph itself were also found to be four or five times larger than those for the homopolymer. In a homogeneous solution, where both the fluorophore and quencher can move freely, k_q approximates the value of diffusion-controlled kinetics when the quencher is sufficiently effective. The difference in the redox potential between the fluorophore and quencher can roughly be a measure of the effectiveness of the quenching agent in a homogeneous solution[22]. In this sense, parallel with the fact that k_q's for the monomer

model (QM) with MHEA and DHEA in both solvents are very close to the diffusion-controlled limit, both quenching agents are regarded as being effective enough. Thus, we may interpret that the less accessibility of the quencher molecule to the fluorophore surrounded in the polymer matrix is reflected in the lower values of k_q observed for the polymer in both DMF and water.

For comparison with the anionic copolymers (APh), the oxidative quenching of QPh with BHET and FA was also investigated. The fluorescence of QPh was effectively quenched by BHET. The quenching data for QPh are, qualitatively, very similar to those for APh (Table IX), indicating that the hydrophobic interaction plays an important role in the quenching. On the contrary, the quenching with FA was much different between them (Table X). The fluorescence

Table IX. Rate constants for the fluorescence quenching of QPh and APh by BHET in aqueous solution

Sample	f_{Ph}	τ/ns	K_{SV}/M^{-1}	$k_q \times 10^{-9}/M^{-1}s^{-1}$
QPh-47	0.47	34	1500[a)]	44
QPh-14	0.14	42	71.7	1.7
QM	—	44	215	4.9
APh-58	0.58	20	610[a)]	30
APh-15	0.15	37	145	3.9
AM	—	34	171	5.0

a) Calculated from the initial slope of the Stern-Volmer plot.

quenching of QPh with this quenching agent was found to occur quite effectively in pure water, in which FA anions are probably electrostatically bound to the cationic sphere of QPh. The Stern-Volmer plots strongly deviated downward from the linear relation and the apparent second-order rate constants for the quenching estimated from the initial slope were found to be extremely high; all values fell in the range of 1-6 x 10^{11} M^{-1} s^{-1} for QPh-FA systems (Table X). However, in acidic solution, the fluorescence was quenched far less effectively than in pure water; the plots obeyed the Stern-Volmer relation and k_q was of the order of 10^9 $M^{-1}s^{-1}$ (Table X). This drastic difference in the quenching behavior of QPh in pure and acidic aqueous solutions is shown in Figure 7. It should be stressed that no such difference was observed with the monomer model shown in Figure 7. These results indicate a dramatic effect of a potential field generated by polyions with a high density of fixed charge along the polymer chain. A single charge combined in the neighborhood of a fluorophore, as in the case of QM, is not sufficiently effective to bind the quencher electrostatically and thus facilitate the quenching process. On the other hand, the fluorescence of APh was quenched less effectively than that of QPh in pure water. However, in spite of the electrostatic repulsion between the anionic segments of APh and FA anion, the k_q's for APh are not much smaller than that for the monomer model (AM) (Table X).

Tavle X. Rate constants for the fluorescence quenching of QPh and APh by FA in aqueous solution

Sample	f_{Ph}	τ/ns	K_{SV}/M^{-1}		$k_q x10^{-9}/M^{-1}s^{-1}$	
			pure	acidic[a)]	pure	acidic[a)]
QPh-47	0.47	34	20000[b)]	279	590	8.2
QPh-14	0.14	42	4380	88.4	100	2.1
QM	—	44	224	—	5.1	—
APh-58	0.58	20	97.2	—	4.9	—
APh-15	0.15	37	72.1	—	1.9	—
AM	—	34	116	—	5.0	—

a) Measured in 0.2 N H_2SO_4 solution.

b) Calculated from the initial slope of the Stern-Volmer plot.

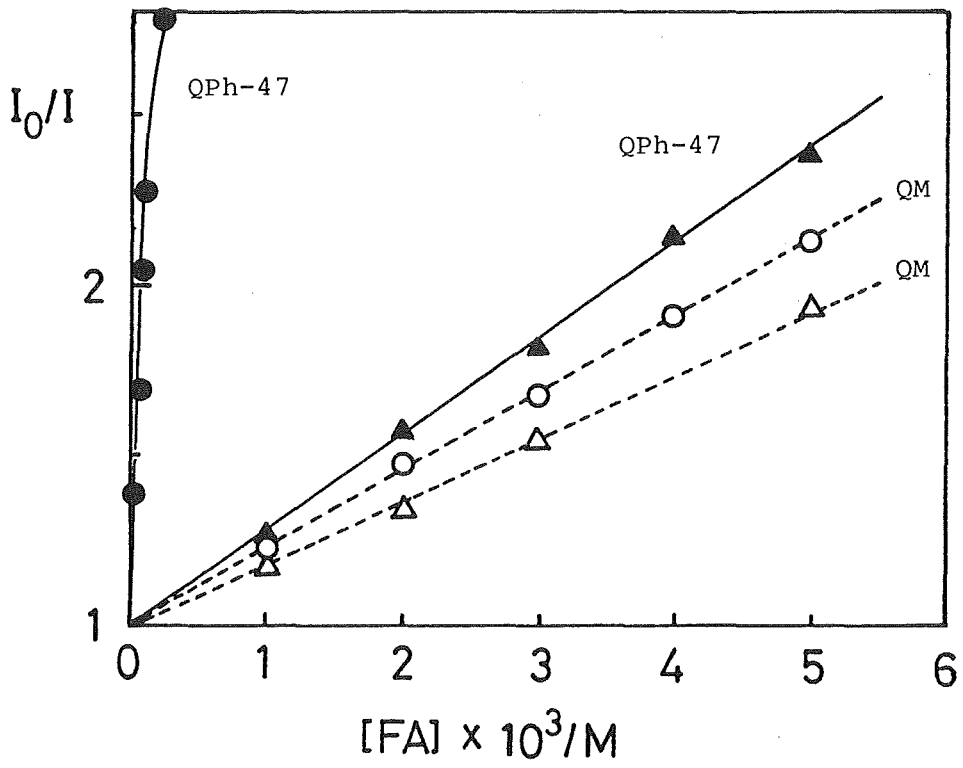

Figure 7. Stern-Volmer plots for the fluorescence quenching of QPh-47 and QM by FA in aqueous solutions: —●— and ---○---, QPh-47 and QM in pure water; —▲— and ---△---, QPh-47 and QM in 0.2 N H_2SO_4, respectively.

3-3-4. A Kinetic Model for Downward Curvature in a Stern-Volmer Plot

In the previous sections, we have encountered the remarkable observation that the fluorescence from the Ph groups in amphiphilic copolymers is quenched by amphiphilic quenchers such as BHET in aqueous solutions far more effectively than predicted by diffusional quenching. In such cases, plots of I_0/I versus the quencher concentration showed strong downward deviations from the Stern-Volmer equation. The apparent Stern-Volmer constant $K_{SV,0}$ calculated from the initial slope of the plots showed conspicuously large values, indicating extreme effectiveness of the quencher even when its concentration is extremely low. These facts obviously reflect the intrinsic heterogeneous character of the aqueous solution of these amphiphilic polymer, which requires the development of new concepts in reaction kinetics. We propose in this section a specific kinetic model for such systems on the basis of a multi-step equilibrium for the binding of the amphiphilic quenchers to the hydrophobic microdomains.

Distribution of Quenchers

We assume that all hydrophobic chromophores in amphiphilic copolymers such as block copolymer (b-VPh) and random copolymer (APh) self-associate through the hydrophobic interaction in aqueous media to form microdomains with an average aggregation number $\bar{n}$. Amphiphilic quenchers are taken up by hydrophobic microdomains leading to the distribution of the quencher

molecules among the domains and bulk aqueous phase. In analogy to micellar systems[12,23-31], a stepwise association model can be assumed to this process:

$$[M_{n,i-1}] + [Q] \overset{K_i}{\rightleftharpoons} [M_{n,i}], \text{ where } i=0,1,2, \cdots \quad (1)$$

where $[M_{n,i}]$ is the concentration of the microdomain of average aggregation number $\bar{n}$ associated with i quencher molecules, [Q] the concentration of the quencher in the bulk aqueous phase, and K_i the binding constant of the ith association step. We assume that at each step the rate constant for the association of quencher is equally given by k_a whereas that for the quencher escape is proportional to the number of quenchers bound in the microdomain; thus the distribution of the quencher molecules among the microdomains obeys Poisson statics[12,23-31]. In this situation the total concentration of the microdomain is given by

$$\sum_{i=0}^{\infty} [M_{n,i}] = [M_{n,0}] \sum_{i=0}^{\infty} \{(K_1[Q]^i/i!\}$$

$$= [M_{n,0}]\exp(K_1[Q]) \quad (2)$$

The total residual concentration of chromophore [M] can be written as

$$[M] = n[M_{n,0}]\exp(K_1[Q]) \quad (3)$$

The analytical concentration (macroscopic concentration) of quenchers bound in the microdomains is

$$\sum_{i=1}^{\infty} i[M_{n,i}] = [M_{n,0}]K_1[Q]\exp(K_1[Q]) \quad (4)$$

Therefore, the concentration of the quencher in the bulk aqueous phase is given by

$$[Q] = \{n/(K_1[M] + n)\}[Q]_0 \qquad (5)$$

where $[Q]_0$ is the analytical total concentration of the quenchers added to the system.

Steady-state Fluorescence Quenching

In Chapter 2, we discussed that the hydrophobic microdomains of such polymers as b-VPh and APh assume a rigid structure where the segmental motion of the chromophore groups is highly restricted as a result of strong hydrophobic interaction. This situation is considered to be favorable to the energy-transfer process[32]. Therefore, if a chromophore is excited in the microdomain, then the excitation may "delocalize" throughout the microdomain as a result of energy migration[33]. This is a distinctive feature of the hydrophobic microdomain which is entirely composed of chromophores, while in common surfactant aggregates compartmentation of a single chromophore occurs under common experimental conditions. It is now assumed that the quenching process due to the quenchers associated with the microdomains is described by the first-order rate constant $k_{q,1}$ and that $k_{q,1}$ is independent of the number of quenchers present in the domains. This assumption seems to be reasonable when the delocalization of the excited state throughout the domain is taken into consideration. On the other hand, in surfactant micellar systems, it is assumed that the first-order

rate for the static quenching proportionally increases with the number of quencher molecules contained within a micelle[23,24,27,31]. This assumption is valid only in the situation where the intramicellar encounter frequency between the fluorophore and the quenchers is the decisive factor in the quenching process[24]. Obviously this is not the case for the system in the present study, where rapid intradomain migration of excitation energy to sites at which quenchers are bound leads to an effective static quenching. On the basis of the above assumptions we propose a simple kinetic model as

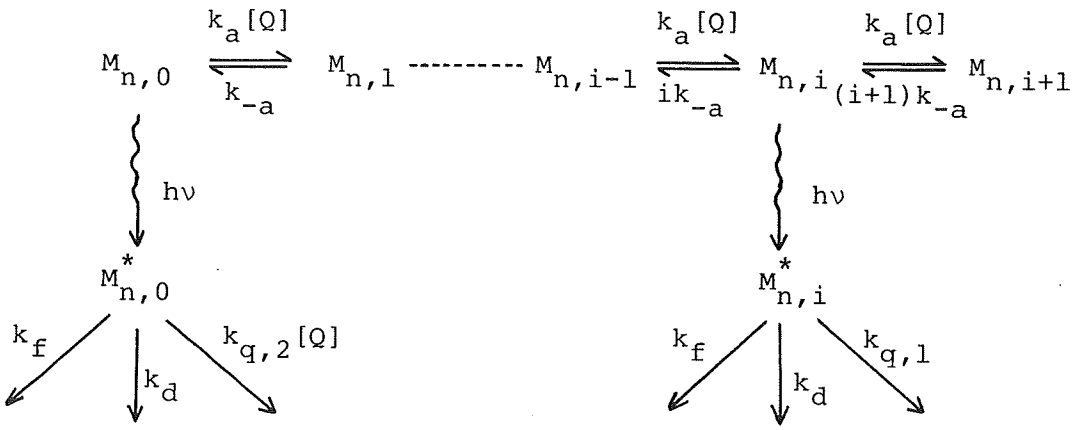

Scheme I

where k_{-a} is the dissociation rate constant of the first step association of quenchers to the microdomain, k_f and k_d the radiative and non-radiative decay constants, and $k_{q,2}$ the second-order rate constant for the diffusional quenching, respectively. We consider here only situations where the decay of the excited microdomain is fast relative to the exchange rate of the quencher molecules among the microdomains and the

bulk phase. The steady-state solution for scheme (I) leads to the concentrations of the excited microdomains as follows:

$$[M^*_{n,0}] = \left(\frac{I_a}{k_f + k_d + k_{q,2}[Q]}\right)\frac{n[M_{n,0}]}{[M]} \tag{6}$$

$$\sum_{i=0}^{\infty}[M^*_{n,i}] = \frac{\{k_f+k_d+k_{q,2}[Q]+(k_{q,1}-k_{q,2}[Q])n[M_{n,0}]/[M]\}I_a}{(k_f+k_d+k_{q,2}[Q])(k_f+k_d+k_{q,1})} \tag{7}$$

where I_a is the rate of light absorption. The ratio of the expected fluorescence intensities in the presence and in the absence of quencher is

$$\frac{I}{I_0} = \frac{\tau I_a}{\sum_{i=0}^{\infty}[M^*_{n,1}]} \tag{8}$$

where τ is the lifetime of the excited state in the absence of quenchers. Combination of eqs. (3), (5), (7), and (8) leads to

$$\frac{I_0}{I} = \frac{(1+\tau k_{q,1})(A+B[Q]_0)}{A+B[Q]_0+\tau(Ak_{q,1}-nk_{q,2}[Q]_0)\exp\{-(nK_1/A)[Q]_0\}} \tag{9}$$

where $A = K_1[M] + n$ and $B = n\tau k_{q,2}$. From eq. (9) one can easily see

$$\lim_{[Q]_0\to 0}(I_0/I) = 1 \tag{10}$$

$$\lim_{[Q]_0\to\infty}(I_0/I) = 1 + \tau k_{q,1} \tag{11}$$

Consequently, eq. (9) represents a downward curvature which is asymptotic to $1 + \tau k_{q,1}$ with the intercept of $I_0/I = 1$ in the I_0/I versus $[Q]_0$ coordinates. It is noted that for $K_1 \longrightarrow 0$ one obtains the Stern-Volmer equation $I_0/I = 1 + \tau k_{q,2}[Q]_0$ from eq. (9). The initial slope of the curve for eq. (9) is given by

$$\lim_{[Q]_0 \to 0} \left\{ \frac{d(I_0/I)}{d[Q]_0} \right\} = \frac{n(\tau k_{q,2} + K_1)}{K_1[M] + n} \qquad (12)$$

One can regard the initial slope as the apparent quenching coefficient $K_{SV,0}$. Eq. (12) reveals the linear relationship between the reciprocal of the $K_{SV,0}$ and the total residual concentration of chromophores added in the system as follows:

$$\frac{1}{K_{SV,0}} = \frac{K_1}{n(\tau k_{q,2} + K_1)}[M] + \frac{1}{\tau k_{q,2} + K_1} \qquad (13)$$

In the extreme case where $K_1 >> \tau k_{q,2}$, eq. (13) can be approximated as

$$\frac{1}{K_{SV,0}} \simeq \frac{1}{n}[M] + \frac{1}{K_1} \qquad (14)$$

Hence, from the slope and the intercept of the plot of $1/K_{SV,0}$ versus [M] one can estimate n and K_1, respectively. On the other hand, if $\tau k_{q,2} >> K_1$, then the simple Stern-Volmer relation $K_{SV,0} = \tau k_{q,2}$ is valid.

Application to the Experimental Result

We now describe our observations in the experiment on the quenching of the Ph fluorescence in the amphiphilic block copolymer (b-VPh) in aqueous solution[34]. As shown in Figure 4(a), the data shows strong downward deviation from the simple Stern-Volmer relation. The relationship between I_0/I and $[Q]_0$ was obtained for various concentrations of the Ph residue [M]. The $K_{SV,0}$ calculated from the initial slopes of the Stern-Volmer-type plots were plotted as a function of [M] to obtain a linear relationship as shown in Figure 8. From the intercept, $\tau k_{q,2} + K_1 = 3.7 \times 10^4\ M^{-1}$ was obtained. Because the τ for the fluorophore of the Ph residues in the block copolymer (b-VPh-23) is 2×10^{-7} s[34] and because the $k_{q,2}$ cannot exceed the value predicted from the diffusion-controlled limit ($\sim 7 \times 10^9\ M^{-1}s^{-1}$), the theoretical upper limit for the $\tau k_{q,2}$ is predicted to be $\sim 1.4 \times 10^3\ M^{-1}$. Therefore, the contribution of the dynamic quenching with BHET present in bulk can approximately be negligible; thus we could estimate $K_1 \sim (3.6\text{-}3.7) \times 10^4\ M^{-1}$. In these situations eq. (14) can be applied. From the slope of the plot in Figure 8 we could also estimate $n \simeq 26$, which coincides with the degree of polymerization of the Ph sequence in the block copolymer. Interestingly, this result indicates that in the concentration range employed in the peresent study the block copolymer forms a monomolecular microdomain in aqueous solution.

According to the present simple kinetic model, the general formulation for the downward curvature in a Stern-Volmer-type

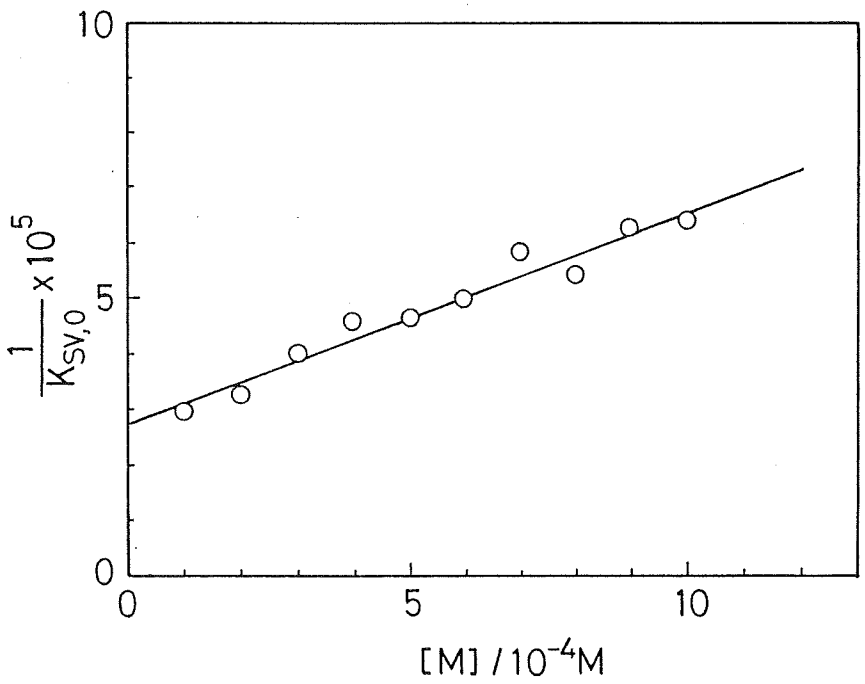

Figure 8. Dependence of the reciprocal of $K_{SV,0}$ on the residual concentration of Ph groups of b-VPh-23 in aqueous solutions: The solution contains 4.84×10^{-5} M of BHET as fluorescence quencher.

plot (eq. (9)) is given as a combination of the static and dynamic mechanisms. However, another possible interpretation of the downward curvature could be an idea that a Langmuir adsorption curve may simply reflect the plot. This could happen in the situation where only a limited number of the quenchers in the aqueous phase could be bound to the microdomains because a limited number of the binding sites may actually be available. This idea, however, seems to fail to explain the quenching behavior which involves both static and dynamic mechanisms occurring concurrently as in the following example. In the comparison of the Stern-Volmer-type plots among the copolymers of various Ph contents the plot tends to become more straight in nature (viz. the contribution of the dynamic quenching increases) with decreasing content of Ph in the copolymer. These facts seem to be only explicable by eq. (9) where n and K_1 decrease as the Ph content decreases.

The validity of this simple kinetic model has yet to be verified from various different aspects; e.g., analysis of the transient fluorescence quenching, computer simulation of eq. (9) for various examples, comparison of the binding constant with those determined by other techniques, etc.

3-4. Conclusion

The copolymers with higher hydrophobic-unit contents were found to take up a large amount of amphiphilic quencher through hydrophobic interaction in aqueous solution, resulting in the facilitation of the fluorescence quenching of the copolymers. In such cases, the quenching does not occur simply through the diffusional process. A kinetic model involving both the dynamic and static mechanisms well explains the characteristic behavior of quenching in aqueous media. Electrostatic binding of ionic quencher with the copolymer also resulted in severe quenching. This electrostatic effect on the quenching will be further investigated in the next chapter. These results suggest that the back reaction is also affected by the microenvironmental effects (hydrophobic and/or electrostatic) of the copolymers.

References

1) J. H. Fendler and E. J. Fendler, "Catalysis in Micellar and Macromolecular Systems", Academic Press, New York (1975).

2) K. Kalyanasundaram, Chem. Soc. Rev., 7, 453 (1978).

3) D. A. Holden and J. E. Guillet, Macromolecules, 13, 289 (1980).

4) C. A. Dornfeld and G. H. Coleman, "Organic Syntheses" Collective Vol. III, John Wiley and Sons Inc., New York, 1955, p701.

5) R. G. Jones, Q. F. Soper, O. K. Behrens, and J. W. Corse, J. Am. Chem. Soc., 70, 2843 (1948).

6) Y. Abe and H. Pei-Chin, Yukigoseikagaku, 33, 277 (1975).

7) F. F. Blicke and C. E. Maxwell, J. Am. Chem. Soc., 64, 428 (1942).

8) M. H. Benn, C. N. Owen, and A. M. Creighton, J. Chem. Soc. (London), 2800 (1958).

9) M. Yokoyama, Y. Fukui, N. Yamamori, and H. Mikawa, Abstracts of Papers, Molecular Structure Symposium, Fukuoka, 1980, p352.

10) P. J. Elving and C. Teitelbaum, J. Am. Chem. Soc., 71, 3916 (1949).

11) E. S. Pysh and N. C. Yang, J. Am. Chem. Soc., 85, 2124 (1963).

12) Y. Waka, K. Hamamoto, and N. Mataga, Photochem. Photobiol., 32, 27 (1980).

13) D. R. Arnold, N. C. Baird, J. R. Bolton, J. C. D. Brand,

P. W. N. Jacobs, P. de Mayo, and W. R. Ware, "Photochemistry", Academic, New York, 1974, p109.

14) section 2-3-2.

15) D. Ng and J. E. Guillet, Macromolecules, 15, 728 (1982) and references cited therein.

16) For example, T. Nakahira, T. Sakuma, S. Iwabuchi, and K. Kojima, J. Polym. Sci., Polym. Phys. Ed., 20, 1863 (1982).

17) A. M. Kotliar and H. Morawetz, J. Am. Chem. Soc., 77, 3692 (1955).

18) J. C. Leyte and M. Mandel, J. Polym. Sci., A, 2, 1879 (1964).

19) M. Nagasawa, T. Murase, and K. Kondo, J. Phys. Chem., 69, 4005 (1965).

20) section 3-3-1.

21) W. M. Clark, "Oxidation-Reduction Potentials of Organic systems", R. E. Kringer Publ. Co., New York, 1972.

22) D. Rehm and A. Weller, Ber. Bunsenges. Phys. Chem., 73, 834 (1969).

23) M. Tachiya, Chem. Phys. Lett., 33, 289 (1975).

24) S. S. Atik and L. A. Singer, Chem. Phys. Lett., 59, 519 (1978).

25) S. S. Atik, C. L. Kwan, and L. A. Singer, J. Am. Chem. Soc., 101, 5696 (1979).

26) S. S. Atik and J. K. Thomas, J. Am. Chem. Soc., 103, 3345 (1981).

27) A. Yekta, M. Aikawa, and N. J. Turro, Chem. Phys. Lett.,

63, 543 (1979).

28) P. P. Infelta, Chem. Phys. Lett., 61, 88 (1979).

29) M. Maestri, P. P. Infelta, and M. Grätzel, J. Chem. Phys., 69, 1522 (1978).

30) Y. Waka, K. Hamamoto, and N. Mataga, Chem. Phys. Lett., 53, 242 (1978).

31) Y. Waka, K. Hamamoto, and N. Mataga, Chem. Phys. Lett., 62, 364 (1979).

32) N. J. Turro, Pure Appl. Chem., 49, 405 (1977).

33) A. Somersall and J. E. Guillet, Macromolecules, 5, 410 (1972).

34) section 3-3-2.

Chapter 4

Electrostatic Effect of Amphiphilic Copolymers on the Forward Electron Transfer

4-1. Introduction

Separation of photoproducts formed in the photosensitized electron transfer reaction is crucial for efficient chemical conversion and storage of light energy. A number of microscopically heterogeneous systems such as micelles and surfactant vesicles were employed to control the rates of light-induced electron transfer (forward reaction) and subsequent back electron transfer (back reaction)[1]. It is obvious that charges on these organized assemblies play some role to control the reaction rate and direction. In most cases, however, electrostatic attraction or repulsion between the microheterogeneous surface and the reactants operates in the same direction in both forward and back reaction and thus high overall quantumn efficiency seems not to be achieved. Namely, an acceleration of the forward reaction through electrostatic attraction can also lead an increase of the rate of back reaction[2-5], and a retardation of the back reaction through electrostatic repulsion also tends to be accompanied by a decrease of the rate of forward reaction[6,7].

Recently, Calvin et al.[8,9] and Grätzel et al.[10] independently reported that the back reaction could be retarded without decreasing the rate of the forward reaction by using a zwitterionic analogue of methyl viologen as an electron acceptor. Also Brugger and Grätzel[11] demonstrated that the retardation of the back reaction could be realized as a consequence of significant shift in the hydrophilic-lipophilic

balance of surfactant electron acceptor occurring upon electron transfer in CTAC micelles.

On the other hand, Meisel, Rabani, and co-workers[12-15] have demonstrated that the electrostatic interaction of the potential field of polyelectrolyte with charged species are useful to some extent in controlling the rate of photoinduced electron transfer reaction. Recently, Okubo and Turro[16,17] studied the kinetics of binding between sodium poly(styrene-sulfonate) and cationic phosphorescence probes and the effect of polyelectrolyte in the quenching mechanism of these probes by the phosphorescence decay method. They demonstrated that both hydrophobic and electrostatic interactions affect the binding constants and the quenching rate constants of the probes.

Amphiphilic copolymers consisting of electrolyte segments and hydrophobic chromophores are regarded as organic assemblies, because they, when brought into water, tend to form micellar structures in which hydrophobic aggregates are confined in a polyelectrolyte outer shell[18]. Consequently, from the view point of the molecular design of polymers having both the reaction center and the microenvironment that vectrially drives a reaction in a desired direction, it is interesting to investigate fundamentally the microenvironmental effect of these polymers on the photoinduced electron transfer. In Chapter 3, it was demonstrated that the fluorescence from the excited Ph groups in these copolymers was quenched effectively by amphiphilic quenchers such as BHET in aqueous solutions, suggesting that the rate of the forward reaction

was greatly increased because of an increase of effective concentration of the amphiphilic quencher around the copolymer as a result of hydrophobic interaction. Also it was found that the electrolyte segments of the copolymers affect the rate of fluorescence quenching with an ionic quencher in aqueous solutions. This result motivated us to study how the rate of undesirable back reaction following the photoinduced electron transfer can be retarded by the same microenvironmental effect.

The photosensitized electron transfer is governed by both forward and back reactions. The forward reaction is conveniently followed by fluorescence quenching as described in Chapter 3. The back reaction can be investigated directly by flash photolysis and indirectly by observing the accumulation of the photoproduct[19]. For the latter method, viologens (1,1'-dialkyl-4,4'-bipyridinium) are one of the most appropriate electron acceptors because these compounds are susceptible to one-electron reduction, producing cation radicals, which are long-living under anaerobic conditions and show a characteristic absorption at 602 nm[20]. Here, we investigated the photoreduction of electrically neutral viologen, 4,4'-bipyridinium-1,1'-bis(trimethylenesulfonate) (SPV) with anionic amphiphilic polymers (APh) as sensitizers to see how the electrostatic interaction affects the back reaction. It is expected that the electrolyte segments in these polymers retard the back reaction of photoproducts. For a better understanding of this electrostatic effect on the photoredox reaction, we examined the forward and back reactions separately

in detail. This chapter concerns with the fluorescence quenching of amphiphilic copolymers, APh and QPh, using methyl viologen (MV^{2+}) or SPV as an oxidative quencher. These results are compared with those of the monomer model compounds.

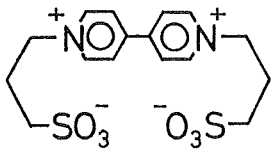

SPV

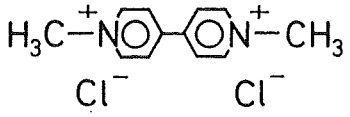

MV^{2+}

4-2. Experimental

Quenchers

4,4'-Bipyridinium-1,1'-bis(trimethylenesulfonate) (SPV) was prepared according to the method of Grätzel et al.[10] with some modification: To a solution of 5.5 g (0.045 mol) of 1,3-propanesulton in 10 ml of methanol was added 2.3 g (0.015 mol) of 4,4'-bipyridyl in 10 ml of methanol. The reaction mixture was stirred at 35 °C for 5 h. The precipitate was filtrated and washed with methanol. The crude product was further purified by precipitation from the aqueous solution into an excess of aceton three times: yield 4.2 g (71 %);

NMR(D_2O) δ 2.42-2.82(m,4H), 3.11(t,4H), 4.97(t,4H),and 7.43-8.41 ppm(m,8H).

Anal. $C_{16}H_{20}N_2O_6S_2 \cdot 0.5\ H_2O$ Calcd: C, 46.93%; H, 5.17%; N, 6.84%; S, 15.66%. Found: C, 46.93%; H, 5.18%; N, 6.77%; s, 15.80%.

1,1'-Dimethyl-4,4'-bipyridinium dichloride (methyl viologen, MV^{2+}) was purchased from Aldrich, and used without further purification.

Materials

Syntheses of amphiphilic copolymers (APh and QPh) and the related monomer models (AM and QM) are described in Chapter 1 and Chapter 3, respectively.

Measurements

Spectral measurements were performed in the same manner described in Chapter 3.

4-3. Results and Discussion

In Chapter 3, we pointed out that the fluorescence quenching occurred effectively as a consequence of hydrophobic and/or electrostatic interactions between quenchers and amphiphilic copolymers consisting of fluorophores. In this chapter, we used SPV (electrically neutral quencher) and MV^{2+} (cationic quencher) to gain further insight into the electrostatic effect on the fluorescence quenching of the excited Ph groups in the amphiphilic copolymers containing anionic segments (APh) or cationic segments (QPh). The half-wave reduction potentials for SPV and MV^{2+} were determined by cyclic voltammetry to be -0.63 V (vs. SCE) and -0.68 V (vs. SCE) in aqueous solutions, respectively. These values were in good agreement with those in the literature[10]. Estimates of excited-state oxidation potential of Ph (-2.07 V vs. SCE[21]) based on the spectral data and the ground-state oxidation potential suggest that the fluorescence quenching of Ph by these viologens occurs by electron transfer from excited Ph to the viologens. The lowest-energy absorption band of these compounds appears at 260 nm, which is sufficiently shorter wavelength than that of the phenanthryl group. Thus, the fluorescence quenching due to energy transfer can be precluded. Considering the energy difference between the singlet and triplet excited states of Ph (0.90 eV[22]), oxidation potential of the triplet-excited Ph (-1.17 V vs. SCE) is also sufficiently negative compared with the reduction

potentials of the viologens. Therefore, the electron transfer from the triplet state to these viologens is also a likely pathway. However, the fluorescence quenching study can still provide a practical tool for a rough assessment of the easiness of the overall forward electron transfer process from excited Ph.

The fluorescence from the Ph residue in these amphiphilic copolymers was sufficiently quenched by both SPV and MV^{2+} in aqueous solutions. Figure 1 illustrated the Stern-Volmer plots for APh with various f_{Ph} in aqueous solutions. The data for APh showed some scattering, but gave essentially linear plots in the range of the quencher concentrations shown in Figure 1. With MV^{2+} as a quencher, the fluorescence quenching of APh was clearly observed even at concentrations in the 10^{-6} M range, whereas with SPV the fluorescence was quenched to about the same extent at concentrations of the order of 10^{-4} M. This implies that electrostatic attraction between MV^{2+} and APh brings about a considerable enhancement of the quenching process. It is also important to note that the quenching depends remarkably on f_{Ph}. This effect will be discussed later.

Table I summarizes K_{SV} and k_q for the fluorescence quenching of APh of various f_{Ph} and the monomer model (AM). The k_q values for MV^{2+} were always much larger than those for SPV for all the anionic copolymers. Furthermore, these values for MV^{2+} reached the order of 10^{12} $M^{-1}s^{-1}$. These remarkable observations are explicable in terms of the increased local concentration of MV^{2+} around the fluorophore as a result of

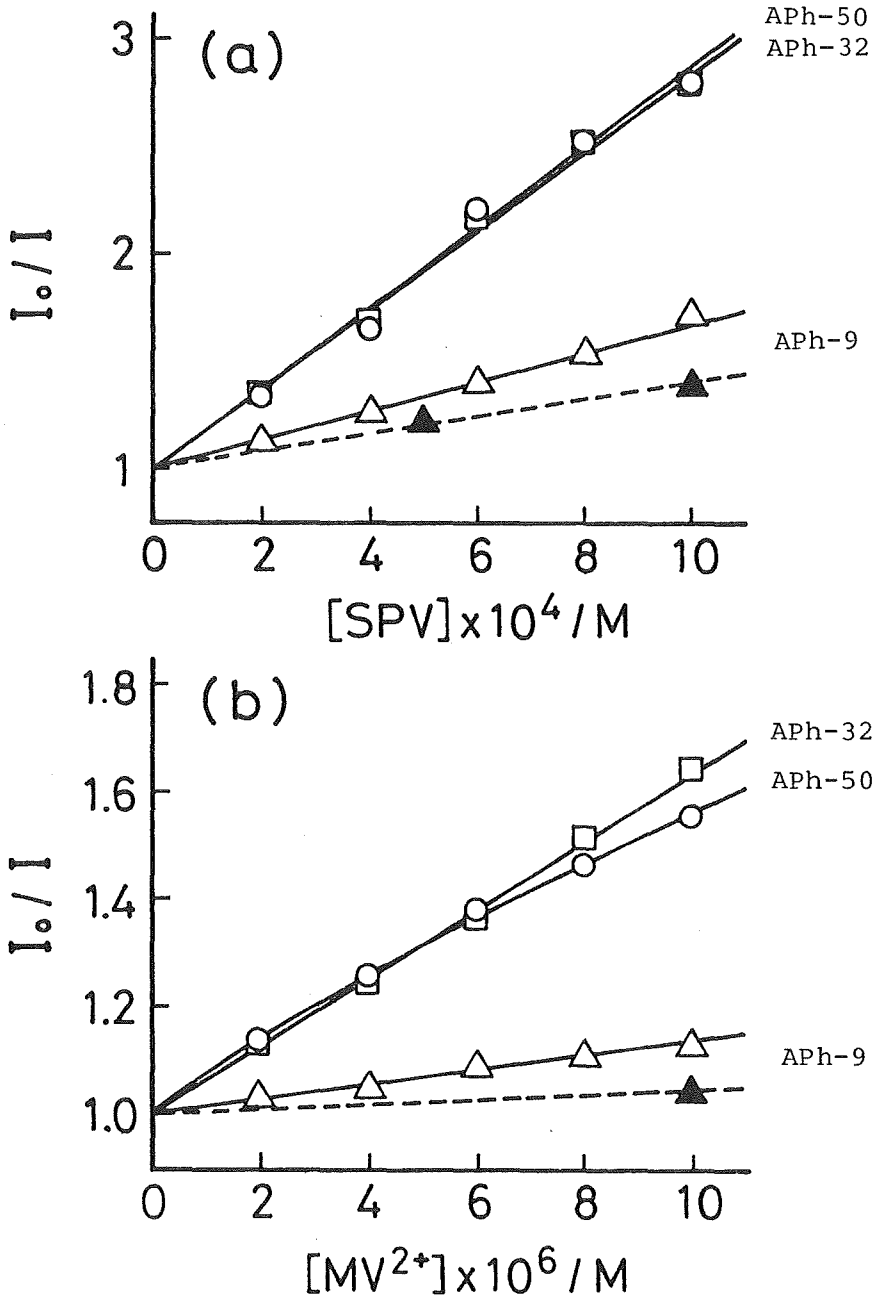

Figure 1. Stern-Volmer plots for APh-SPV system (a) and for APh-MV^{2+} system (b) in aqueous solution: ○, APh-50; □, APh-32; △, APh-9; ▲, APh-9 in aq. NaCl (μ=0.4); $[VPh]_{residue}=2x10^{-4}$ M.

Table I. Rate constants for the fluorescence quenching of APh by SPV and MV^{2+} in aqueous solution[a)]

Sample	added substance	f_{Ph}	τ/ns	K_{SV}/M^{-1}		$k_q x10^{-9}/M^{-1}s^{-1}$	
				SPV	MV^{2+}	SPV	MV^{2+}
APh-50		0.50	33	1850	69000[b)]	56	2100
APh-50	PAMPS($2x10^{-3}$M)	0.50	33	925	13900	28	420
APh-32		0.32	38	1810	63900	48	1700
APh- 9		0.09	38	675	14300	17	380
APh- 9	NaCl (0.2M)	0.09	38	351	5550	9.2	146
Ph/SDS[d)]		—	40[c)]	710[b,c)]	1600[b,c)]	ca.20	ca.40
AM		—	34	472	1070	14	31
AM	NaCl (0.2M)	—	34	458	530	13	16

a) $[VPh]_{residue}=2x10^{-4}$ M.

b) Calculated from the initial slope of the Stern-Volmer plot.

c) Measured without deaeration.

d) $[SDS]=5x10^{-2}$ M.

electrostatic interaction between MV^{2+} and the anionic segments of APh. Similar phenomena were often encountered with charged interfacial systems such as micelles[23,24] and polyelectrolyte[12,13,17,25]. It should be stressed that no such difference between MV^{2+} and SPV was observed with the monomer model (AM) (Table I).

Careful studies for the absorption spectra of aqueous solutions of APh and MV^{2+} let us to notice a slight change in the spectral shape of the Ph absorption band in the tail of the longer wavelength side. On addition of the 10^{-4}-10^{-3} M range of MV^{2+} to aqueous solution of APh, a new absorption band at 390 nm became apparent (Figure 2). This observation is an indication of the formation of ground-state EDA (electron donor acceptor) complexes between Ph and MV^{2+}. Such an EDA complex formation of MV^{2+} with some other aromatic compounds has also been observed in micellar media[26-28]. In order to quantitatively assess the complexation, the formation constants, K_{CT}, were determined by using the Benesi-Hildebrand equation[29]. In Table II K_{CT} values for various systems are listed. An extremely high value of K_{CT} was obtained for the APh-MV^{2+} system (much larger than those obtained so far for aromatic compounds-MV^{2+} complexes in SDS solutions[26]). This result indicates that the concentration of MV^{2+} in sufficiently close vicinity of the Ph residue was remarkably increased in the polymer system to facilitate the complexation. Furthermore, it is worth noting that these values are in parallel with the quenching rate parameters (Table II). These facts suggest that

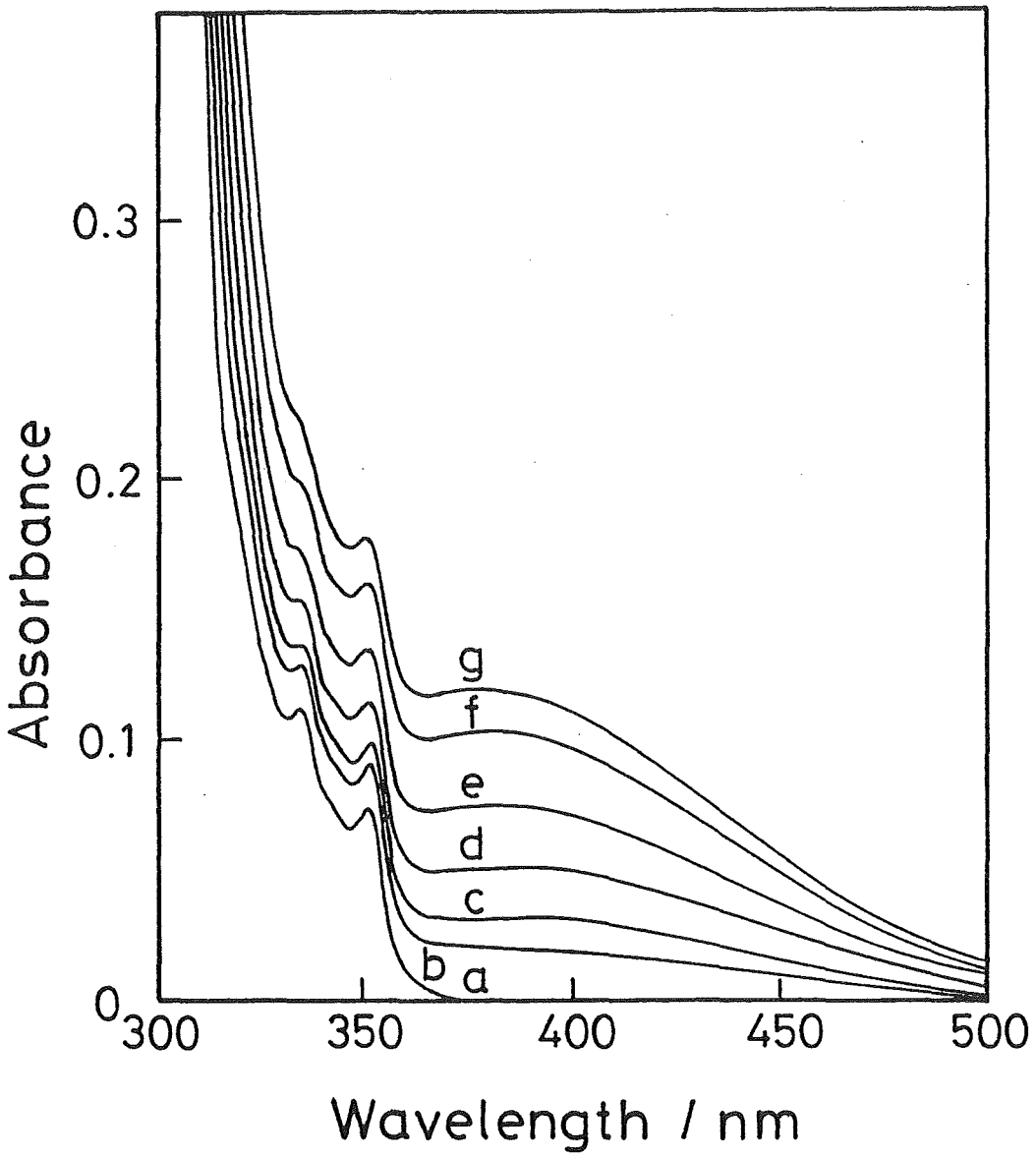

Figure 2. Absorption spectra of APh-9 in aqueous solution in the presence of various concentration of MV^{2+}: $[VPh]_{residue}=2.5\times10^{-4}$ M; $[MV^{2+}]=0$, 0.5, 1.1, 2.1, 4.2, 10, 50 $\times10^{-4}$ M for plots a-g, respectively.

both values of K_{SV} and K_{CT} for the APh-MV^{2+} system are extremely overestimated, because these values were simply calculated from the Stern-Volmer and Benesi-Hildebrand equations, respectively, by using the analytical concentration (macroscopic concentration) of MV^{2+}. Russell and Whitten[27,28] demonstrated that the association constants, K_A, corrected for this concentration effect of the SDS micelle were similar to that for the complex of the surfactant derivative of trans-stilben and MV^{2+} in acetonitrile. Consequently, apparent K_{SV} and K_{CT} values may be regarded as parameters indicating the concentration efficiency of MV^{2+}. Kinetics of the fluorescence quenching in the presence of ground-state interaction were discussed in the literature[30]. However, we could not apply these kinetics as such to the present case because the estimation of the effective concentration of quencher was impossible.

Table II. Formation constants of ground-state complexes and Stern-Volmer constants for various systems

	SPV		MV^{2+}	
Donor	K_{CT}/M^{-1} a)	K_{SV}/M^{-1} b)	K_{CT}/M^{-1} a)	K_{SV}/M^{-1} b)
APh-9	106	675	2800	14300
Ph/SDS	348	710	844	1600
AM	75	472	552	1070

a) $[VPh]_{residue}=4\times10^{-4}$ M for Ph/SDS and AM systems;
$[VPh]_{residue}=2.5\times10^{-4}$ M for APh-9 system.
b) $[VPh]_{residue}=2\times10^{-4}$ M.

The effect of ionic strength (μ) on the quenching was studied to confirm further the interaction of the polyelectrolyte with the charged species. An addition of NaCl to ionic strength (μ) = 0.4 decreased the k_q value to about one-third of that at $\mu \simeq 0$ for the APh-MV^{2+} system (Table I, Figure 1(b)). This is mainly due to the screening of electrostatic attraction beween APh and MV^{2+}. It should be noted that the salt effect was also observed for the model compound (AM), although the extent of the effect was less than the polymer case. This is indicative of the nature of AM tending to aggregate to form a micelle-like structure even at low concentrations (see Chapter 5).

It is interesting to note that k_q's for SPV were of the order of 10^{10} $M^{-1}s^{-1}$, which seems to be a little larger than the diffusion-controlled limit (Table I). This observation may imply the contribution of some attractive interaction between SPV and APh; probably through electrostatic attraction between the pyridinium cation sites of SPV and the anionic segments of APh. This idea was supported by the fact that the rate of the fluorescence quenching of APh with SPV decreased when NaCl was added (0.2 M of NaCl decreased the k_q value for APh-9 from 1.7×10^{10} $M^{-1}s^{-1}$ to 9.2×10^{9} $M^{-1}s^{-1}$ as shown in Table I). A similar observation was also reported by Grätzel et al.[10]. Namely, the fluorescence quenching of zinc tetrakis-(sulfonatophenyl)porphrin ($ZnTPPS^{4-}$) with zwitterionic analogues of MV^{2+} was decreased with an increase of ionic strength. This speculation was further rationalized by the

experimental result that the fluorescence quenching for the corresponding cationic copolymer (QPh) with SPV was less effective than that for APh as will be discussed later (Table III).

In Figure 1, one would notice the remarkable dependence of the fluorescence quenching on f_{Ph}. Similar phenomena were observed in Chapter 3, which were explained on the basis of the local concentration of quenchers around the fluorophore, resulting from the hydrophobic interaction. In the present case, the k_q value for MV^{2+} depends more on f_{Ph} than that for SPV, the electrostatic interaction is believed to be a main factor. However, both MV^{2+} and SPV being amphiphilic molecules of fairly large size with the positive charges localized on the nitrogen atoms, the hydrophobic interaction may also occur between the hydrophobic part of these molecules and the Ph residues in the copolymers. Therefore, one may envisage a "crossover effect" of these electrostatic and hydrophobic interactions occurring cooperatively, thus the formation of the ground-state complex would be highly favored. Under the present experimental conditions, an aqueous solution of APh-9 contains about 10 times larger amount of electrolyte groups ($-SO_3^-$) than that of the APh-50 solution, although the residual concentration of Ph groups are identical. When a polyelectrolyte, sodium poly(2-acrylamido-2-methylpropanesulfonate) (PAMPS) was added to the solution of APh-50 so that the residual concentration of the electrolyte groups is equal to that for the solution of APh-9, the k_q value for APh-MV^{2+} system was

decreased from 2.1 x 10^{12} $M^{-1}s^{-1}$ to 4.2 x 10^{11} $M^{-1}s^{-1}$ (Table I). The latter value is fairly close to that of APh-9. These facts suggest that the lower k_q values for the copolymers containing larger amount of electrolyte groups, namely, the copolymers with lower f_{Ph} are attributed to the decrease of effective concentration of the quencher around the aromatic groups in the copolymer because of the progressive electrostatic association of the quenchers with the electrolyte sequences which are remote from the Ph residues.

Table I also includes the quenching data for Ph solubilized in SDS micelles, where the fluorescence quenching with both SPV and MV^{2+} was less effective than that for the polymer system. This may be interpreted in the same way as above. Namely, this may be due to the fact that the effective concentration of the quencher around the fluorophore is decreased because of the presence of SDS micelles containing no fluorophore (the average number of Ph per micelle is ca. 0.25), and may also be due to the difference of the solubilized sites of Ph (hydrophobic fluorophore) and the quencher (amphiphilic compound) in the micelles.

Figure 3 shows the Stern-Volmer plots for the fluorescence quenching of the corresponding cationic polymer, QPh. On the contrary to the APh system, the fluorescence quenching of QPh with MV^{2+} was much less effective than that of APh. This is in parallel with the fact that no EDA complex formation of QPh and MV^{2+} was observed. The quenching data for QPh and the monomer model (QM) are summarized in Table III. In the case of MV^{2+},

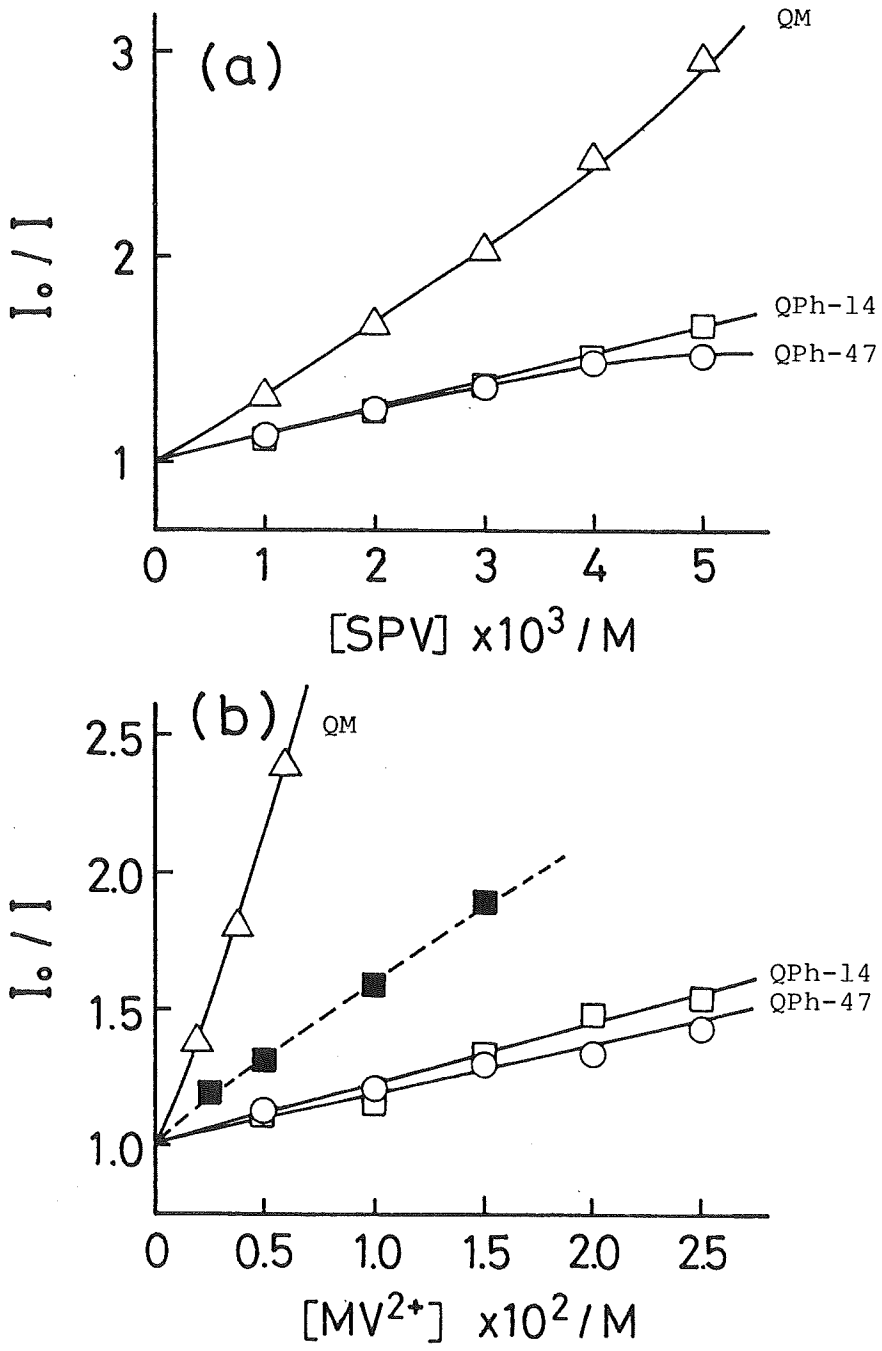

Figure 3. Stern-Volmer plots for QPh-SPV system (a) and for QPh-MV^{2+} system (b) in aqueous solution: ○, QPh-47; □, QPh-14; △, QM; ■, QPh-14 in aq. NaCl (μ=0.4); $[VPh]_{residue}=2\times10^{-4}$ M.

Table III. Rate constants for the fluorescence quenching of QPh by SPV and MV^{2+} in aqueous solution[a)]

Sample	added substance	f_{Ph}	τ/ns	K_{SV}/M^{-1}		$k_q x10^{-9}/M^{-1}s^{-1}$	
				SPV	MV^{2+}	SPV	MV^{2+}
QPh-47		0.47	34	130[b)]	19.0	3.8	0.56
QPh-14		0.14	42	130	22.4	3.1	0.53
QPh-14	NaCl (0.2 M)	0.14	42	127	74[b)]	3.0	1.7
Ph/CTAB[d)]		—	17[c)]	21.8[c)]	∿0[c)]	ca.1	∿0
QM		—	44	320[b)]	190[b)]	7.3	4.3
QM	NaCl (0.2 M)	—	44	370[b)]	320[b)]	8.4	7.3

a) $[VPh]_{residue}=2x10^{-4}$ M.

b) Calculated from the initial slope of the Stern-Volmer plot.

c) Measured without deaeration.

d) $[CTAB]=5x10^{-3}$ M.

the k_q value for QM was very close to the rate constant for diffusion-controlled reactions, whereas these values for QPh were of the order of 10^8 $M^{-1}s^{-1}$. These results indicate that the cationic segments of QPh effectively prevent the access of MV^{2+} to the polymer. A strong salt-effect on the quenching for QPh support this speculation (Figure 3(b), Table III). It is of interest to note that the fluorescence of Ph solubilized in CTAB micelles was not quenched at all by MV^{2+}. This indicates that the surface charge of CTAB micelles is more effective to prevent the access of MV^{2+} to the fluorophore than that of QPh as evident in Table III.

4-4. Conclusion

The present study demonstrated that an electrostatic potential field generated by macroions in amphiphilic copolymer is so powerful that it can alter the rate of fluorescence quenching at least by an order of magnitude in aqueous solutions. This strong electrostatic interaction was also found to favor the formation of ground-state EDA complex between Ph and viologen.

References

1) D. G. Whitten, J. C. Russell, and R. H. Schmehl, Tetrahedron, 38, 2455 (1982).

2) Y. Moroi, A. M. Braun, and M. Grätzel, J. Am. Chem. Soc., 101, 567 (1979).

3) Y. Moroi, P. P. Infelta, and M. Grätzel, J. Am. Chem. Soc., 101, 573 (1979).

4) A. Slama-Schwok, Y. Feitelson, and J. Rabani, J. Phys. Chem., 85, 2222 (1981).

5) D. Meisel, J. Rabani, D. Meyerstein, and M. S. Matheson, J. Phys. Chem., 82, 985 (1978).

6) P. A. Brugger, P. P. Infelta, A. M. Braun, and M. Grätzel, J. Am. Chem. Soc., 103, 320 (1981).

7) R. H. Schmehl and D. G. Whitten, J. Phys. Chem., 85, 3473 (1981).

8) I. Willner, J. W. Otovos, and M. Calvin, J. Am. Chem. Soc., 103, 3203 (1981).

9) I. Willner, J. M. Yang, C. Laane, J. W. Otovos, and M. Calvin, J. Phys. Chem., 85, 3277 (1981).

10) P. A. Brugger, M. Grätzel, T. Guarr, and G. McLendon, J. Phys. Chem., 86, 944 (1982).

11) P. A. Brugger and M. Grätzel, J. Am. Chem. Soc., 102, 2461 (1980).

12) D. Meisel and M. S. Matheson, J. Am. Chem. Soc., 99, 6577 (1977).

13) C. D. Jonah, M. S. Matheson, and D. Meisel, J. Phys. Chem.,

83, 257 (1979).

14) D. Meyerstein, J. Rabani, M. S. Matheson, and D. Meisel, J. Phys. Chem., 82, 1879 (1978).

15) R. E. Sassoon and J. Rabani, J. Phys. Chem., 84, 1319 (1980).

16) T. Okubo and N. J. Turro, J. Phys. Chem., 85, 4034 (1981).

17) N. J. Turro and T. Okubo, J. Phys. Chem., 86, 1535 (1982).

18) Chapter 2.

19) Chapter 5.

20) E. M. Kosower and J. L. Cotter, J. Am. Chem. Soc., 86, 5524 (1964).

21) section 3-3-1.

22) J. B. Birks, "Photophysics of Aromatic Molecules", Wiley-Interscience, New York, 1970, p184.

23) R. H. Schemehl and D. G. Whitten, J. Am. Chem. Soc., 102, 1938 (1980).

24) R. H. Schmehl, L. G. Whitesell, and D. G. Whitten, J. Am. Chem. Soc., 103, 3761 (1981).

25) I. A. Taha and H. Morawetz, J. Am. Chem. Soc., 93, 829 (1971).

26) F. M. Martens and J. W. Verhoeven, J. Phys. Chem., 85, 1773 (1981).

27) J. C. Russell and D. G. Whitten, J. Am. Chem. Soc., 103, 3219 (1981).

28) J. C. Russell and D. G. Whitten, J. Am. Chem. Soc., 104, 5937 (1982).

29) H. A. Beneshi and J. H. Hildebrand, J. Am. Chem. Soc., 71, 2703 (1949).

30) T. L. Nemzek and W. R. Ware, J. Chem. Phys., 62, 477 (1975).

Chapter 5

Electrostatic Effect of Amphiphilic Copolymers on the Back Electron Transfer

5-1. Introduction

In order to estimate the electrostatic effect of amphiphilic copolymers on the back reaction of the light-induced electron transfer reaction, we investigate the photosensitized reduction of viologens using amphiphilic copolymers having phenanthryl groups as photosensitizer in aqueous solution. In Chapter 4, the fluorescence quenching of these polymers was examined as a practical measure of the forward reaction. It was found that the quenching was accelerated with a charged viologen of opposite sign to the polymer and was retarded with a viologen of the same sign. These results imply that the electrolyte segments in amphiphilic copolymers also control the rate of back reaction.

In this chapter, we discuss the back reaction in detail. We observed the accumulation of the photoproducts in the presence of a sacrificial electron donor, triethanolamine (TEOA), under steady state illumination. Rate constants of the back electron transfer were calculated in some cases from laser photolysis data. Furthermore, the potential field effect of macroions on the electron transfer reactions was simulated by electrochemical redox reactions.

5-2. Experimental

Materials

Syntheses of amphiphilic copolymers (APh and QPh) and the monomer models (AM and QM) are described in Chapter 1 and Chapter 3, respectively.

Synthesis of SPV is described in Chapter 4.

Measurements

Steady-state irradiations were carried out by using a 500-W super-high pressure mercury lamp (Usio Electric Co.) in conjunction with a cut-off filter (UV-37, Toshiba Glass Co.) at room temperature. The sample solution was sealed in a quartz cell under vacuum. Accumulation of the photo-reduced product ($SPV^{\cdot}$ or $MV^{+\cdot}$) was followed by the absorbance at the 602-nm band (ε(602 nm) = 12800 $M^{-1}cm^{-1}$ for $SPV^{\cdot}$ [1] and ε(603 nm) = 12400 $M^{-1}cm^{-1}$ for $MV^{+\cdot}$ [2]).

Laser flash photolysis was carried out by using the second harmonic (347.1 nm) of a NEC ruby laser SLG-2018 with a Q-switch (0.85 J per flash at 694.3 nm with a pulse width of 20 ns). A 150-W xenone arc lamp was used for a monitoring beam. Sample solutions were placed in a 1-cm quartz cell and were deaerated under vacuum.

Electrochemical measurements were performed in a conventional single-compartment cell equipped with a platinum-wire counter electrode and a saturated potassium chloride calomel reference electrode (SCE). The working electrode was prepared from a pyrolytic graphite electrode (Nippon Carbon

Co., 5 mm x 5 mm x 2 mm) as illustrated in Figure 1. The electrode was coated by carefully syringing 20 μl of a 0.91 wt % methanolic APh-50 solution onto a freshly cleaved basal plane of the electrode and allowing the methanol to evaporate at room temperature. The coverage was ca. 1.2×10^{-7} mol/cm^2 (for sulfonate residue). All measurements were obtained using a NF function generator FG-121B and a Hokuto Potentiostat HA-301 at scan rate, 16 mVs^{-1}. The sample solutions were deaerated by bubbling with argon for 5 min.

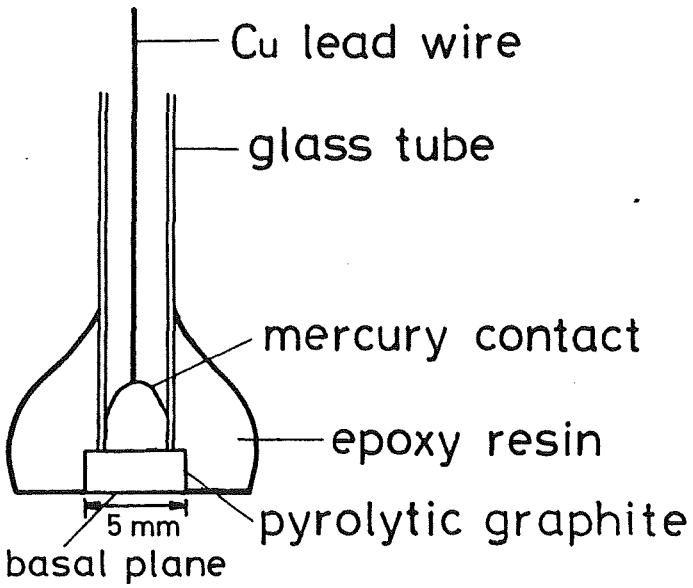

Figure 1. Pyrolytic graphite electrode.

5-3. Results and Discussion

5-3-1. Steady State Photochemical Reduction of Viologens

Irradiation of a deaerated solution containing APh and SPV or MV^{2+} with light ($\lambda \geq 370$ nm), by which phenanthryl groups (Ph) of APh were excited, resulted in the accumulation of viologen radicals ($SPV^{\cdot}$ or $MV^{+\cdot}$) in the presence of TEOA. This photoreduction includes following processes:

$$Ph \xrightarrow{h\nu} Ph^{*} \quad (1)$$

$$Ph^{*} + SPV \text{ (or } MV^{2+}) \longrightarrow Ph^{+\cdot} + SPV^{\cdot} \text{ (or } MV^{+\cdot}) \quad (2)$$

$$Ph^{+\cdot} + SPV^{\cdot} \text{ (or } MV^{+\cdot}) \longrightarrow Ph + SPV \text{ (or } MV^{2+}) \quad (3)$$

$$Ph^{+\cdot} + TEOA \longrightarrow Ph + TEOA_{ox} \quad (4)$$

Since the rate of reaction of $Ph^{+\cdot}$ with water is relatively slow as described later, reduction of $Ph^{+\cdot}$ by TEOA (eq. 4) occurs preferencially; i.e., TEOA can function as a sacrificial donor and hence Ph is reproduced. Among these processes the rates of forward and back reactions (eqs. 2 and 3) are considered to be particularly variable through the electrostatic interaction between the electrolyte segments of APh and an ionic substrate (MV^{2+}) or ionic photoproducts ($SPV^{\cdot}$ or $MV^{+\cdot}$). The forward reaction was estimated by means of fluorescence quenching in Chapter 3. In this chapter, we describe the effect of these amphiphilic copolymers on the back reaction first by observing the accumulation of the photoproducts.

In Figure 2(a), concentrations of $SPV^{\cdot}$ and $MV^{+\cdot}$ formed for APh-9 are plotted as a function of irradiation time. Accumulation of $SPV^{\cdot}$ was apparently faster than that of $MV^{+\cdot}$.

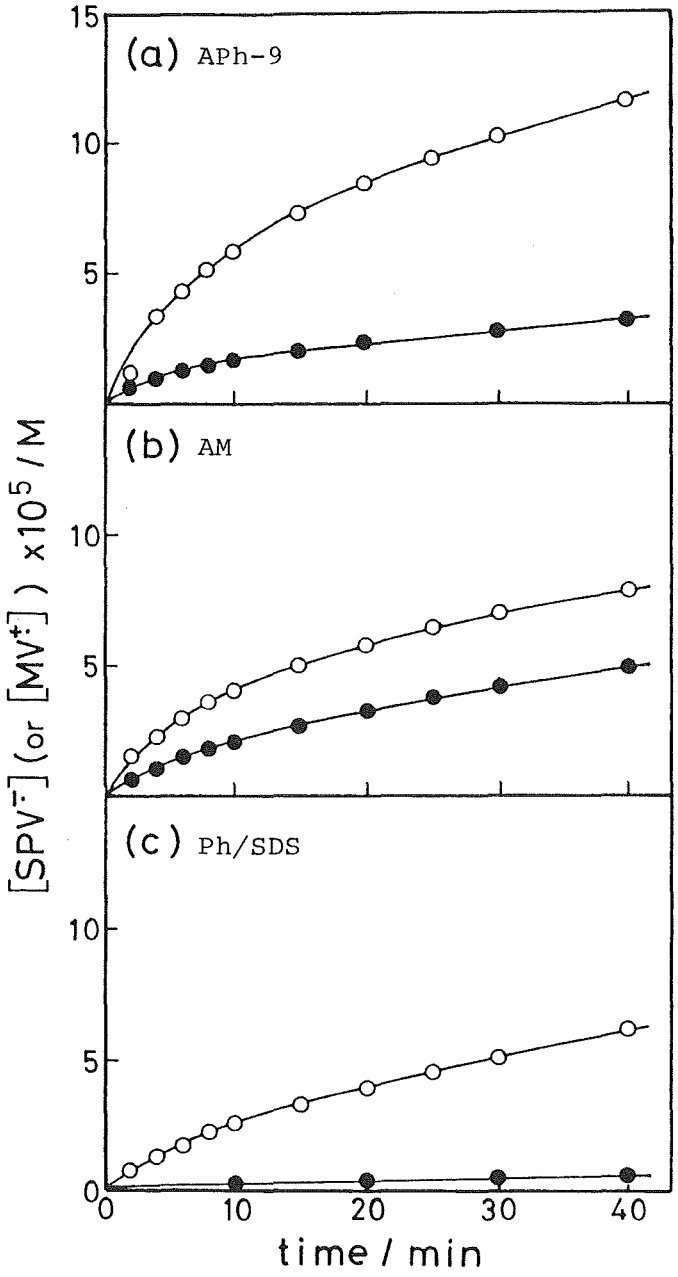

Figure 2. Accumulation of $SPV^{\cdot-}$ or $MV^{\cdot+}$ as a function of irradiation time with APh-9 (a), AM (b), and Ph/SDS (c) as photosensitizer: $[VPh]_{residue}=5\times10^{-4}$ M; [SPV] (or $[MV^{2+}]$) = 2.5×10^{-3} M; [TEOA] = 2.5×10^{-3} M; ○, SPV; ●, MV^{2+}.

This result seems, at a glance, to be opposite to what is expected from the experimental results of the fluorescence quenching in Chapter 4; MV^{2+} quenched the fluorescence of APh far more effectively than SPV, suggesting that the forward reaction (eq. 2) is far more favorable with MV^{2+} than with SPV. These facts clearly indicate that the electrostatic interaction between the electrolyte segments of APh and the photoproducts strongly affects the rate of the back reaction (eq. 3). Namely, $SPV^{\cdot}$ which acquires a negative charge as a result of the photoreduction is efficiently repelled by the anionic segments of APh, leading to the facilitation of charge separation. On the other hand, $MV^{+\cdot}$ which still has a positive charge after the reduction remains attracted by the anionic segments, resulting in the rapid back reaction.

The related monomeric model compound, AM, showed less electrostatic effect on the photoreduction (Figure 2(b)). In fact we had not expected the difference of the yields between $SPV^{\cdot}$ and $MV^{+\cdot}$ as observed in Figure 2(b). This may be attributed to the nature of AM tending to form a micelle-like structure even at low concentrations. This speculation was rationalized by the experimental results of the uptake of a hydrophobic fluorescence probe, CyD[3,4]. As shown in Figure 3, the emission spectra from CyD showed a shift from 510 to about 550 nm along with the decrease of the emission intensity in the presence of 10^{-4} M of AM, presumably due to the formation of dimer or higher aggregates of CyD[3]. This indicates that several molecules of AM aggregate in this concentration range, which

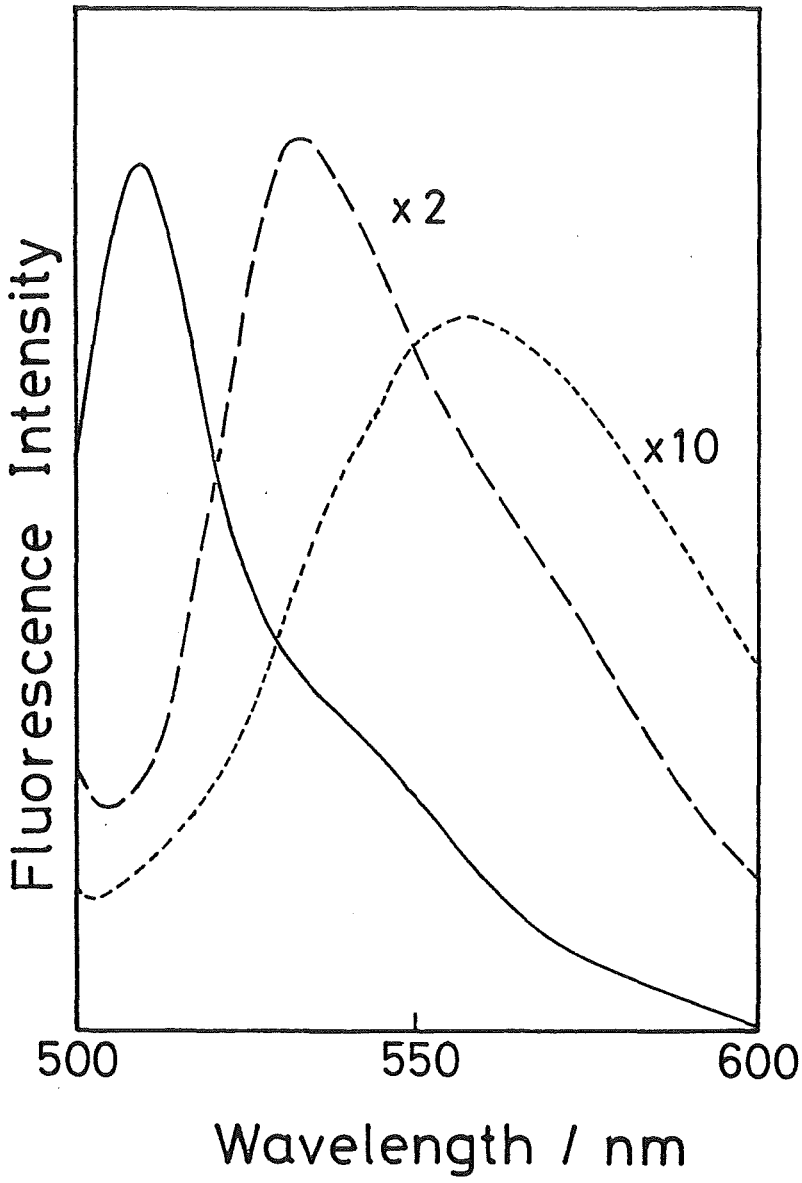

Figure 3. Fluorescence spectra of CyD in aqueous solution in the presence of various concentration of AM: [CyD]=5×10^{-7} M; excitation wavelength, 485 nm; ———, [AM]=0 M; --------, [AM]=3×10^{-4} M; – – – –, [AM]=3×10^{-3} M.

take up more than one molecule of CyD. At higher concentrations than 10^{-3} M, the peak shifted back to about 530 nm and the intensity increased, indicating that CyD was taken up in isolation because a larger number of aggregates were formed at higher concentrations.

For comparison Figure 2(c) shows the effect of the surfactant micelles on the photoreduction. With Ph solubilized in SDS micelles as a photosensitizer, $SPV^{\cdot}$ was efficiently accumulated probably due to the retardation of the back reaction through electrostatic repulsion between $SPV^{\cdot}$ and the charged surface of the micelles. On the other hand, much less accumulation of $MV^{+\cdot}$ was detected. The SDS micelles contain a large amount of anionic electrolyte groups (0.05 M). Thus, even though $MV^{+\cdot}$ may be produced by the photoreduction, they cannot escape from the back electron transfer because of the tight binding of $MV^{+\cdot}$ to the micellar surface. As for the yields of the photoproduct, $SPV^{\cdot}$, the polymer system seems to be more effective than the micellar system (Figure 2(a) and 2(c)). The yields of photoproducts for various systems after irradiation for 30 min are summarized in Table I. The rate constants of fluorescence quenching obtained previously[5] are also listed.

The ionic strength has a strong effect on the forward and back reactions and hence on the accumulation of the photo-products. On addition of salt to the polymer solution, the yield of $SPV^{\cdot}$ slightly decreased and that of $MV^{+\cdot}$ increased (Table I). These observations may be interpreted by the sum of the salt-effects on the forward and back reactions. There is

appreciable electrostatic attraction between SPV and APh and added salt screens this attractive interaction[5]. Added salt also screens the electrostatic repulsion of $SPV^{\cdot}$ with the anionic segments of APh. These effects lead to the decrease of the forward quenching rate and the increase of the rate of back reaction, resulting in net decrease in the $SPV^{\cdot}$ accumulation on addition of salt. In the case of MV^{2+}, on the other hand, since the forward reaction decreases on addition of salt, the enhancement of the accumulation of $MV^{+\cdot}$ as a result of salt-effect may be solely due to the decrease of the back reaction. A small salt-effect in the AM systems is indicative of the small electrostatic effect of AM. In Table I, one would notice the dependence of the yields of photoproducts

Table I. Quenching rate constants and yields of viologen radicals in the steady state photoreduction in APh systems

Sample	$k_q \times 10^{-9}/M^{-1}s^{-1}$		$[SPV^{\cdot}] \times 10^5/M$ [a]	$[MV^{+\cdot}] \times 10^5/M$ [a]
	SPV	MV^{2+}		
APh-50	56	1900	13.9	8.48
APh-32	48	1700	11.7	7.33
APh- 9	17	380	10.2	2.77
APh- 9 (μ=0.4)	9.2	130	8.81	6.47
AM	14	31	7.04	4.20
AM (μ=0.4)	13	16	6.17	4.53
Ph/SDS	ca.20	ca.40	5.13	0.49

a) The yields of photoproducts after irradiation for 30 min. $[VPh]_{residue}=5\times10^{-4}$ M; [SPV](or $[MV^{2+}]$)$=2.5\times10^{-3}$ M; $[TEOA]=2.5\times10^{-3}$ M.

and of k_q on f_{Ph}. Although the yields increased with increasing f_{Ph} for both SPV and MV^{2+}, the ratio of the yields ($[SPV^{\cdot}]/[MV^{+}]$) was larger for the copolymer with lower f_{Ph}. Namely, the copolymer containing a larger amount of electrolyte groups shows an increasing electrostatic effect on the photoreduction. This result implies that the high charge density of the electrolyte segments around the photosensitizer play an important role for the efficient charge separation.

With the corresponding cationic copolymer, QPh, as a photosensitizer, drastic change in the accumulation of viologen radicals was observed (Table II). No photoproducts for both SPV and MV^{2+} could be detected in the presence of QPh-14. No MV^{+} is accumulated probably because the electrostatic repulsion prevents MV^{2+} from gaining access to QPh-14[5]. With SPV, the

Table II. Quenching rate constants and yields of viologen radicals in the steady state photoreduction in QPh systems

Sample	$k_q \times 10^{-9}/M^{-1}s^{-1}$ SPV	$k_q \times 10^{-9}/M^{-1}s^{-1}$ MV^{2+}	$[SPV^{\cdot}] \times 10^{5}/M$ [a]	$[MV^{+}] \times 10^{5}/M$ [a]
QPh-47	3.6	0.49	2.55	1.75
QPh-14	3.1	0.53	0	0
QPh-14 (μ=0.4)	3.0	1.4	0	0
QM	7.7	5.0	4.52	3.15
QM (μ=0.4)	8.4	7.5	—	—

a) The yield of photoproducts after irradiation for 30 min; $[VPh]_{residue}=5\times10^{-4}$ M; [SPV](or $[MV^{2+}]$)$=2.5\times10^{-3}$ M; $[TEOA]=2.5\times10^{-3}$ M.

back reaction is so enhanced by the electrostatic attraction between $SPV^{\bar{\cdot}}$ and polycation that no accumulation of $SPV^{\bar{\cdot}}$ must have been observed. These speculation is compatible with the fact that the photoproducts in the presence of QPh-47 (lower charge density of polycation than QPh-17) and QM (with a single charge) accumulated with the irradiation time (Table II).

5-3-2. Laser Flash Photolysis of APh-SPV System

Excitation of a deaerated solution containing APh-9 and SPV with a 347.1-nm laser pulse resulted in the appearance of a transient absorption band due to $SPV^{\bar{\cdot}}$. Figure 4(a) and 4(b) illustrate the decay profiles of $SPV^{\bar{\cdot}}$ followed at 602 nm for the APh and AM systems, respectively. In the case of the APh-SPV system, up to several msec after the laser pulse, $SPV^{\bar{\cdot}}$ continued to disappear by the back reaction with Ph^{+} (eq. 3) (about first 70 % of total decay of $SPV^{\bar{\cdot}}$ followed a second-order rate low). In the longer time domain, however, a part of $SPV^{\bar{\cdot}}$ was observed as a permanent product probably because of the degradation of Ph^{+} in the reaction with water. The second-order rate constants for the back electron transfer were calculated to be $k_b = 8.7 \times 10^7\ M^{-1}s^{-1}$ for APh-SPV and $k_b = 2.8 \times 10^9\ M^{-1}s^{-1}$ for AM-SPV. This large retardation of the back reaction in the polymer system is obviously attributed to the electrostatic repulsion between the reduced product ($SPV^{\bar{\cdot}}$) and the electrolyte segments of APh. In fact, addition of salt decreases the electrostatic effect of the

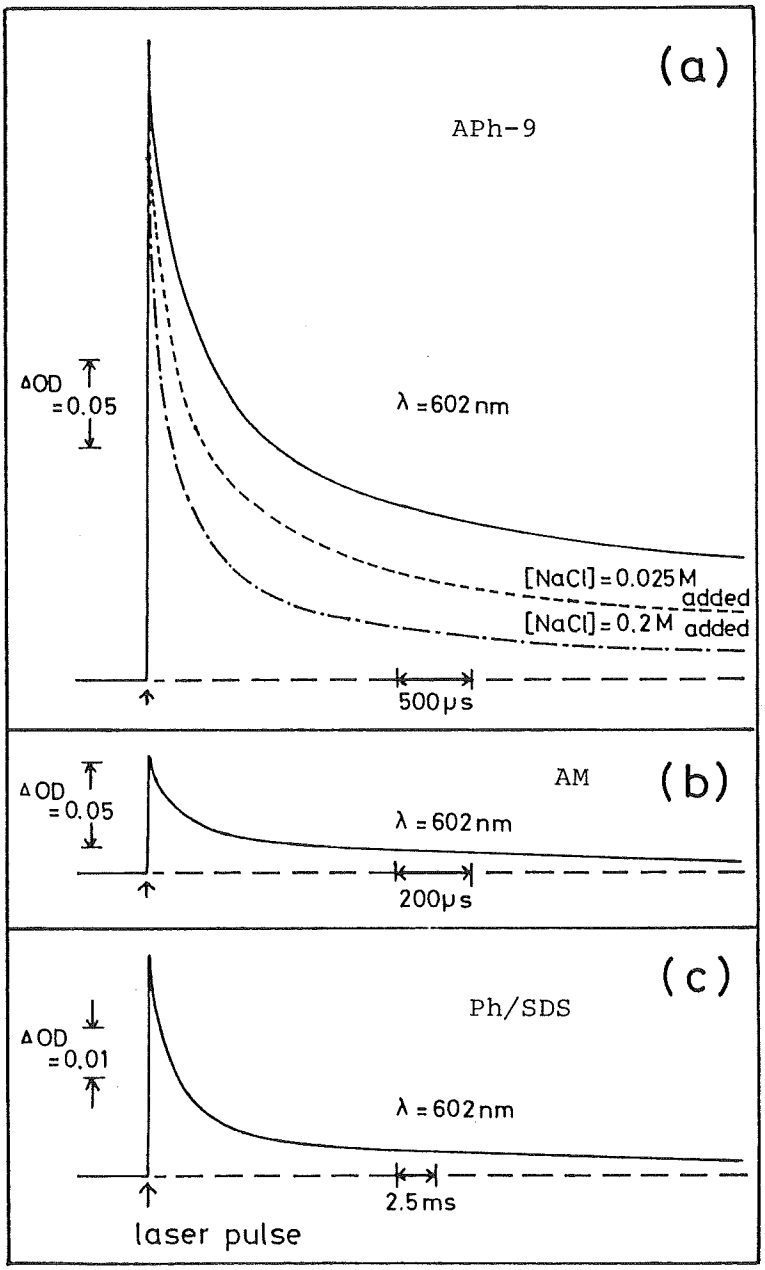

Figure 4. Transient absorption changes of $SPV^{\cdot}$ at 602 nm following excitation of APh-9 (a), AM (b), and Ph/SDS (c): $[VPh]_{residue}=2.5\times10^{-3}$ M; $[SPV]=10^{-2}$ M; ———, [NaCl]=0 M; --------, [NaCl]=0.025 M; —·—·—, [NaCl]=0.2 M.

polymer, leading to the increase of back reaction as observed in Figure 4(a). At 0.025 M of added NaCl k_b increased to 2.5 x 10^8 $M^{-1}s^{-1}$ and at 0.2 M of NaCl k_b = 5.2 x 10^8 $M^{-1}s^{-1}$. This result provided a strong evidence for the occurrence of the large electrostatic repulsion. It should be noted that the estimated initial yield of $SPV^{\cdot}$ produced by the laser flash was much higher for APh-9 than that for AM (Figure 4(a) and 4(b)). Since the efficiency of the forward electron transfer is not much different in both systems[5], this may be due to the much faster back reaction in AM that we could not detect in the present study.

The elctrostatic effect of polyelectrolyte on the photoinduced electron transfer reactions has been investigated by Meisel, Matheson, Rabani, and co-workers[6-8]. They reported an effect of potassium poly(vinyl sulfate) on the initial yields of the photoelectron transfer. However, the retarding effect of polyelectrolyte on the back reaction appears to be small (e.g., k_b = 4 x 10^9 $M^{-1}s^{-1}$ for $Ru(bpy)_2(CN)_2$-$Fe(CN)_6^{3-}$-polybrene system[8]). In contrast, the k_b value in the present study is remarkably small and comparable to other interfacial systems such as surfactant micelles (k_b = 4 x 10^7 $M^{-1}s^{-1}$) reported by Grätzel et al.[9] and the colloidal SiO_2 system (k_b = 5.7 x 10^7 $M^{-1}s^{-1}$) by Calvin et al.[1,10]. These comparison reveals that unlike potassium poly(vinyl sulfate) the amphiphilic polyelectrolyte in the present study serves as one of the most effective microenvironments for the prevention of the back electron transfer. The reduced k_b value was also obtained for Ph solubilized in SDS micelles (k_b = 6.8 x 10^7 $M^{-1}s^{-1}$)

(Figure 4(c)). However, the estimated initial yield of $SPV^{\cdot}$ was remarkably low, presumably because of a lower fraction of the escape of $SPV^{\cdot}$ from the geminate ion pair. This fact may imply that SPV preferably resides inside of the micelles and the electron transfer takes place mostly within the micelle and not across the charged surface. It should be noted that k_b for the AM-SPV system ($k_b = 2.8 \times 10^9$ $M^{-1}s^{-1}$) was smaller than that of a diffusion-controlled limit ($k_{diff} \simeq 7 \times 10^9$ $M^{-1}s^{-1}$)[11]. This result suggests the aggregation of AM again.

Replacement of SPV with MV^{2+} caused a drastic change in the rate of back reaction. In the APh-MV^{2+} system most of $MV^{+\cdot}$ decays within 100 μsec and its decay did not follow a second-order rate low (data not shown). In the micellar system the decay of $MV^{+\cdot}$ was too fast to be detected by the present laser photolysis experiment. These results indicate that the anionic segments of APh and the charged surface of SDS micelles still associate with $MV^{+\cdot}$ even after the electron transfer. In this situation the back reaction may not simply be a bimolecular process.

Although the kinetics of such back reactions awaits a further study, the results of the laser photolysis are substantially consistent with those obtained from the steady-state photosensitized reduction.

5-3-3. Electrochemical Simulation of Controlled Charge Separation of Ionic Species by an Amphiphilic Copolymer

Having found the remarkable electrostatic effect of amphiphilic polyelectrolyte on the photo-redox reaction, we further confirmed the same effect in the electrochemical redox reaction. We measured the cyclic voltammetry of various redox species in aqueous solution using a pyrolytic graphite electrode coated with APh-50. This electrode was stable in aqueous solution even though APh-50 was a water-soluble polymer, probably due to the tight adsorption of the hydrophobic (phenanthryl) groups of APh on the basal plane of the electrode.

Figure 5(a) shows cyclic voltammograms for SPV (electrically neutral species) with a bare and a polymer-coated electrode. The voltammogram of SPV with a bare electrode exhibits ideal reversible behavior of one-electron reduction regardless of the concentration of supporting electrolyte (Na_2SO_4), although the peak potential separation was dependent on the electrolyte concentration. With the polymer-coated electrode, however, the shape of voltammogram was remarkably different at lower ionic strength (Figure 5 (a-1)), i.e., the reoxidation wave of $SPV^{\cdot}$ (electrochemically reduced species) almost disappeared. At higher ionic strength, on the other hand, the reoxidative wave appeared and the voltammogram recovered the reversible behavior (Figure 5(a-2)). These impressive phenomena may be interpreted by the electrostatic effect of the amphiphilic copolymer. The

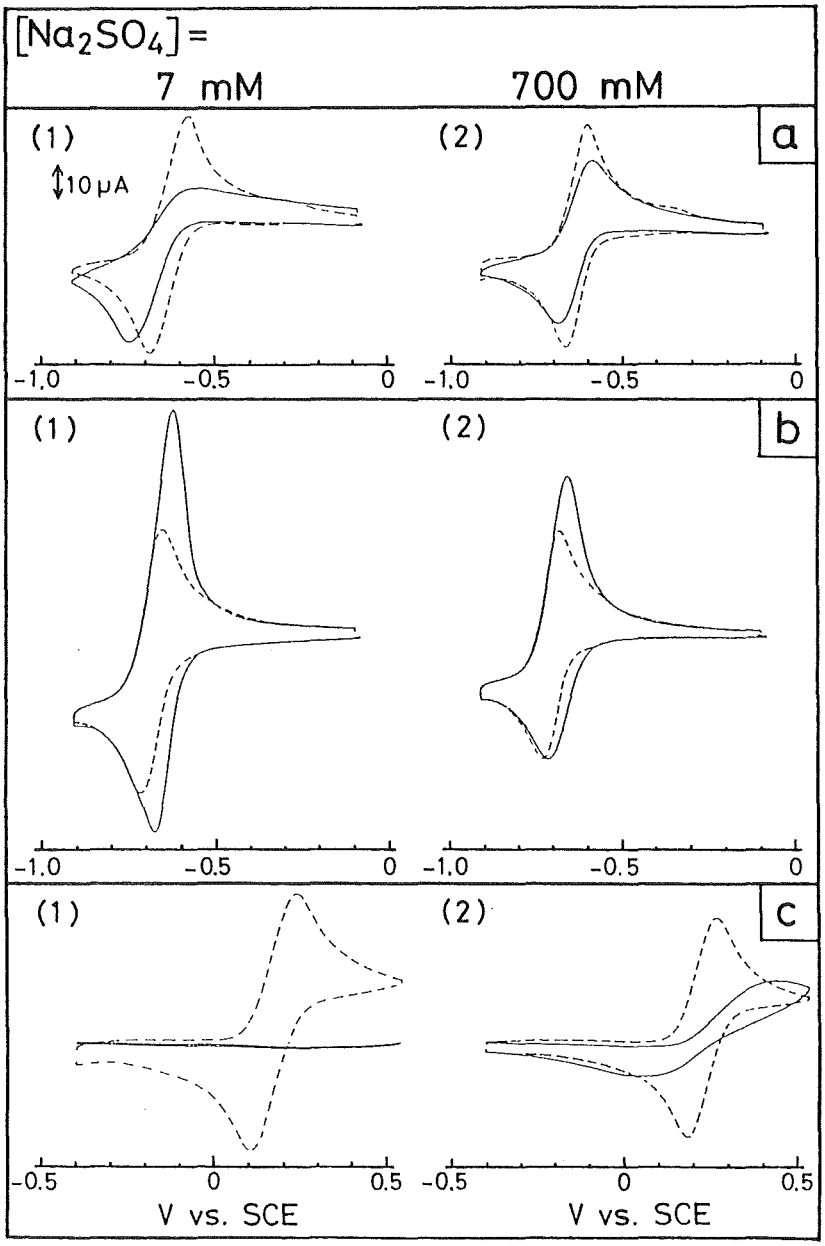

Figure 5. Cyclic voltammograms for SPV (a), MV^{2+} (b), and $K_4[Fe(CN)_6]$ (c) with a bare graphite electrode and a polymer-coated electrode: scan rate, 16 mVs^{-1}; [SPV], $[MV^{2+}]$, $[K_4[Fe(CN)_6]]=2.5x10^{-3}$ M; (1) $[Na_2SO_4]$=7 mM; (2) $[Na_2SO_4]$= 700 mM; --------, bare electrode; ———, polymer-coated electrode.

potential field made of the anionic segments of APh forces $SPV^{\cdot}$ to diffuse away from the electrode surface through electrostatic repulsion, leading to the lack of the reduced species ($SPV^{\cdot}$) on the electrode in an anodic scan cycle. Addition of salt decreases this electrostatic effect of the polymer. Consequently, this electrostatic potential field on the electrode was found to be useful to control the electrode reaction of various ionic species. Figure 5(b) shows the cyclic voltammograms for MV^{2+} (cationic species). An increase in the peak height of both reduction and reoxidation waves was observed with the polymer-coated electrode at lower ionic strength (Figure 5(b-1)), indicating the electrostatic adsorption of the electroactive species on the electrode. As expected an addition of salt decreased this concentration effect of the polymer (Figure 5(b-2)). Figure 5(c) shows the cyclic voltammograms for $Fe(CN)_6^{4-}$ (anionic species). At the lower ionic strength, neither reduction nor oxidation wave was observed with the polymer-coated electrode (Figure 5(c-1)). This indicates that the anionic segments of APh effectively prevent the access of $Fe(CN)_6^{4-}$ to the electrode. Increasing the ionic strength, the redox reaction slightly occurred (Figure 5(c-2)).

5-4. Conclusion

We demonstrated a remarkable electrostatic effect of the electrolyte segments of amphiphilic copolymers on the charge separation. Comparison with polyelectrolyte and micellar systems reveals that the amphiphilic copolymers in the present study serves as one of the most effective microenvironments for the prevention of the back electron transfer. Furthermore, the electrostatic potential field made up of the polyions was found to be useful to control other chemical or electron transfer reaction of various ionic species.

References

1) I. Willner, J. M. Yang, C. Laane, J. W. Otovos, and M. Calvin, J. Phys. Chem., 85, 3277 (1981).

2) E. Steckhan and T. Kuwana, Ber. Bunsenges. Phys. Chem., 78, 253 (1974).

3) section 2-3-1.

4) R. Humphry-Baker, M. Grätzel, and R. Steiger, J. Am. Chem. Soc., 102, 847 (1980).

5) section 4-3.

6) D. Meyerstein, J. Rabani, M. S. Matheson, and D. Meisel, J. Phys. Chem., 82, 1879 (1978).

7) C. D. Jonah, M. S. Matheson, and D. Meisel, J. Phys. Chem., 83, 257 (1979).

8) R. E. Sassoon and J. Rabani, J. Phys. Chem., 84, 1319 (1980).

9) P. A. Brugger, M. Grätzel, T. Guarr, and G. Mclendon, J. Phys. Chem., 86, 944 (1982).

10) I. Willner, J. W. Otovos, and M. Calvin, J. Am. Chem. Soc., 103, 3203 (1981).

11) D. R. Arnold, N. C. Baird, J. R. Bolton, J. C. D. Brand, P. W. N. Jacobs, P. de mayo, and W. R. Ware, "Photochemistry", Academic Press, New York, 1974, p109.

Summary

In an expectation as potential media for photosensitized electron transfer reactions, various types of polymers carrying both electrolyte and hydrophobic (aromatic) segments were prepared by radical and anionic polymerizations. Behavior of these copolymers in aqueous solution indicated a pronounced hydrophobic interaction of a number of aromatic groups in the copolymer with high aromatic content. The microdomains formed were found to be highly hydrophobic in nature but less capable to solubilize substrate than the surfactant micelles. The fluorescence spectra of the copolymers containing Ph groups imply the presence of an excimerlike interaction of Ph groups in aqueous solution. Such various phenomena originating from the hydrophobic aggregation were more remarkable in the block copolymer systems.

We attempted to use these microdomains as the media for photoelectron transfer reaction in aqueous solution. We demonstrated that the forward electron transfer was facilitated by the uptake of amphiphilic quenchers through hydrophobic interaction. Namely, the fluorescence of the Ph residue in the copolymers in aqueous solutions was quenched by an amphiphilic quenchers (e.g., BHET) far more effectively than by a hydrophilic quenchers (e.g., FA). This tendency is particularly strong for the copolymer with high f_{Ph} in APh and QPh systems and is most remarkable for the block copolymer (b-VPh) systems. Electrostatic interaction of a charged quencher with the

electrolyte segments of amphiphilic copolymers also remarkably affected the rate of fluorescence quenching.

Further, we demonstrated a remarkable electrostatic effect of the electrolyte segments of these copolymers on the charge separation. In fact, the viologen radical ($SPV^{\bar{\cdot}}$) was efficiently accumulated because the electrostatic repulsion between $SPV^{\bar{\cdot}}$ and the anionic segments of APh leads to the facilitation of charge separation. The rate constant of back reaction for this system is more than 30-fold slower than that observed in the monomer model system.

Consequently, we demonstrated in this study that the each process of the photosensitized electron transfer reaction can be controlled to some extent by the use of amphiphilic copolymers as reaction media. From these results, we expect that the appropriately combined use of hydrophobic and electrostatic interactions in the well designed amphiphilic polymer and quencher (electron donor or acceptor) system may satisfy the requirement for achievement of high overall quantum efficiency, i.e., facilitation of forward and prevention of back reactions. In our laboratory, further studies are in progress along this line.

List of Publications

The content of this thesis have been published or will be published in the following papers and communications:

1. Copolymers of 2-Acrylamido-2-methylpropanesulfonic Acid and Aromatic Vinyl Compounds as Potential Media for Photosensitized Electron Transfer Reactions
   Y. Morishima, Y. Itoh, and S. Nozakura
   Makromol. Chem., 182, 3135 (1981).

2. Syntheses of Amphiphilic Block Copolymers. Block Copolymer of Methacrylic Acid and 9-Vinylphenanthrene
   Y. Morishima, T. Hashimoto, Y. Itoh, M. Kamachi, and S. Nozakura
   Makromol. Chem., Rapid Commun., 2, 507 (1981).

3. Amphiphilic Copolymers of Some Aromatic Vinyl Compounds and an Electrolytic Monomer As Potential Media for Photosensitized Electron Transfer: Fluorescence Quenching by an Amphiphilic Electron Acceptor in Aqueous Media
   Y. Itoh, Y. Morishima, and S. Nozakura
   J. Polym. Sci., Polym. Chem. Ed., 20, 467 (1982).

4. Amphiphilic Block Copolymer of 9-Vinylphenanthrene and Methacrylic Acid: Fluorescence Quenching of Phenanthrene Residue in Aqueous Medium
   Y. Morishima, Y. Itoh, T. Hashimoto, and S. Nozakura
   J. Polym. Sci., Polym. Chem. Ed., 20, 2007 (1982).

5. Amphiphilic Copolymers Consisting of Vinylphenanthrene and Cationic Segments. Fluorescence Quenching by Amphiphilic Quenchers in Aqueous Media
Y. Morishima, T. Tanaka, Y. Itoh, and S. Nozakura
Polym. J., 14, 861 (1982).

6. Fluorescence Quenching in Aqueous Solution of Amphiphilic Copolymers: A Kinetic Model for Downward Curvature in a Stern-Volmer-type Plot
Y. Morishima, Y. Itoh, and S. Nozakura
Chem. Phys. Lett., 91, 258 (1982).

7. Charge Separation in the Light-induced Electron Transfer Reaction of Amphiphilic Copolymers Consisting of Polyanion and Phenanthrene Segments
Y. Itoh, Y. Morishima, and S. Nozakura
J. Polym. Sci., Polym. Lett. Ed., 21, 167 (1983).

8. Amphiphilic Copolymers as Media for Light-induced Electron Transfer I. Electrostatic Effect on the Forward Reaction as Studied by Fluorescence Quenching
Y. Itoh, Y. Morishima, and S. Nozakura
Photochem. Photobiol., 39, 451 (1984).

9. Amphiphilic Copolymers as Media for Light-induced Electron Transfer II. Electrostatic Effect on the Back Electron Transfer
Y. Itoh, Y. Morishima, and S. Nozakura
Photochem. Photobiol., 39, 603 (1984).

10. Functional Polyelectrolytes As Novel Media for Light-Induced Electron Transfer
Y. Morishima, Y. Itoh, S. Nozakura, T. Ohno, and S. Kato
Macromolecules, 17 (1984) in press.

Other related papers:

1. Syntheses of Some Polymeric Dyes and Sensitized Photoelectrode Processes by the Polymer-Coated Electrodes
Y. Morishima, M. Isono, Y. Itoh, and S. Nozakura
Chem. Lett., 1149 (1981).

2. Syntheses of Amphiphilic Block Copolymers. Block Copolymers of Methacrylic Acid and p-N,N-dimethylaminostyrene
Y. Morishima, T. Hashimoto, Y. Itoh, M. Kamachi, and S. Nozakura
J. Polym. Sci., Polym. Chem. Ed., 20, 299 (1982).

3. Electrochemical Electron-Transfer Process of Polymers Containing N-Methylphenothiazine
Y. Morishima, Y. Itoh, and A. Koyagi
J. Polym. Sci., Polym. Chem. Ed., 21, 953 (1983).